Offshore Wind
Gravity Based Foundations

Workability Evaluation of the
Float-out & Submerge Installation Method

Charalampos (Babis) Romanidis

Offshore Wind
Gravity Based Foundations

Workability Evaluation of the Float-out & Submerge Installation Method

by

Charalampos (Babis) Romanidis

to obtain the double degree of
MSc Offshore and Dredging Engineering at Delft University of Technology
and
MSc Marine Technology at Norwegian University of Science and Technology
to be defended publicly on Tuesday July 7, 2026 at 13:00.

Student number:	6278612	
Project duration:	January, 2026 – July, 2026	
Thesis Committee Chairman:	Prof. dr. A. V. Metrikine	TU Delft
Daily Supervisor:	Dr. ir. B. C. Ummels	TU Delft
Committee Member:	Prof. E. Bachynski-Polić	NTNU
Company Supervisor:	D. van Rooijen	Temporary Works Design (TWD)

An electronic version of this thesis is available at http://repository.tudelft.nl/.

TU Delft NTNU EWEM TWD

Preface

The present thesis report represents the final step in obtaining the European Wind Energy Master's, a double degree awarded jointly by Delft University of Technology (TU Delft) and the Norwegian University of Science and Technology (NTNU). Completing it has at times been inspiring and effortless, yet moments of struggle and hardship were equally present. Overall, this master's programme has been a valuable experience beyond my wildest dreams. It has helped me understand myself better and strengthen some of my weaknesses, and it has reminded me that the journey is what matters most.

First, I would like to thank Prof. A. V. Metrikine for chairing my graduation committee and for his insightful feedback. I am equally grateful to Prof. Erin Bachynski-Polić for her guidance during my time in Norway and for raising the questions that helped me understand a little more of the entirely new, for me, field of offshore marine dynamics. I would also like to thank Dominik Hochhausler and Dylan van Rooijen from TWD for their support and critical discussions. Finally, I would like to express special gratitude to B. C. Ummels, whose enthusiasm and interest in the topic were always present, even when my own were lacking. I truly appreciate your attitude and our engaging discussions about wind energy, which reignited my own enthusiasm in the moments I needed it most.

Last, but most importantly, I would like to thank the people who were not directly involved in this work but who supported me by keeping my morale high throughout the process. My family in Greece, who have always been there for me and always will be, as I will be there for them. My old, dear friends: although we are thousands of miles apart, we keep our spirits high. And my new friends made along the way, with whom I have shared both the happiness and the hardship of this master's programme.

Thank you all for your support. I look forward to the exciting new endeavours the future holds.

Charalampos (Babis) Romanidis
Delft, June 2026

«Μην καταδέχεσαι να ρωτάς: "Θα νικήσουμε; Θα νικηθούμε;". Πολέμα!»

— Νίκος Καζαντζάκης, *Ασκητική* —

"Do not condescend to ask:'Will we be victorious? Will we be defeated?'. Fight on!"

— Nikos Kazantzakis, *Salvatores Dei* —

Summary

The transition towards ever larger offshore wind turbines has renewed industry interest in Gravity Based Foundations (GBFs), which offer a competitive and low-carbon alternative to conventional steel substructures. Their principal drawback, however, is their considerable mass, which complicates transport and installation (T&I) and restricts the number of vessels capable of handling them. The Float-out & Submerge (F&S) method offers a promising means of bypassing heavy-lift operations, yet it has so far been demonstrated only at the Blyth Offshore Demonstrator project (2018), where it was applied to 8.3 MW turbines. Its suitability for the modern generation of turbines therefore remains unproven. This thesis investigates how the workability of the F&S method can be improved for GBFs supporting modern 15 MW offshore wind turbines.

As no representative foundation design was available for this turbine class, an automated design algorithm was first developed. The algorithm implements a preliminary, capacity-factor based design method, enriched with constraints specific to the F&S configuration, and is coupled to a fully parametrised geometry generated in Autodesk Inventor through Python scripting. When validated against the realised Blyth design, the method reproduced the foundation mass to within approximately 5%. Up-scaling to the 15 MW class resulted in a 30% increase in total mass.

The installation process was subsequently modelled in OrcaFlex as a multibody, time-domain simulation, with hydrodynamic properties obtained from OrcaWave and with second-order wave effects and viscous damping explicitly included. A response-based operability assessment was carried out for the two governing installation sub-phases (station-keeping and landing), and the resulting limits were benchmarked against site-specific metocean data in accordance with the relevant DNV guidelines.

The analysis revealed that the mass-optimal foundation is not necessarily the most installable one. Workability was shown to improve by tuning the dynamic response of the tugboat-structure system to the wave climate of the specific site. A smart-ballasting strategy, realised by redistributing ballast to shift the roll natural period away from the dominant wave energy, raised the conditional workability of the station-keeping sub-phase from 29.5% to 75.5%, although its effect on the landing sub-phase was marginal. A bridle mooring arrangement was found to benefit the landing sub-phase instead raising workability from 45.7% to 58.6%. The study concludes by recommending an integrated design procedure that incorporates installability requirements, such as static stability and natural-period targeting, alongside the established structural criteria.

Contents

List of Figures

List of Tables

Abbreviations

Abbreviation	Explanation
AHTS	Anchor Handling Tug Supply
API	American Petroleum Institute
AWD	Adverse Weather Downtime
BOD	Blyth Offshore Demonstrator
BP	Bollard Pull
CFD	Computational Fluid Dynamics
CoG	Centre of Gravity
DLC	Design Load Case
DNV	Det Norske Veritas
DOF	Degree Of Freedom
DP	Dynamic Positioning
DtP	Distance-to-Port
F&S	Float-out & Submerge
FSC	Free-Surface Correction
GBF	Gravity Based Foundation
GBS	Gravity Based Structure
GM	Metacentric Height
HL	Heavy Lift
HLV	Heavy Lift Vessel
HT	Harbour Tugboat
HTV	Heavy Transport Vessel
IEC	International Electrotechnical Commission
JUV	Jack-up Vessel
LOA	Length Over All
MBL	Minimum Breaking Load
MP	Monopile foundation
MPE	Most Probable Extreme
MSL	Mean Sea Level
MWS	Marine Warranty Service
O&G	Oil and Gas
OEM	Original Equipment Manufacturer
ORI	Operability Robustness Index
OWF	Offshore Wind Farm
PLF	Partial Load Factor
QTF	Quadratic Transfer Function
RAO	Response Amplitude Operator
RC	Reinforced Concrete
SPMT	Self-Propelled Modular Transporter
T&I	Transport and Installation
TSHD	Trailing Suction Hopper Dredger
WOW	Weather Operational Window
WTG	Wind Turbine Generator
WTIV	Wind Turbine Installation Vessel

1 Introduction

1.1. Offshore Wind Energy Outlook

Over the past decade, there has been a significant shift towards renewable energy sources as part of the global transition to more sustainable energy systems. Wind energy has played a central role in this transition. Specifically, in the European Union, installed wind capacity reached $247\,\mathrm{GW}$ in 2025, generating $465\,\mathrm{TWh}$ of electricity and meeting $19\,\%$ of the Union's electricity demand [7].

Offshore wind has become an increasingly important component of this expansion, with both its total capacity and relative share rising year by year, as shown in Figure 1.1. This growth has been driven largely by offshore developments in the United Kingdom, Germany, the Netherlands, Denmark, and Belgium. These countries share a common advantage, access to the North Sea, a region with favourable conditions for offshore wind. These include high wind energy density, relatively shallow water depths of up to approximately $40\,\mathrm{m}$, and sandy seabeds that provide sufficient soil bearing capacity for bottom-fixed foundations, as well as close proximity to major demand centres. In addition, the potential for large-scale developments capable of meeting the growing electricity demand associated with the broader electrification of various sectors has further supported this expansion.

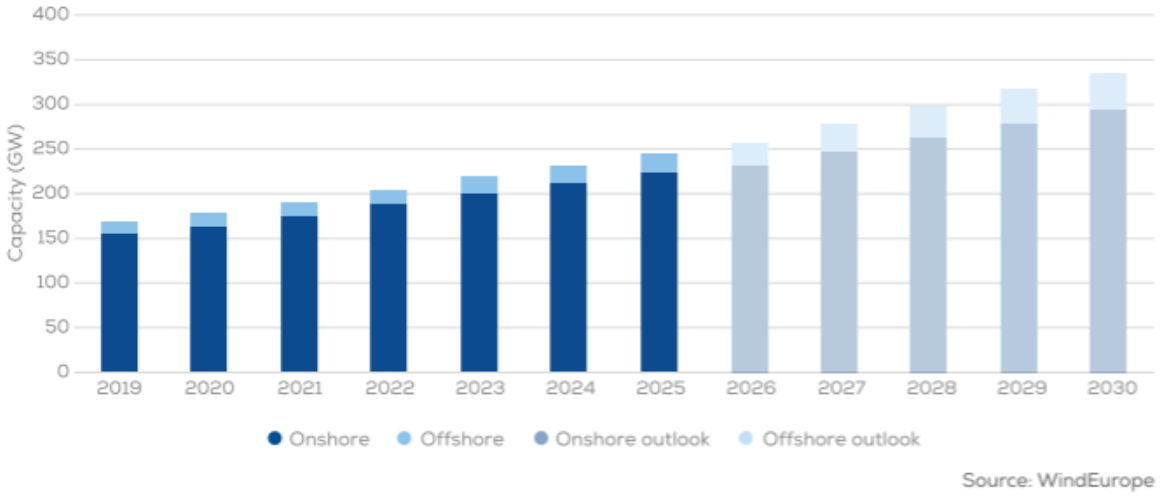

Figure 1.1: Outlook of wind energy cumulative installed capacity in Europe [55].

The outlook projected by WindEurope in Figure 1.1 sets a target of $90\,\mathrm{GW}$ of installed offshore wind capacity in the European Union by 2030, as part of the longer-term objective of reaching $300\,\mathrm{GW}$ by 2050. This ambition, together with the commitment from governments and industry to strengthen cooperation towards these goals, was underlined at the North Sea Summit held in Hamburg in January 2026, marked by the signing of the North Sea Investment Pact. This initiative aims to remove existing

barriers and de-risk offshore wind investments, thereby contributing to securing Europe's electricity supply [49].

1.2. Offshore Wind Foundations

1.2.1. Foundation Types

Offshore wind turbine foundations are a critical component of the infrastructure required to enable offshore wind energy generation. These foundations are strongly influenced by site-specific conditions and must be designed to accommodate varying water depths and soil characteristics. An overview of the most commonly used bottom-fixed foundation (FOU) technologies is presented in Figure 1.2.

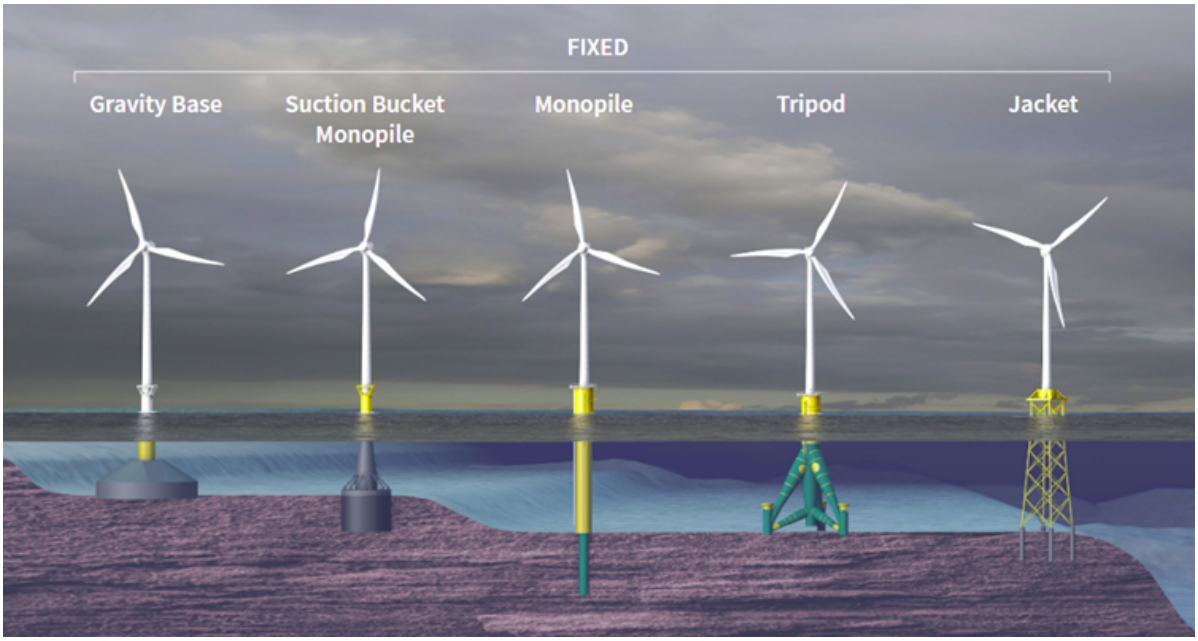

Figure 1.2: Foundation types used for bottom-fixed offshore wind installations [48].

As illustrated in Figure 1.3, the market share of different foundation types has evolved over time. Monopiles (MPs) have dominated the past decade, primarily due to their suitability for North Sea conditions and their relative ease of industrialisation, which has been essential in supporting the industry's required annual growth.

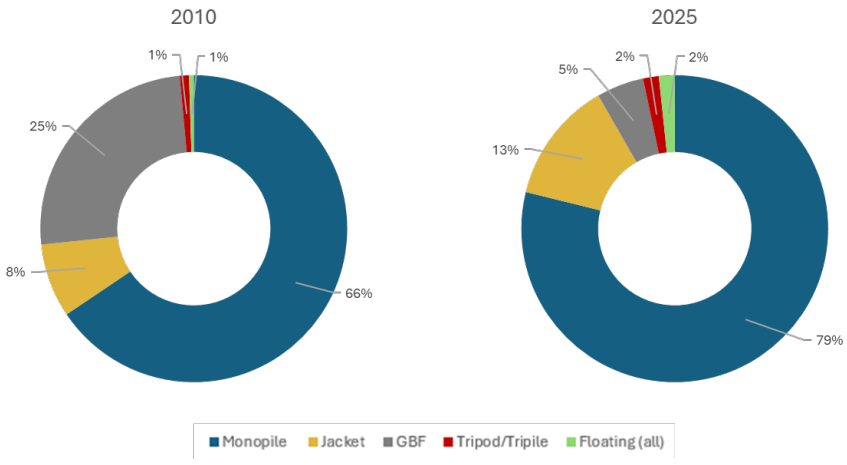

Figure 1.3: Market share evolution of different foundation types between 2010 and 2025 [39].

In contrast, gravity based foundations (GBFs) have experienced limited deployment in recent years.

Although they were used in early offshore wind projects, their competitiveness declined as developments moved further offshore, where monopiles proved more efficient.

Nevertheless, renewed interest in concrete support structures is emerging, particularly in regions where their advantages are more pronounced. For example, GBFs have been applied in the Baltic Sea, where complex soil conditions complicate piling operations and where concrete provides improved ice resistance compared to steel [39].

1.2.2. Manufacturing Cost

Foundations represent one of the largest non-recurring capital expenditures (CAPEX) of an offshore wind farm (OWF). As shown in Figure 1.4, foundations account for approximately 16% of the total CAPEX [40].

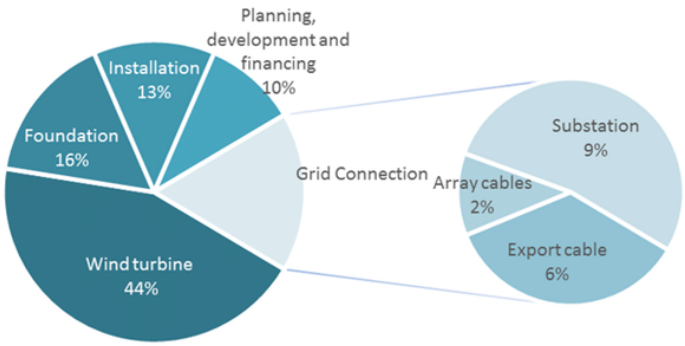

Figure 1.4: Cost breakdown of an offshore wind farm [10].

However, this percentage strongly depends on the selected foundation type, which is influenced by a range of design parameters, including turbine characteristics, metocean conditions, water depth, and soil properties. The primary cost driver for foundations is the cost of steel, which is determined by global commodity markets and is subject to significant price volatility [46].

1.2.3. Environmental Footprint

Many offshore wind tenders are awarded through so-called “beauty contests”. In this context, evaluation is not limited to the electricity strike price, but also includes qualitative criteria such as system integration, ecological performance, and overall project viability.

As a result, the environmental footprint of projects, typically expressed in terms of CO_2e/MW, is assessed more rigorously. This footprint varies significantly across foundation types, largely due to differences in steel content. More specifically, emissions for concrete foundations are estimated at 237 t CO_2e/MW, whereas steel-based solutions reach approximately 554 t CO_2e/MW for jackets and 600 t CO_2e/MW for monopiles [45].

In addition, increasing concerns regarding underwater noise during foundation installation have led many tender authorities to introduce sound exposure level (SEL) limits as part of their evaluation criteria [48].

Finally, design for decommissioning is becoming increasingly important as the industry expands and moves towards a more sustainable and circular economy model.

1.3. Foundation Installation

1.3.1. Vessel Availability

One of the key limiting factors behind the shortfall in achieving offshore wind development ambitions is the availability of suitable installation vessels [37]. Although the global fleet has expanded by 34 vessels over the past decade, with increased capacities and enhanced installation capabilities, constraints remain. The lead time for the delivery of these vessels is typically around 3–4 years, highlighting the mismatch between industry targets and current capacity [56].

It is estimated that, to meet the established targets, Europe's installation capacity must increase from the current 10 GW/year to 15 GW/year. This scale-up requires approximately 9.5 bn EUR of investment across the value chain, of which 4.2 bn EUR is allocated to new installation vessels [49]. The aforementioned scarcity of installation vessels also leads to a gap between supply and demand, causing day rates to rise disproportionately and, consequently, increasing offshore wind project costs [19].

Furthermore, it is important to note that most offshore wind specialised vessels are shared between Wind Turbine Generator (WTG) and foundation installation campaigns [29]. This further highlights the potential advantages of alternative foundation installation methods in unlocking the maximum capacity of the global fleet.

A categorisation of the vessels used in the offshore wind sector, together with indicative day rates, is provided in Appendix A.

1.3.2. Vessel Operational Limits

In addition to limited vessel availability, project developers and contractors face constraints related to the operational capabilities of existing installation vessels. As wind turbine and foundation component sizes and masses continue to increase, vessel lifting capacities are being pushed to their limits. As shown in Figure 1.5, crane capacities for modern jack-up vessels (JUVs) are capped at approximately $3000\,\mathrm{t}$. While this is generally sufficient for WTG components, it becomes marginal for the installation of heavier foundations such as jackets or GBFs.

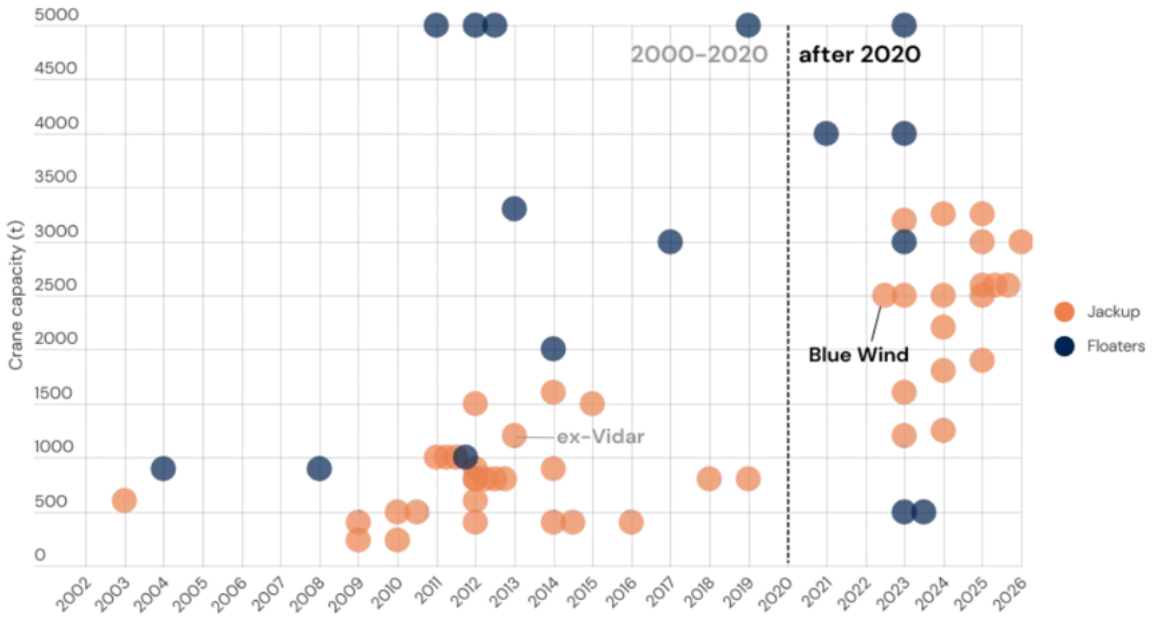

Figure 1.5: Trends in vessel crane capacities with respect to year of construction [56].

In contrast, dynamically positioned (DP) floating installation vessels can achieve lifting capacities of $5000\,\mathrm{t}$ or higher. However, these vessels are subject to stricter weather-related operational limits, as further discussed in Appendix A. Moreover, their availability is highly constrained, with fewer than 10 operational units currently in service, often competing simultaneously with demand from the oil and gas (O&G) sector.

Consequently, designing within vessel operational limits and aligning installation strategies accordingly has become a critical factor in offshore wind farm project execution.

1.4. Operability & Workability

Operability is broadly defined as the ability of a system to carry out its specified work safely and effectively, given all relevant constraints. These constraints encompass environmental, technical, logistical, and human factors that collectively govern the successful execution of an offshore marine operation, and fundamentally influence both the duration and total cost of an installation campaign [6].

Workability is a more specific concept, representing the environmental component of operability. It is defined as the fraction of time during which the environmental conditions at a site remain within the operational limits of the system, such that the marine operation can be safely executed. Its evaluation therefore requires knowledge of both the long-term environmental statistics at the site and the operational limit criteria of the system [2]. The industry standard for expressing workability is in 3-hour intervals, in alignment with the resolution of standard metocean hindcast databases.

A key performance indicator for quantifying workability is the Operability Robustness Index (ORI), defined as the fraction of operable sea states over the total number of sea states in the scatter diagram:

$$\text{ORI} = \frac{N_{\text{operable}}}{N_{\text{total}}} \times 100\% \tag{1.1}$$

Downtime is the complement of workability, corresponding to the fraction of time during which at least one operability criterion is not met:

$$\text{Downtime} = 1 - W \tag{1.2}$$

Downtime attributable specifically to environmental conditions exceeding operational limits is termed Adverse Weather Downtime (AWD). Understanding the seasonality of installation campaigns is equally important, as installation windows are sometimes limited to only three to four months per year; even marginal improvements in workability can therefore have a significant impact on overall project delivery.

Regarding temporal classification, marine operations are designated as *weather restricted* if their planned duration is less than 72 hours, meaning that accurate short-range weather forecasts can be relied upon to plan execution. Operations exceeding 72 hours are classified as *weather unrestricted*, for which long-term statistical methods must be applied instead [53].

Workability can be established using two fundamentally different approaches.

Weather-based workability expresses operational limits directly in terms of environmental parameters, most commonly the significant wave height H_s and wind speed. A sea state is classified as workable if the environmental conditions remain below prescribed thresholds, irrespective of the actual structural or vessel response. This approach is straightforward to apply and is commonly used in preliminary planning studies, where a conservative limiting H_s of 1.5–2.0 m is often adopted [44]:

$$W = \frac{T\big(H_s \leq H_{s,\text{lim}}\big)}{T_{\text{total}}} = P\big(H_s \leq H_{s,\text{lim}}\big) \tag{1.3}$$

Response-based workability defines operational limits in terms of the system's actual dynamic response, such as maximum allowable displacement, rotation, or acceleration of the floating structure. A sea state is classified as workable only if the computed response remains within prescribed limits under those conditions. This approach is physically more rigorous and requires time-domain or frequency-domain dynamic simulations for each sea state in the scatter diagram:

$$W = \frac{T\big(\text{response} \leq \text{response}_{\text{lim}}\big)}{T_{\text{total}}} \tag{1.4}$$

In this study, response-based workability is adopted, as it is more representative of the actual system behaviour and enables a more meaningful comparison between design variants. The corresponding operational limit criteria are derived from project-specific requirements and published industry guidelines such as DNV-ST-N001 [16].

1.5. Research Objective & Scope

Considering all the aforementioned facts, a clear objective emerges to increase the efficiency and capacity of new offshore wind installations. GBFs could be a feasible solution to address this growing demand and accelerate project deployment globally by leveraging their inherent advantages. However, a set of challenges must be resolved to enable their wider adoption in commercial projects.

As highlighted earlier, the main challenge for this type of foundation lies in its enormous mass, which makes transport and installation (T&I) particularly difficult. The largest turbines installed on lifted GBFs are 7 MW units at the Fécamp project in 2022, where the foundations weighed approximately 7000 tonnes, limiting installation to only three vessels worldwide [8]. Considering that modern, currently

installed 15 MW class turbines require significantly higher load-bearing capacities, it becomes evident that the mass of these foundations will increase even further.

In parallel, several concepts have been proposed within the industry to address the T&I challenge, mainly by introducing alternative installation methods. These concepts primarily focus on float-out & submerge (F&S) approaches [38], aiming to bypass traditional heavy lift operations. However, only a limited number of these concepts have been tested in demonstration projects, and none have yet been deployed at commercial scale in offshore wind farms. Moreover, the suitability of the F&S method has only been demonstrated for 8.3 MW wind turbines in the Blyth Offshore Demonstrator (BOD) project in 2018.

The above considerations led to the formulation of the main research question and the respective sub-questions, as presented below.

Main Research Question

How can the workability of the F&S method for modern offshore wind turbine GBFs be improved?

The following sub-questions are defined to support the main research question:

1. How does a GBF designed for F&S installation scale to support modern 15 MW wind turbines?
2. How can the installation process be modelled more accurately to increase understanding and simulation confidence?
3. What are the main factors governing the operability of the installation process?
4. How can installation workability be improved for a specific site location?

Overall, the goal of this thesis work is to provide an improved understanding of the F&S method, increasing confidence in this T&I approach, accelerating the adoption of GBFs in offshore wind projects, and contributing to the further development of the sector.

1.6. Approach

In order to address the research questions defined in the previous section, a structured methodology was developed. An overview of the adopted methodology for the scope of this thesis is presented in Figure 1.6.

Initially, based on the conducted literature review, the most advanced GBF concept realised to date using the Float-out & Submerge (F&S) installation method was identified and examined. The selected concept was originally designed for an 8 MW-class wind turbine, which was considered no longer representative of currently installed offshore wind turbines. Its design, manufacturing, transportation, and installation processes were therefore analysed in order to identify potential limitations, operational challenges, and installation bottlenecks.

Subsequently, the foundation concept was up-scaled to accommodate modern large-scale wind turbines. The GBF was re-designed following a simplified Front-End Engineering Design (FEED) methodology proposed in the literature for preliminary foundation design. The resulting configuration served as the baseline design for the present study. The geometry was developed in *Autodesk Inventor* and fully parametrised, allowing automated updates through Python scripts for efficient design iteration and optimisation.

Based on the understanding acquired regarding the installation sequence and the F&S methodology, a numerical model was then developed in *OrcaFlex* to perform time-domain simulations of the installation process. Particular focus was placed on the final sub-phase of installation prior to seabed mating, which was considered the most critical in terms of structural motions and operational control. The detailed model set-up and included components are presented in the Chapter 4. Hydrodynamic properties were calculated using *OrcaWave* and subsequently imported into the time-domain model. In

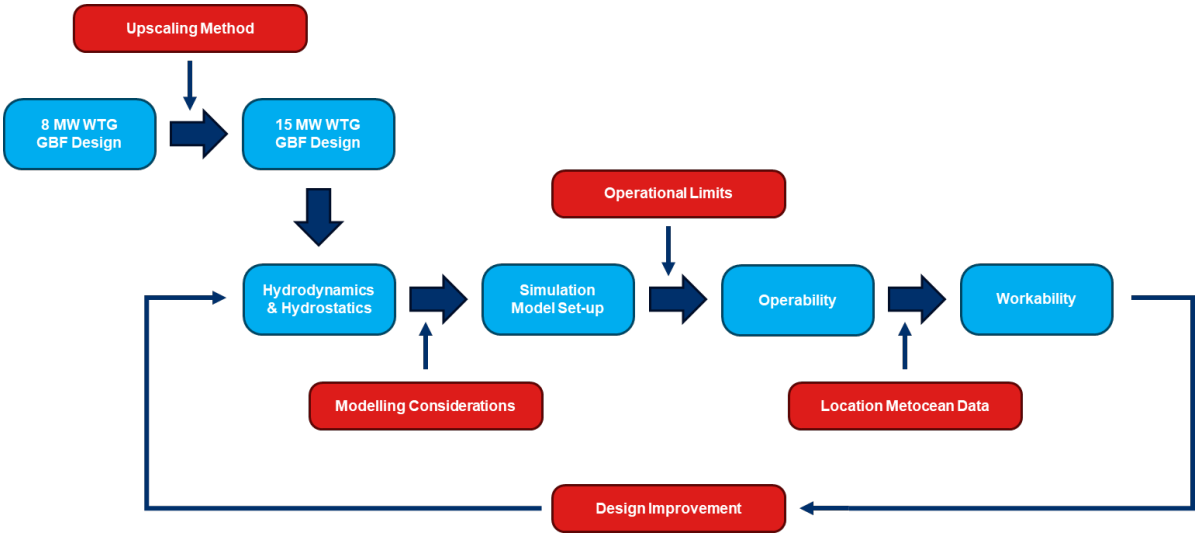

Figure 1.6: Overview of the methodology followed in the present study.

addition, sensitivity studies were conducted to improve the quality, robustness, and numerical accuracy of the simulations.

Following the model development, a set of response criteria was established to assess whether the installation operation could be performed within the required safety and positioning tolerances. The operability of the installation method was then evaluated through post-processing of the simulation results using Python-based analysis tools.

Finally, the obtained operability limits were benchmarked against metocean data from a representative offshore location. Combined with the application of relevant industry standards and guidelines (e.g. DNV marine operations standards), this enabled the workability of the proposed installation methodology to be assessed for realistic offshore conditions.

After evaluating the operability and workability of the baseline installation method, and identifying its main limitations and bottlenecks, an effort was made to investigate potential improvements. The proposed enhancement strategy was selected with the intention of maintaining practical applicability while requiring minimal additional equipment or major design modifications. This process led to the development of the improved design concept, which is presented in the relevant chapter.

The performance of both the baseline and improved configurations was subsequently benchmarked, evaluated, and discussed. The resulting analysis provided a deeper understanding of the installation behaviour of floating GBFs and led to the formulation of a proposed installation methodology, while also identifying topics requiring further investigation.

1.7. Report Outline

This report is organised into seven chapters, the structure of which is outlined below.

Chapter 1 has introduced the context and motivation of the present work, defined the research objective and scope, and presented the methodology adopted to address the research questions.

Chapter 2 reviews the state of the art of Gravity Based Foundations and of the Float-out & Submerge (F&S) installation method. It discusses the renewed interest in self-buoyant foundations, the integrated nature of their design, and the manufacturing and port infrastructure they require, before describing the individual phases of the F&S method. The Blyth Offshore Demonstrator (BOD) concept is identified here as the baseline for the study.

Chapter 3 presents the up-scaling of the baseline foundation to support a modern 15 MW turbine. The adopted design load case and limit states are defined, and the preliminary design procedure is described, together with its underlying assumptions and constraints. The resulting parametrised geometry serves as the baseline design for the remainder of the work.

Chapter 4 details the development of the numerical simulation model. The hydrodynamic properties of the foundation are computed in OrcaWave and imported into a multibody, time-domain OrcaFlex model. The modelling assumptions are stated, and several modelling considerations (the internal free-

surface effect, the mesh resolution, the viscous damping, and the second-order wave loads) are examined through dedicated sensitivity studies.

Chapter 5 evaluates the operability and workability of the baseline installation method. The installation operation and its two critical sub-phases, station-keeping and landing, are identified, and a set of response-based operability criteria is established. The resulting operability limits are then benchmarked against the metocean conditions of a representative offshore site to obtain the baseline workability.

Chapter 6 investigates strategies for improving the workability of the method. Following a comparison of the candidate concepts, the smart-ballasting approach is examined in detail, and a bridle mooring arrangement is subsequently assessed as a complementary measure targeting the landing sub-phase.

Chapter 7 summarises the main conclusions of the study with respect to the research questions, and sets out recommendations for further work. Supporting material on offshore installation vessels, Gravity Based Foundations, the foundation design calculations, and the complete set of operability and workability figures is provided in Appendices A to D.

2

State-of-the-art

2.1. Renewed Interest in GBFs

A renewed interest in GBFs has been emerging over the past several years, driven by a convergence of market and technical pressures that erode the competitive advantage of monopiles [39]. As the offshore wind industry expands rapidly, the production capacity of monopile and jacket manufacturers is increasingly strained, creating supply chain bottlenecks that affect project timelines and costs [36]. This has prompted developers to reconsider alternative foundation concepts, including GBFs, which rely on a different supply chain based on concrete construction and local fabrication. Figure 2.1 shows the largest commercial OWF project realised with GBF foundations, Fécamp in France.

The sustained increase in global steel prices represents a further significant driver [46]. Because GBFs rely predominantly on reinforced concrete, their material cost is considerably less sensitive to steel market fluctuations, making them a more financially stable option in an environment of volatile commodity prices [22].

The scarcity of suitable installation vessels is also a contributing factor. The global fleet of Heavy Lift Vessels (HLVs) and WTIVs is limited, and demand has significantly outpaced supply as the number of projects entering their construction phase has grown rapidly, pushing day-charter rates to historically high levels [19]. GBFs installed via the F&S method rely on standard tugboats rather than specialised HLVs, offering a potential route to decoupling installation cost from vessel scarcity.

Beyond cost, site conditions in emerging offshore wind markets are also reasserting the relevance of GBFs. They are particularly competitive in locations with rocky or heterogeneous seabeds unsuitable for pile driving, and in regions where ice loading is a governing design condition [39].

Figure 2.1: Installation (left) and construction quay (right) of the Fécamp OWF GBFs.

These drivers are reflected in recent industry developments. The commissioning of the Fécamp OWF (2022) in France, with 71 GBFs supporting 7 MW turbines at approximately 30 m depth, represents the most advanced large-scale GBF project executed using conventional HL methods to date [1]. The BOD project (2018) in the UK demonstrated the viability of the F&S method at commercial scale.

In addition, GBFs have been adopted at sites with challenging conditions, including Tahkoluoto (Finland) and Vindpark Vänern (Sweden) in iced environments [53], and Hydropower Rudong (China) in an intertidal setting. A detailed account of the historical development, design generations, and novel concepts of GBFs is provided in Appendix B.

2.2. Self-buoyant Foundations

2.2.1. State of the Art

The current state of the art, representing what can be considered a fourth generation of GBFs, has emerged to address the crane capability and cost limitations of conventional heavy lift operations by introducing self-buoyant designs compatible with the F&S method. The most prominent realised example is the Blyth Offshore Demonstrator (BOD) project (2018) in the UK, operated by EDF Renewables in Northumberland. Five MHI Vestas V164-8.3 MW turbines are supported on hybrid steel-concrete foundations designed by Royal BAM, in water depths of up to 42 m [39]. Figure 2.2 presents the tow-out phase of the self-buoyant GBF prior to installation.

The hybrid design concept is central to the BOD foundation. The lower section consists of a reinforced concrete caisson (slab and cone), which provides the required dead weight and buoyancy during the float-out phase. The upper section is a steel cylindrical shaft, equivalent in function to a monopile, which interfaces with the turbine tower. This configuration leverages the structural efficiency of each material. Concrete provides cost-effective mass and durability in the submerged section, whereas steel offers the precision and fabrication ease needed at the tower interface and the fatigue resistance required in the splash zone. The result is a foundation that is both self-buoyant and structurally optimised for in-place operation, without the need for HLVs during installation [39].

Each foundation consists of three sections from bottom to top: a wide reinforced concrete slab ($D_2 = 30$ m), a conical transition ($h_2 = 10$ m), and a steel cylindrical shaft ($D_1 = 6$ m, $h_1 = 32$ m), as shown in Figure 2.3. Key properties are summarised in Table 2.1. The concrete caisson contains approximately 2% steel reinforcement by weight and relies on its hollow interior for buoyancy during tow-out. Once on site, controlled seawater ballasting lowers the structure onto the prepared seabed, after which sand ballast is added to achieve the required operational dead weight [54].

Figure 2.2: BOD self-buoyant GBF being towed out at River Tyne, Newcastle, UK [39].

The BOD project remains the only commercial-scale application of the F&S method for GBFs in the North Sea, and its foundation design serves as the baseline concept for the present thesis investigation.

2.2.2. Integrated Design Approach

One of the defining characteristics of GBF design and development, particularly for the F&S method, is the strong interdependency between three core engineering domains: the structural design of the foundation, the selected manufacturing method, and the planned T&I strategy [22]. Unlike monopile

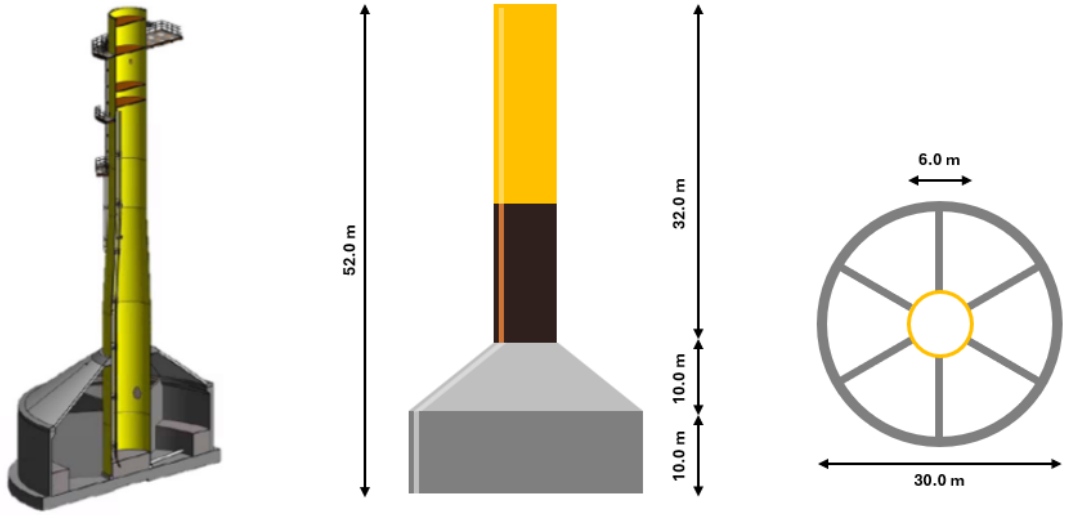

Figure 2.3: Sectional view and main dimensions of the BOD GBF design [54].

Table 2.1: BOD GBF main geometric and mass properties [54].

Parameter	Symbol	Value	Units
Height – Total	h_{tot}	52	m
Height – Pile	h_1	32	m
Height – Cone	h_2	10	m
Height – Base	h_3	10	m
Diameter – Pile	D_1	6	m
Diameter – Base	D_2	30	m
Mass (w/o ballast)	M_{net}	5600	t

foundations, where these domains can be developed in relative independence, GBF engineering decisions are highly coupled, and changes in one domain invariably propagate to the others, as illustrated in Figure 2.4.

For self-buoyant GBFs in particular, the floating stability during tow-out and the controlled ballasting behaviour during submersion impose constraints on the caisson geometry, namely the base diameter, the height of the hollow section, and the vertical position of the centre of gravity. These constraints must be satisfied simultaneously with the structural requirements for in-place operation [45]. This means that T&I loads, as prescribed in DNV-RP-N103 [13], must be fully integrated into the structural design from the outset rather than treated as a secondary check. The selected manufacturing method and port infrastructure further constrain the achievable geometry and the maximum construction tolerances [21].

In practice, the industry approach is to evaluate multiple combinations of design concepts, manufacturing alternatives and T&I strategies together, identifying the optimal combination for each specific project rather than optimising each domain in isolation [22].

2.2.3. Manufacturing & Port Infrastructure

The concrete used in GBF caissons is highly reinforced, with the steel reinforcement ratio varying considerably across different designs and T&I concepts. Reported values range from as low as 3.6% [31] to as high as 18.7% [44], depending on the structural requirements and the loads imposed during the installation phase. As a consequence, the effective density of the concrete caisson is considerably

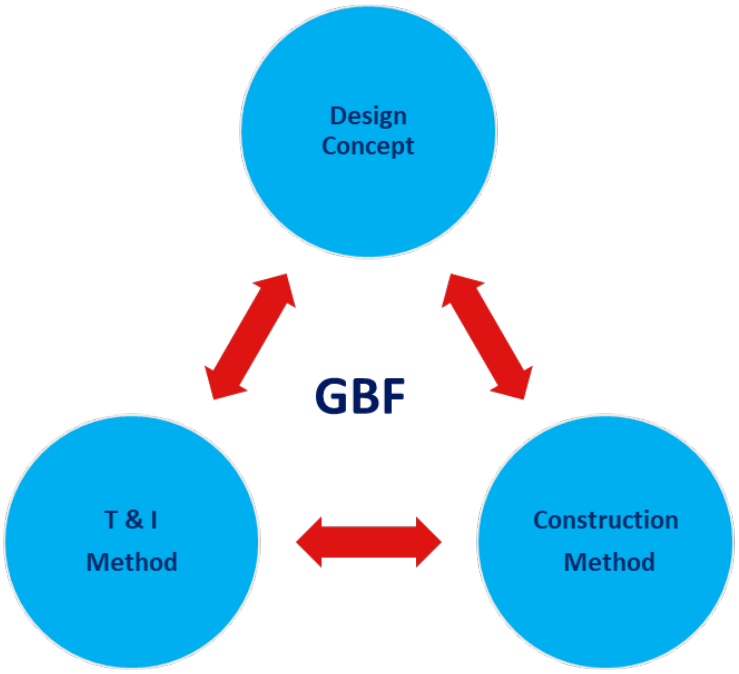

Figure 2.4: The design concept, construction and T&I method are strongly interdependent for GBFs.

higher than plain concrete, with values around $2850\,\mathrm{kg\,m^{-3}}$ typically reported for reinforcement ratios in the region of 10% [38]. Mass properties of concrete structures carry an uncertainty of up to approximately 10% based on project experience [6], which must be accounted for in structural and stability analyses.

GBF fabrication demands significant port or quayside infrastructure in close proximity to the project site, as concrete foundations are substantially heavier than equivalent steel foundations and cannot be economically transported over long distances [21]. Three main construction methods have been applied in existing projects, as shown in Figure 2.5:

- **Dry dock construction** was employed in the earliest OWFs, including Vindeby and Middelgrunden, and remains relevant for self-buoyant designs such as the BOD project. The foundation is constructed within a dry dock that is subsequently flooded, enabling the structure to float-out directly without any heavy lift load-out operation. Dry dock dimensions, particularly width, may however act as a limiting factor for the construction of large-footprint GBFs.
- **Floating pontoon construction** was used for projects such as Nysted and Lillgrund, where foundations were built directly on transport barges or pontoons. This minimises port land requirements but ties up the pontoons for the full duration of construction, and still requires heavy lift operations for offshore installation.
- **Quayside construction** has been adopted for third-generation GBFs at Thornton Bank and Fécamp. It requires large, structurally reinforced quayside areas. Once complete, the foundations are transferred to transport barges using either self-propelled modular transporters (SPMTs) in a roll-off operation or dedicated heavy lift equipment.

More recently, the slip-forming technique has gained attention as a method to improve the industrialisation of concrete construction. Applied for example during the fabrication of the Hywind Tampen spar foundations, slip-forming enables continuous vertical construction and can significantly reduce cycle times for large concrete structures [52].

Both dry dock and quayside construction are compatible with the F&S method, provided that the design achieves sufficient self-buoyancy. In the dry dock approach, the structure floats out directly upon dock flooding, avoiding load-out altogether. In the quayside approach, a controlled slide-in or roll-off operation into the water can be adopted, after which the foundation is towed to site. The choice

Figure 2.5: Manufacturing methods for GBFs: dry dock construction (left), floating pontoon construction (centre), and quayside construction (right) [22].

between the two depends primarily on the available port infrastructure, the foundation footprint and the local logistical constraints of each project.

2.3. Float-out & Submerge Method

2.3.1. Method Overview

Two main approaches exist for the installation of GBFs offshore: the conventional heavy lift (HL) method and the float-out & submerge (F&S) method. The former has been the industry standard for all three conventional GBF generations, while the latter represents a more recent and less explored alternative that is the focus of the present thesis. Both methods require similar seabed preparation prior to installation and scour protection works after placement, as illustrated in Figure 2.6. In the HL method, the foundation is fabricated either on a quayside or directly on a floating barge, transported to the project site on a heavy transport vessel (HTV) or barge, and lifted onto the prepared seabed using an HLV or SSCV [39]. A hybrid approach combining buoyancy assistance with heavy lift was applied at the Thornton Bank OWF, where foundations were partially submerged during transport to reduce crane line loads, with the same vessel used for load-out, transport and installation [22].

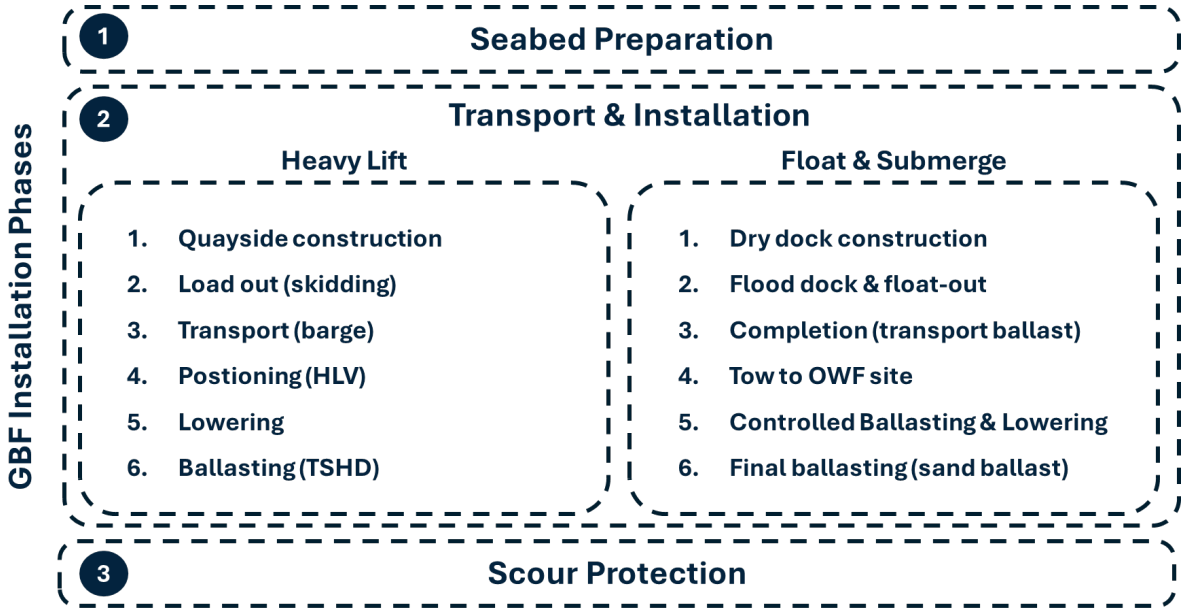

Figure 2.6: Overview of the two main GBF T&I methods [21].

The F&S method attempts to eliminate offshore heavy lift operations entirely by designing the foundation to be self-buoyant. This enables fabrication using all conventional construction approaches (quayside, dry dock or slip-forming), while also easing port logistics and offering alternative handling

approaches. Transport to the project site can be performed either by towing individual foundations using standard tugboats or by utilising semi-submersible heavy transport vessels (HTVs) for batch deliveries. The operational principle of the F&S method resembles immersed tunnel construction. This was recently demonstrated at large scale in the Fehmarnbelt Fixed Link project, where precast concrete elements of approximately $73\,000\,\mathrm{t}$ each are floated out and submerged into a dredged seabed trench [25]. The F&S method is examined in detail in the following subsections.

2.3.2. Seabed Preparation & Scour Protection

Seabed preparation is a prerequisite for GBF installation, required to ensure adequate bearing capacity and a level contact surface beneath the caisson. The process involves dredging the seabed to a specified depth, typically up to several metres, followed by the placement of a gravel or crushed-rock bedding layer to achieve the required levelness and stiffness. For a representative case requiring approximately 3 m of dredging, the operation duration is reported to be around three to four days per foundation [21]. The quality of this preparation is particularly critical for GBFs because, unlike pile foundations, they do not have an embedded structural element to redistribute contact loads. Any unevenness in the bedding layer can lead to non-uniform stresses beneath the caisson base, potentially causing post-installation settlement or tilt under the cyclic loading of the operating turbine [54]. In some project designs, cement grout injection between the caisson base and the seabed is employed after touchdown to fill remaining voids and improve contact uniformity [21].

Scour protection is applied after foundation placement to mitigate the localised seabed erosion caused by the acceleration of sea currents around the caisson base. Without adequate protection, the progressive formation of a scour hole can alter the contact stress distribution beneath the foundation and push loading conditions beyond design limits [39]. A graded rock or gravel layer is typically placed around the foundation footprint to a specified radius and thickness, following established industry guidelines [28]. Both phases are illustrated in Figure 2.7.

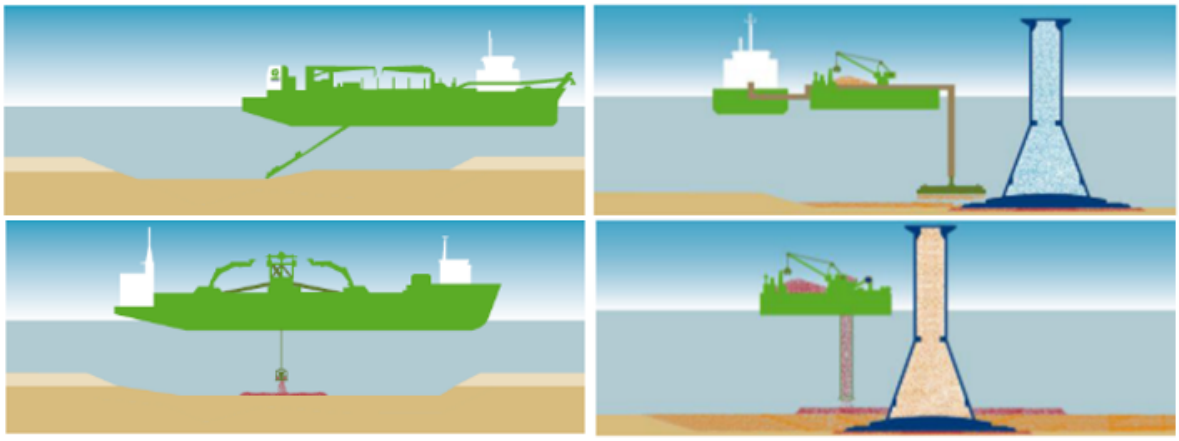

Figure 2.7: Seabed preparation procedure (left) and scour protection application (right) for a GBF [28].

2.3.3. Load-out and Tow-out

For self-buoyant GBFs, the dry dock is the most naturally suited construction and load-out environment, Figure 2.8. Once fabrication is complete, the dock is flooded and the gates opened, allowing the structure to float-out under its own buoyancy. This eliminates the need for SPMTs, heavy lift equipment or crane assistance entirely, reducing port infrastructure requirements and simplifying load-out logistics compared to any other construction method [21]. Once floating, the structure is connected to a spread of tugboats, typically three per foundation, arranged to maintain directional control during the tow from the construction facility to a sheltered nearshore location [21]. Depending on the design draft, partial ballasting may be applied at this sub-phase to adjust the floating condition prior to the open-sea tow. It is important that the floating draft is sufficiently shallow to maintain adequate freeboard and metacentric height, ensuring hydrostatic stability [15].

The self-buoyant design is however not exclusively dependent on dry dock construction. Founda-

Figure 2.8: Load-out of GBFs from quayside (left) and dry dock (right) [39].

tions built on a quayside can be launched into the water via a controlled slide-in or roll-off operation, achieving the same floating condition prior to tow-out. Pontoon-based construction and floating dry docks represent further alternatives, where the foundation is released by controlled immersion of the support platform upon completion. In all cases, once the structure is afloat, the tow-out procedure is identical, and the logistical advantages of the F&S method are fully retained.

2.3.4. Transport to Project Location

Transport of the self-buoyant GBF to the offshore project site is primarily performed by wet tow, using a spread of tugboats or anchor handling tug supply (AHTS) vessels, depending on the open-sea conditions expected along the tow route [21]. Each foundation is typically towed individually to the project location. As an alternative, HTVs can be used for batch deliveries of multiple foundations per trip, improving transport efficiency, as shown in Figure 2.9. The widespread availability of tugboats also allows operations to be scaled up when weather windows permit, with multiple foundations towed simultaneously [38].

Figure 2.9: Heavy duty barge (left) and towed (right) transportation of GBFs to the offshore project site [39].

Transport speed during a wet tow is governed by the tugboat bollard pull (BP), the hydrodynamic drag of the floating structure and the prevailing sea state. Due to the large mass and submerged volume of GBFs, towing is typically performed at speeds of approximately 3–5 knots [20], constrained primarily by towing resistance and structural response limits. A significant wave height of 1.5–2.0 m is generally considered the operational limit for this phase [21]. Transport duration depends primarily on the distance from the construction port to the project site (DtP) and the availability of a sustained weather window sufficient to complete both the tow and the subsequent installation without interruption [44]. For conventional HL operations the required weather operational window (WOW) is typically around 24 hours, while for the F&S method a range of 12–24 hours is expected, depending on site conditions and structure specifications [38].

2.3.5. Controlled Ballasting and Immersion

Once at the project location, controlled immersion of the foundation is performed to achieve the target installation position. The process is split into two main sub-phases, which can be decoupled, offering a key logistical advantage of the F&S method.

The first sub-phase involves seawater ballasting to lower the foundation onto the seabed [21]. Seawater is pumped into the hollow caisson compartments to progressively increase the draft and lower the structure towards the seabed. The ballasting must be conducted in a controlled and symmetric manner to prevent differential flooding, which could induce excessive trim or, in the extreme case, capsizing of the structure. The main steps of this procedure are as follows:

1. Positioning of the floating GBF at the target installation coordinates using the tugboat spread.
2. Controlled ingress of seawater into the designated ballast compartments, with continuous monitoring of draft, trim and list.
3. Progressive lowering of the structure while maintaining the caisson base parallel to the seafloor, to ensure uniform touchdown.
4. Landing of the caisson on the prepared gravel bed, followed by verification of position and inclination.
5. Filling of the caisson with the maximum allowed water ballast to secure its position under prevailing weather conditions.

Once the foundation is secured on the seabed, the first procedure is complete. This marks a critical milestone, as it allows the two sub-phases to be decoupled and the tugboat spread to be released. The T&I process can be either continued immediately, if the weather window duration allows, or be postponed to when workable conditions are present again.

The second sub-phase involves the replacement of the water ballast with sand ballast, Figure 2.10, increasing the dead weight of the GBF to the levels required to withstand the turbine's operational and extreme loads [21].

Figure 2.10: Ballasting equipment during the BOD GBF installation campaign (left). Installed foundation (right) [32].

At the BOD project, this was performed using a specially designed and built bulk vessel with integrated sand storage, mixing, pumping and monitoring systems. The sand ballasting operation was executed as a continuous three-day campaign, during which more than 41000 m^3 of sand was pumped into the five foundations [32].

3

Foundation Up-scaling

3.1. Up-scaling Approach

One of the main research questions addressed in the present thesis is the installation operability of a foundation concept relevant to modern wind turbines currently being installed. Since the BOD design was used for the installation of $8.3\,\mathrm{MW}$ turbines in 2018, representing the largest WTG installed on a GBF to date, up-scaling the design to accommodate a 15 MW turbine was considered necessary.

The GBF was not upscaled by directly enlarging its dimensions. Instead, a preliminary design procedure was followed, ensuring that the resulting design satisfies specific limit states under a selected design load case (DLC) [1, 31].

3.1.1. Design Load Case

A DLC corresponds to a loading condition that may occur during the operational lifetime of the structure and is defined by the environmental conditions (i.e. extreme wind and waves) and the design situation (i.e. rated power or parked condition). A wide range of load cases is provided in the DNV and International Electrotechnical Commission (IEC) standards for the design of offshore WTG foundations with a design life of 25–30 years. The various DLCs are described in detail in [14]. However, performing a complete load analysis exceeded the scope of this thesis. To simplify the calculations and obtain a feasible design, a simplified yet conservative extreme load case was adopted for the evaluation, as proposed in [1]. The details of the selected DLC are presented in Table 3.1.

DLC: Extreme wave load scenario					
Load	**Model**	**Parameter**	**Value**	**Unit**	**Source**
Wind	Extreme turbulence model (ETM)	U_{rated}	10.59	m/s	[26]
		TI	9.7	%	[26]
Wave	50-year Extreme Wave Height (EWH)	$Hs_{50-year}$	16.9	m	[54]
		T_p	12.7	s	[54]
		γ	3.3	-	
Current	Normal current model (NCM)	Vc_{1-year}	1.0	m/s	Expert input
Sea level	Mean sea level (MSL)	SWL	0	m	-

Table 3.1: Extreme wave load scenario (DLC) parameters.

3.1.2. Limit States

For each DLC, relevant limit states (i.e. ULS, FLS, and SLS) must be evaluated. The ULS is often the governing design criterion for GBFs and is therefore typically the first assessment performed during the preliminary design stage [1, 45]. Additional information regarding the limit states and WTG foundation design criteria is provided in Appendix C.

The ULS design checks were performed by evaluating the following capacities of the GBF. Furthermore, an additional capacity check was conducted for the SLS limit state. The capacities were assessed through their corresponding utilisation ratios, where a utilisation ratio greater than 100% indicates that the design exceeds the allowable limit state and should therefore be considered non-feasible.

In more detail:

- **Soil bearing capacity**, which ensures that the soil can safely support the loads transferred from the structure.

$$Bearing\ capacity\ utilisation\ [\%] = \frac{p_u}{q_u}, \tag{3.1}$$

  where p_u is the effective soil stress and q_u is the ultimate bearing capacity.

- **Sliding capacity**, which ensures that the structure will not slide horizontally.

$$Sliding\ capacity\ utilisation\ [\%] = \frac{H}{H_d} \tag{3.2}$$

  where H is the horizontal force acting on the foundation and H_d is the sliding resistance.

- **Tipping capacity**, which ensures that the structure will not overturn due to the environmental overturning moment acting around the mudline.

$$Tipping\ capacity\ utilisation\ [\%] = \frac{M}{M_{st}} \tag{3.3}$$

  where M is the overturning moment induced by the environmental loading and M_{st} is the stabilising moment provided by the GBF self-weight.

- **Full-contact capacity**, which ensures that the bottom surface of the GBF remains in full contact with the soil under all loading conditions.

$$Full-contact\ capacity\ utilisation[\%] = \frac{e}{e_{max}} \tag{3.4}$$

  where e is the load eccentricity and e_{max} is the maximum allowable eccentricity.

The detailed calculation procedures and governing equations are provided in [12, 31, 1] and Appendix C. Furthermore, the relevant partial load factors (PLFs) were incorporated into the assessment of the utilisation ratios, as presented in Table 3.2.

Partial Load Factor	Symbol	Value
ULS - Environmental loads	γ_{env}	1.35
ULS - Permanent loads	γ_{per}	0.90
SLS - Environmental loads	γ_{env}	0.65
SLS - Permanent loads	γ_{per}	0.65

Table 3.2: Partial Load Factors (PLF) for ULS and SLS.

3.2. Implementation Procedure

To implement the proposed design methodology, a Python-based calculation algorithm was developed to perform the capacity checks for a given foundation configuration. The implemented procedure consisted of the following steps:

1. The range of the free design variables is initially defined.

2. A detailed CAD model of the GBF is parametrically modified according to the selected design variables, and the corresponding mass properties of the generated design are extracted.

3. Wind, wave, and current loads are calculated through short-term time-domain simulations (1-hour), considering irregular waves and turbulent wind conditions. The resulting environmental horizontal forces (H) and overturning moments (M) acting on the foundation are then obtained.

4. The foundation capacities are evaluated against the applied loads, including the relevant partial load factors, in order to determine the corresponding utilisation ratios.

5. A feasible design map is generated for the $15\,\mathrm{MW}$ WTG foundation by evaluating all examined capacity criteria.

3.2.1. Assumptions

The design evaluation of the up-scaled GBF was performed under the following assumptions:

- The Morison equation was used to calculate the hydrodynamic loading acting on the GBF, as proposed in [30], since the design wavelength resulted in a ratio marginally within the Morison regime ($\lambda/d > 5$).
- Current conditions were represented using a uniform velocity profile extending from the splash zone to the seabed.
- The soil beneath the foundation was assumed to be cohesionless and drained, considering that appropriate seabed preparation had been performed prior to installation [1].
- The cone height was kept constant in order to limit the number of free design parameters.

3.2.2. Constraints

In addition, a set of design constraints was applied to ensure that realistic foundation configurations were obtained:

- The shaft diameter was fixed at $8.5\,\mathrm{m}$, corresponding to a compatible tower base diameter for a $15\,\mathrm{MW}$ WTG, following expert advice and current Original Equipment Manufacturer (OEM) specifications.
- A blade clearance of $25\,\mathrm{m}$ above the MSL was imposed to define the WTG hub height, following expert advice.
- The deck elevation and air gap were determined according to the guideline proposed in [34] for jacket structures, based on the 50-year significant wave height (H_{max}).
- The shaft thickness was estimated using the API formulation proposed in [3].
- Only the caisson volume was considered available for ballast filling, with the target of fully utilising this volume to achieve the minimum feasible design.
- The maximum slab diameter was limited to $40\,\mathrm{m}$, considering the available space within a floating dry dock that could potentially support such installation projects worldwide.
- The ballast volume fill factor was estimated at 73%, based on the detailed CAD design of the GBF, to account for the actual usable ballast volume.
- The ballast material was assumed to be sand with a density of $\rho_{sand} = 2000\ \mathrm{kg\,m^{-3}}$.

The application of the above assumptions and constraints results in only the slab diameter (D_2) and slab height (h_3) remaining as free parameters governing the foundation design. The output of the algorithm is a feasible design space mapping for the foundation under the pre-defined design conditions.

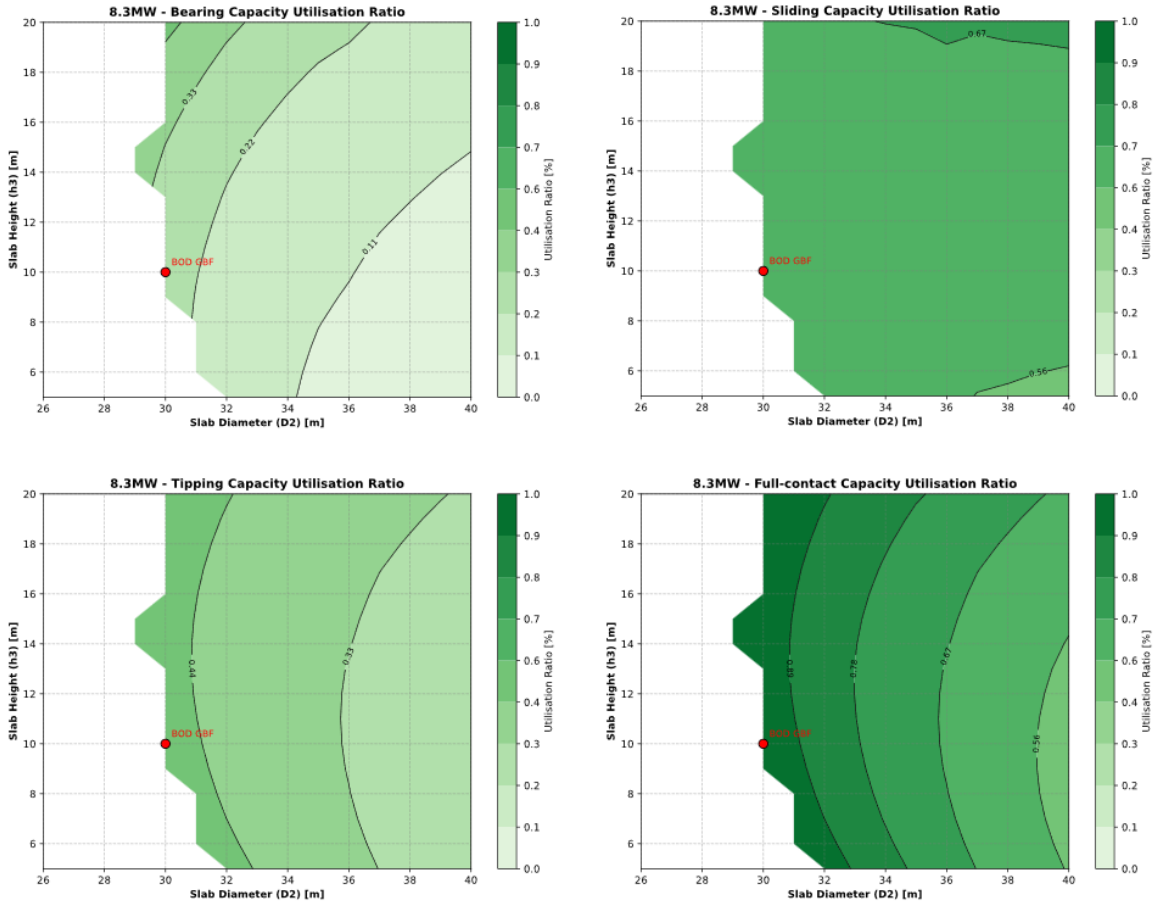

Figure 3.1: Feasible design mapping for the BOD GBF concept. Realised design marked red for validation.

3.3. Method Validation

The design algorithm was first evaluated using the realised BOD project foundation design. The corresponding capacity utilisation ratio maps were obtained, as presented in Figure 3.1. The actual design point is highlighted with a red marker in the maps, demonstrating that the design limits were closely approached in order to achieve a feasible solution with minimum mass and, consequently, reduced cost. The evaluation of the utilisation maps indicates that the full-contact utilisation ratio is the governing constraint limiting the feasible design space, with values close to unity.

Furthermore, the design obtained from the algorithm shows very close agreement with the realised BOD foundation in terms of structural mass, ballast mass, and total system mass when benchmarked against the available project data [33]. The comparison is presented in Table 3.3.

Quantity	Installed Design	Algorithm Design	Units	Diff.
Structural Mass	5600	5616	t	+2%
Ballast Mass	13660	14586	t	+7%
Total Mass	19160	20202	t	+5%

Table 3.3: Comparison between realised and algorithm-based GBF design mass properties

3.4. IEA 15 MW Foundation Design

The validated design algorithm was subsequently applied to a brute-force exploration of the complete design space for the up-scaled foundation. This was achieved by evaluating combinations of slab

diameters (D_2) and slab heights (h_3) within a predefined range.

Figure 3.2 presents the resulting feasible design maps for the $15\,\mathrm{MW}$ GBF under conditions consistent with those of the BOD project. In addition, designs that fell within a 2% deviation from the utilisation factors of the original BOD design were highlighted (red and blue markers). This criterion was introduced to identify solutions that closely replicated the original design behaviour, which was considered a reasonable engineering reference point. Among the shortlisted feasible solutions, only two designs simultaneously satisfied all examined utilisation criteria (blue markers). From these, the configuration with the lower total mass was selected, in line with standard engineering practice aiming to minimise material usage and overall cost.

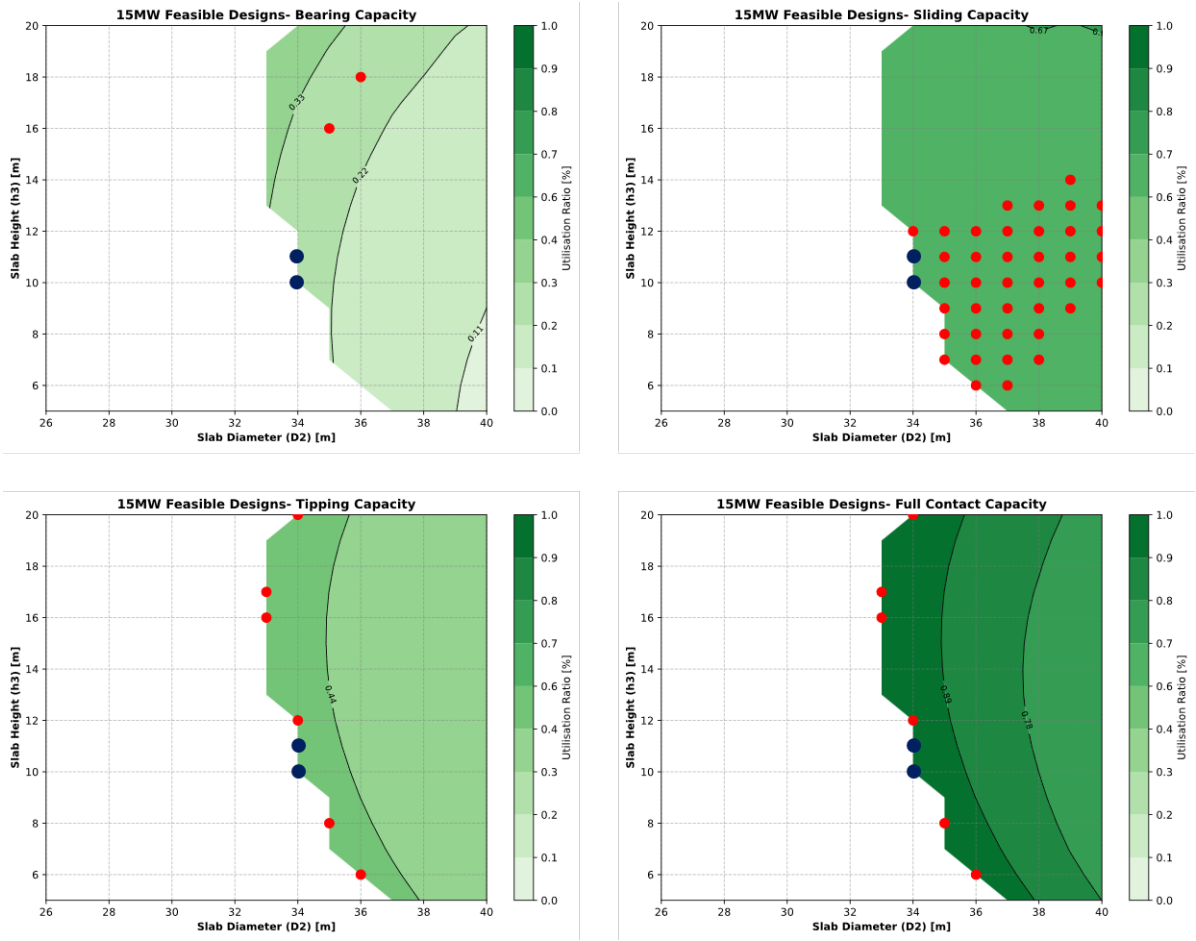

Figure 3.2: Feasible design mapping for the $15\,\mathrm{MW}$ GBF. Marked designs achieve similar utilisation criteria with the BOD reference design.

A comparison between the up-scaled and original designs is provided in Table 3.4. The results indicate that a mass increase of approximately 30% is required when scaling from an $8.3\,\mathrm{MW}$ to a $15\,\mathrm{MW}$ WTG. Notably, the slab height (h_3) remains unchanged, which is considered good practice to avoid increasing the exposure of larger structural elements to wave loading. Instead, the required capacity increase is achieved primarily through an increase in slab diameter (D_2) of 13.3%, ensuring sufficient stability and load-carrying capacity.

Figure 3.3 presents a comparison of the feasible design spaces for both the BOD and the $15\,\mathrm{MW}$ configurations in terms of total mass. It is observed that the selected designs in both cases operate close to full capacity utilisation while simultaneously maintaining a low total mass.

A schematic comparison between the original and up-scaled designs is presented in Figure 3.4, highlighting the main geometric differences.

Finally, the present design methodology is shown to be conservative when compared with the literature. Reference [45], reports a GBF mass of approximately $10\,000\,\mathrm{t}$, with $7500\,\mathrm{t}$ of ballast, for an

Table 3.4: Comparison of GBF design parameters between the Vestas 8.3 MW and IEA 15 MW configurations

Parameter	Symbol	Unit	8.3 MW	15 MW	Diff.
Bearing Capacity Utilisation	BC	%	0.27	0.27	-0.2%
Sliding Capacity Utilisation	SC	%	0.62	0.63	+1.4%
Tipping Capacity Utilisation	TC	%	0.48	0.49	+1.9%
Full-contact Capacity Utilisation	FC	%	0.97	0.98	+1.9%
Slab Height	h_3	m	10.0	10.0	–
Slab Diameter	D_2	m	30.0	34.0	+13.3%
Total Height	h_{total}	m	52.0	52.0	–
Structural Mass	m_{GBF}	t	5600	7300	+30.3%
Ballast Mass	m_{ballast}	t	14600	19100	+30.8%
Total Mass	m_{total}	t	20200	26300	+30.2%

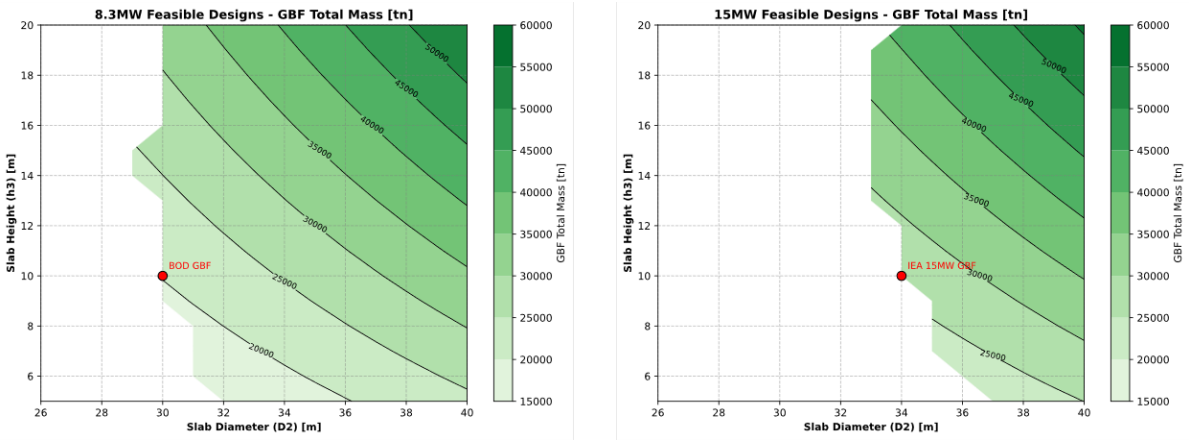

Figure 3.3: Comparison of feasible design total mass mappings for the BOD and 15 MW GBF configurations. Realised and up-scaled designs, respectively, are marked with red colour.

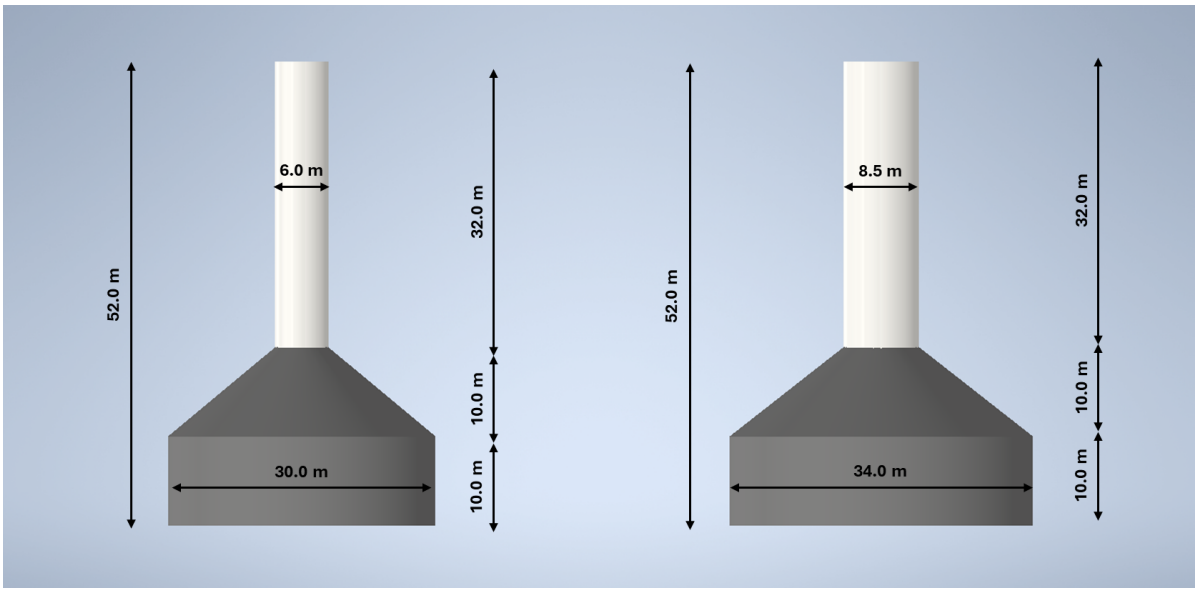

Figure 3.4: Main dimensions comparison between the original and up-scaled GBF designs.

IEA 15 MW WTG at 50 m water depth. However, it should be noted that foundation design is strongly dependent on site-specific conditions, which can significantly influence final design outcomes.

4

Simulation Model Development

4.1. Simulation Framework

Following the development of the up-scaled foundation design, a simulation framework is established to perform time-domain simulations of the installation method. The framework employs *OrcaWave* and *OrcaFlex*, both developed by *Orcina*. The hydrodynamic properties of the GBF are first computed in *OrcaWave* through a boundary element panel method, solving the linear potential flow problem in the frequency domain. The resulting hydrodynamic database is subsequently imported into *OrcaFlex*, where the coupled dynamic system is assembled and solved in the time domain. The model incorporates the tugboat spread moored to pre-laid anchors, replicating the actual installation set-up, as presented in Figure 4.1.

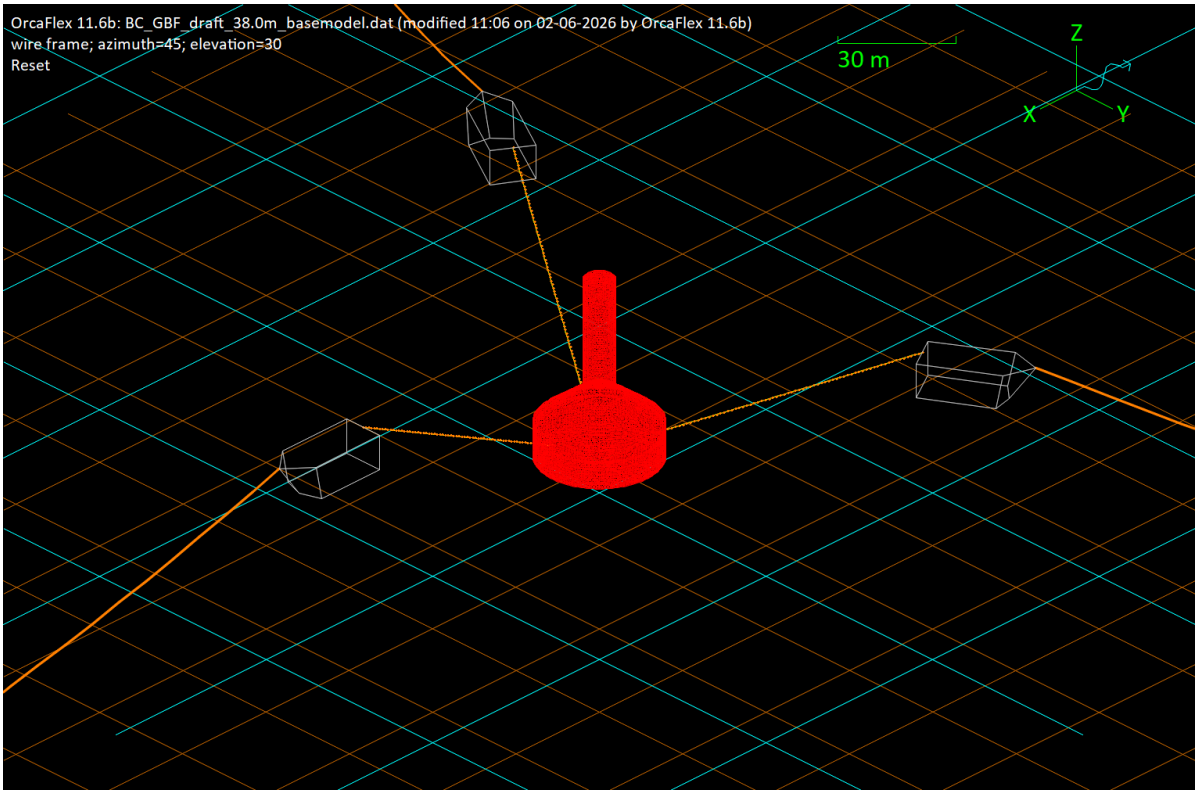

Figure 4.1: OrcaFlex multi-body time-domain simulation model.

A number of modelling considerations are examined prior to the main operability analyses, including the internal free-surface effect on floater stability, hydrodynamic mesh resolution, viscous damping tun-

ing, and second-order wave load modelling accuracy. Each of these is addressed later in this chapter.

4.1.1. Hydrodynamic Analysis

OrcaWave solves the potential flow problem through a boundary element panel method. The primary input is a meshed panel model of the structure, whose geometry and meshing parameters are fully parametrised and generated through a JavaScript-based script using *GeniE* software. Exploiting the double symmetry of the GBF, only one quarter of the geometry is modelled. The mesh is constructed such that the panel topology follows the relevant waterlines at each immersion sub-phase, as illustrated in Figure 4.2, and is subsequently imported into *OrcaWave*, as shown in Figure 4.3.

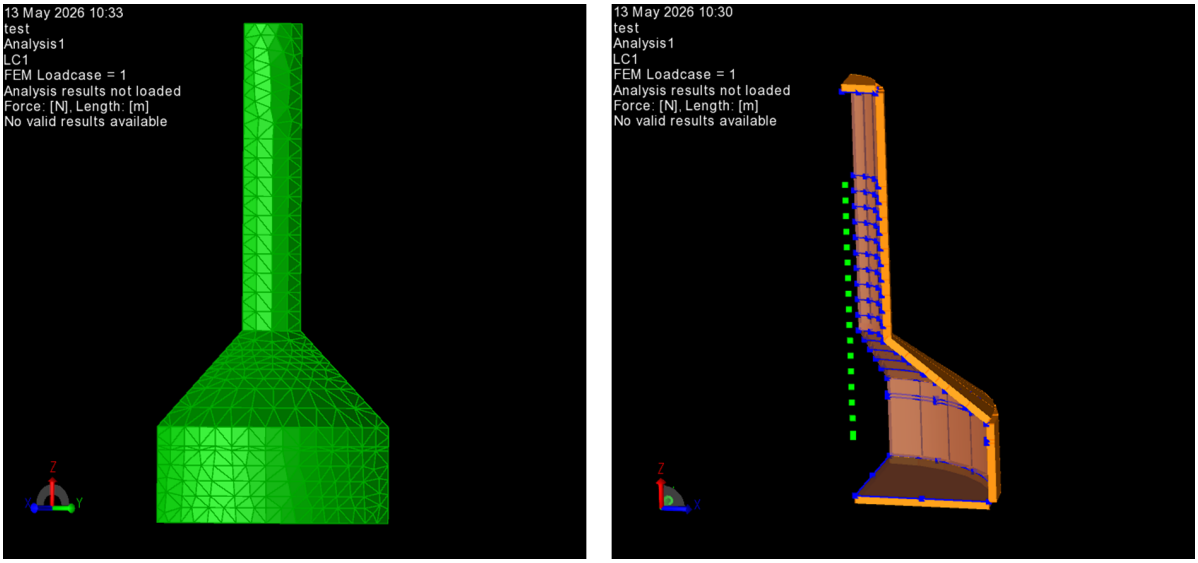

Figure 4.2: Parametrised meshing of the GBF model in *GeniE*, from DNV's *Sesam* suite [43].

The analysis provides the following outputs:

- Hydrostatic restoring matrix
- Added mass as a function of wave period
- Radiation damping as a function of wave period
- Displacement RAOs as a function of wave period
- Load RAOs as a function of wave period

The selection of an appropriate mesh resolution is examined in Section 4.3.2.

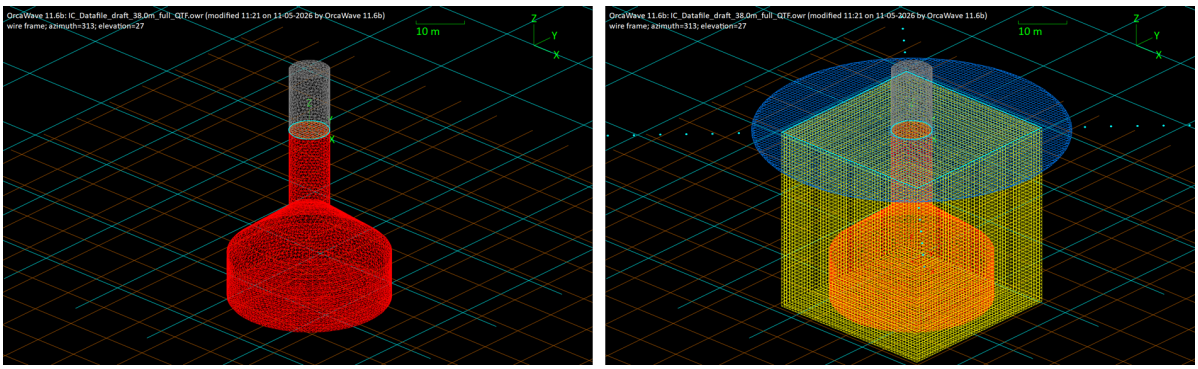

Figure 4.3: Meshed GBF geometry in the *OrcaWave* environment (left). Meshed surface area and control volume for QTF calculation (right).

4.1.2. Time-Domain Simulations

The *OrcaFlex* model represents the GBF as a six degree-of-freedom floating body, connected to a fleet of tugboats via towing lines, as shown in Figure 4.1. Environmental loading is applied through stochastic irregular wave realisations generated from a user-defined wave spectrum, capturing the combined effect of hydrodynamic loading, restoring forces, and environmental excitation under realistic installation conditions.

Numerical time integration is performed using a user-controlled time step and convergence scheme, with settings verified to ensure stability and independence from numerical discretisation. Model generation, batch simulations, and post-processing are fully automated through the *OrcaFlex* Python API, enabling efficient and repeatable parametric evaluation across the full range of environmental conditions and heading combinations considered in this study.

4.2. Simulation Model Assumptions

The following assumptions are adopted in the simulation framework. Each constitutes a deliberate simplification, whose implications are discussed where relevant.

- **Rigid body.** The GBF is modelled as a rigid body, neglecting structural deformations. This is standard practice for global hydrodynamic response analyses of offshore structures.
- **Wind and current loads.** Wind and current loads are excluded from the dynamic simulations. These environmental components are expected to contribute primarily to mean static offsets rather than dynamic excitation, which is the principal driver of operability in this study. Vortex-induced vibration (VIV) is considered negligible for the caisson, where the large diameter and low Keulegan-Carpenter (KC) number place the flow in the inertia-dominated regime; its potential relevance for the slender shaft element is not assessed.
- **Free-surface correction.** The free-surface correction (FSC) is accounted for in static stability calculations but neglected in dynamic analyses, in accordance with DNV-ST-N001 [16]. Its inclusion in the dynamic model would increase the effective roll period, yielding non-conservative response estimates. Analysis is further explained in Section 4.3.1.
- **Seabed proximity effects.** The hydrodynamic analysis is performed for the GBF in open-water conditions, neglecting the influence of seabed proximity on added mass and damping coefficients. This limitation is most significant near the landing phase, where proximity effects are expected to increase the vertical added mass coefficient and modify the heave response.
- **Hydrodynamic coupling.** No hydrodynamic interaction between the GBF and the tugboat fleet is modelled. The multi-body system is coupled exclusively through mechanical connections via towing lines, with vessel shielding and thruster-induced flow effects excluded.
- **Mooring stiffness.** The pre-laid anchor system is represented by a soft mooring configuration. A stiffer arrangement would better reflect the actual station-keeping capacity but risks generating numerically unrealistic snatch loads. The soft mooring approach provides physically plausible line responses while introducing a known limitation in positioning accuracy prediction.
- **Snapshot approach.** Simulations are performed at a fixed structural draft corresponding to the critical installation sub-phase, rather than modelling the continuous immersion process. The vertical descent velocity and the transient variation in hydrodynamic properties with draft are therefore not captured.

4.3. Modelling Considerations

4.3.1. Free-Surface Effect

In structures containing internal compartments that can be partially filled with liquid, the effect of a moving internal free surface must be considered in static stability calculations [13]. The so-called free-surface correction (FSC) reduces the stability of a floating body due to liquid motion within partially filled tanks. As the liquid shifts under external forces, it induces a heeling moment, effectively raising the centre of gravity (CoG) and reducing the metacentric height (GM).

The reduction in metacentric height due to the free-surface effect is given by Equation 4.1, where I is the second moment of area of the free surface and V is the displaced volume of the vessel. This formulation assumes equal densities between internal and external fluids. The corrected metacentric height (GM_{eff}) is then obtained from Equation 4.2.

$$FSC\ [m] = \frac{I\ [m^4]}{V\ [m^3]} \tag{4.1}$$

$$GM_{\text{eff}}\ [m] = GM\ [m] - FSC\ [m] \tag{4.2}$$

To mitigate this effect, standard practice in shipbuilding and floating structures is to subdivide internal volumes into multiple compartments, thereby reducing the impact of slack tanks. In the case of a floating GBF, modelling the internal volume as a single compartment leads to significant stability reduction, potentially resulting in instability ($GM_{\text{eff}} < 0$) across the full draft range during immersion. Subdividing the volume into compartments improves stability considerably.

Figure 4.4 illustrates the variation of metacentric height (GM) with structural draft for different configurations. The simplified case assumes solid ballast, resulting in no GM reduction, while the worst-case scenario considers a single compartment, leading to instability throughout immersion. More realistic cases divide the internal volume into multiple compartments, modelled as equivalent cylindrical tanks to approximate the second moment of area.

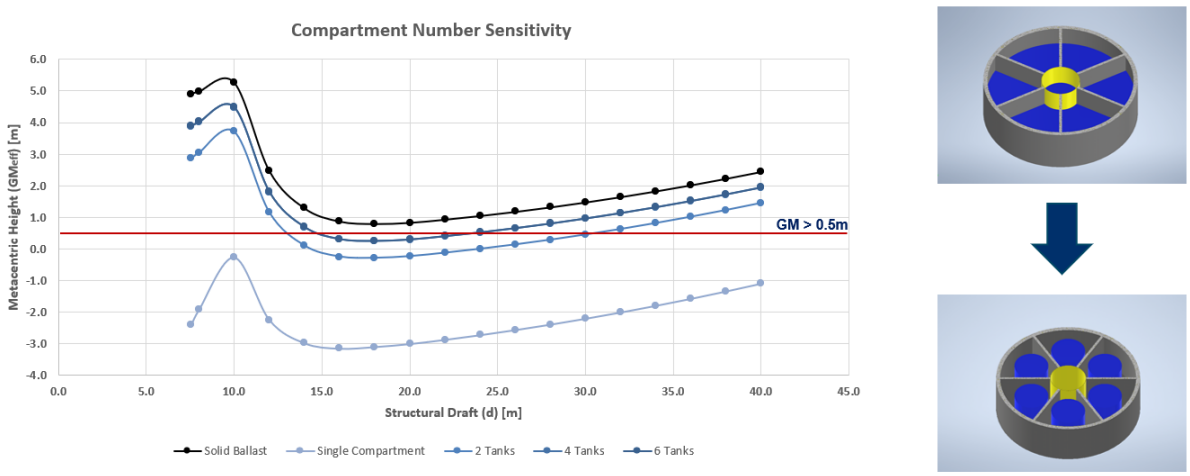

Figure 4.4: Evolution of metacentric height (GM) with draft for different compartment configurations.

As shown in Figure 4.4, the free-surface effect significantly reduces static stability. While the use of compartments improves stability, the benefit becomes marginal when increasing the number from four to six tanks. The six-tank configuration is selected to remain consistent with the original design while allowing flexibility in ballasting operations.

Despite this improvement, the selected configuration remains marginally stable during immersion, with critically low GM values in the draft range of 15–25 m. When applying the DNV guideline requirement of $GM_{\text{eff}} > 0.5$ m [15], the potentially critical draft range extends from 15 m to 25 m. For such conditions, DNV recommends that specific mitigation measures be defined in agreement with the Marine Warranty Service (MWS).

Finally, it is recommended that the free-surface effect, which reduces GM and increases the roll period of the floater, should only be included in dynamic motion analyses if its inclusion does not lead to non-conservative results [15]. In the present study, the free-surface effect is considered in static stability calculations, while it is neglected in dynamic analyses in accordance with this guideline.

4.3.2. Mesh Sensitivity

A mesh sensitivity analysis was performed to determine an appropriate panel size for modelling the structure. The initial panel size was selected based on expert judgement, following the industry rule of thumb given by Equation 4.3 for the relevant wavelength range.

$$L_{\text{panel}} \leq \frac{\lambda}{8} \tag{4.3}$$

Wavelength is obtained from the dispersion relation:

$$\lambda = \frac{gT^2}{2\pi} \tanh\left(\frac{2\pi d}{\lambda}\right) \tag{4.4}$$

Considering a representative range of sea state periods (3–30 s), commonly used in industry applications, and applying Equation 4.4 for a water depth of $d = 40\,\mathrm{m}$, the corresponding wavelength range is approximately $14\,\mathrm{m}$ to $1400\,\mathrm{m}$.

The limiting factor for mesh resolution is the minimum wavelength (λ_{min}), which results in a maximum allowable panel size of $1.75\,\mathrm{m}$. Based on this criterion, three different mesh sizes were evaluated in the diffraction analysis to determine an optimal discretisation for the study. In addition, local mesh refinement was applied near the waterline by prescribing a higher number of elements along selected edges. The investigated mesh configurations are shown in Figure 4.5.

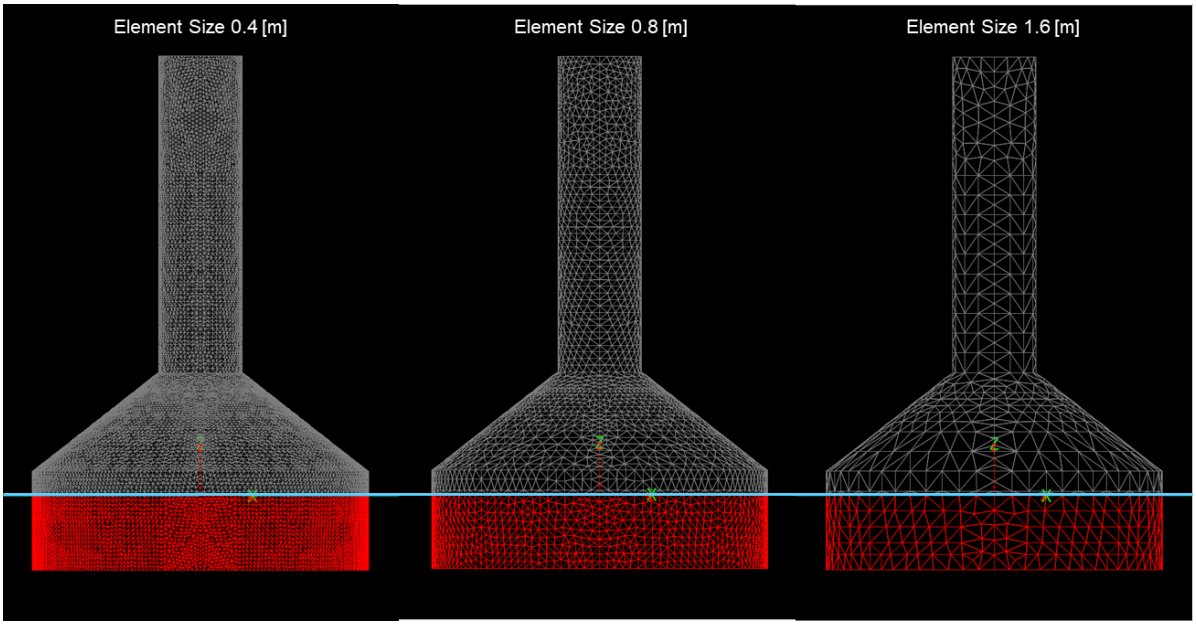

Figure 4.5: Mesh sensitivity study examined element sizes.

Figure 4.6 presents the hydrodynamic response obtained from the potential flow solver for the different mesh resolutions. Very good agreement is observed for surge and heave load Response Amplitude Operators (RAOs), reflecting the relatively simple geometry of the structure. For pitch motion, minor discrepancies appear around the peak response period, with the mid and fine meshes showing close agreement.

The corresponding computational times for the potential flow simulations are summarised in Table 4.1.

Mesh case	Element size [m]	Run-time
Fine	0.4	2 h 20 min
Mid-case	0.8	11.5 min
Coarse	1.6	0.5 min

Table 4.1: Mesh sensitivity study results.

Based on the trade-off between solution accuracy and computational cost, the mid-case mesh with an element size of $0.8\,\mathrm{m}$ was selected for the remainder of the study, as it provides near-identical accuracy to the fine mesh while maintaining significantly reduced simulation time.

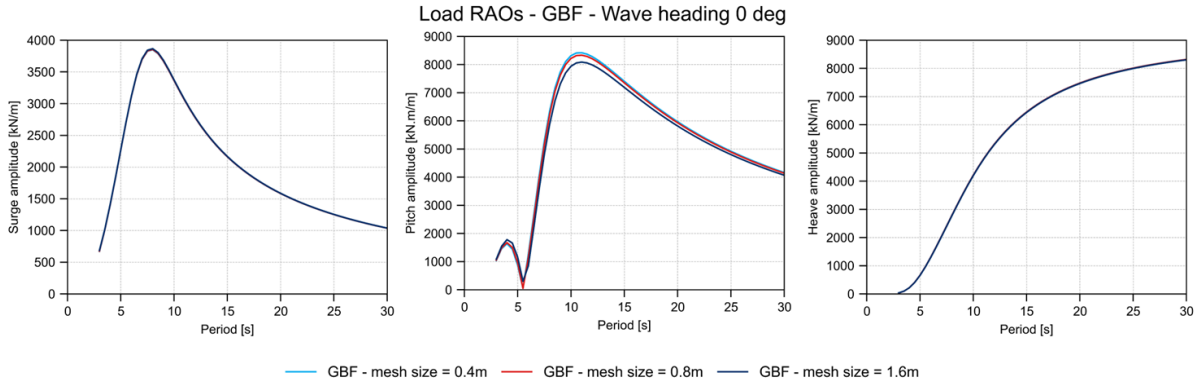

Figure 4.6: Load RAOs comparison for different mesh sizing.

4.3.3. Viscous Damping Tuning

Potential flow theory accounts only for radiation damping and does not capture viscous effects such as skin friction and vortex-induced drag forces acting on floating structures. Consequently, it tends to overpredict roll motions, as viscous phenomena can contribute significantly to the overall damping, particularly in roll and pitch. For this reason, the critical damping coefficient is commonly used as a practical reference to represent the combined damping effects.

Viscous damping is inherently nonlinear and depends on both motion frequency and amplitude. In practice, reliable estimation requires experimental data or Computational Fluid Dynamics (CFD) simulations. Since neither was available in the present study, a literature-based approach was adopted to tune the hydrodynamic model.

Due to the double-plane symmetry of the structure, identical viscous damping values were assumed for surge and sway, as well as for roll and pitch. Following the recommendations of [17], viscous damping was taken as 2% of the critical damping for heave, roll, and pitch, while 1% was used for surge and sway. Yaw damping was neglected, as the yaw response is expected to be of minor importance due to the structural symmetry.

The resulting damping values used in the simulations are presented in Table 4.2, while Figure 4.7 compares the damped and undamped RAOs.

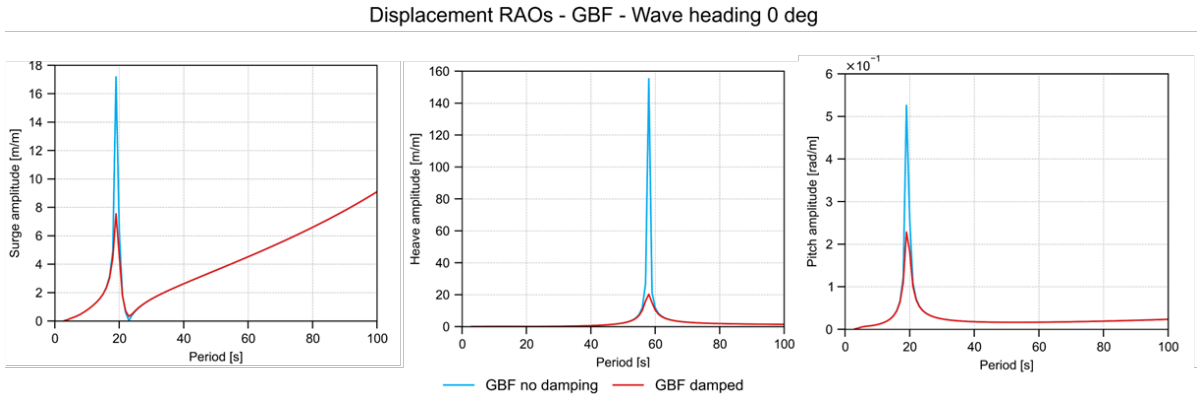

Figure 4.7: Comparison of damped and undamped RAOs

It should be noted that viscous damping was tuned at the natural frequency of each degree of freedom. Since damping coefficients are frequency dependent, a single value cannot represent the full frequency range. However, viscous effects are most important near resonance, where an accurate damping representation is critical. For small motion amplitudes, discrepancies in quadratic viscous damping have limited impact on the response. For higher sea states, larger deviations may occur, although these conditions are beyond the considered installation limits [17].

Table 4.2: Critical and viscous damping values for floater motions

Mode	Symbol	Critical	Viscous (% crit)	Viscous damping	Units
Surge	B_{11}	41.47	1%	0.41	kNs/m
Sway	B_{22}	41.47	1%	0.41	kNs/m
Heave	B_{33}	10545	2%	211	kNs/m
Pitch	B_{44}	3.54×10^6	2%	7.08×10^4	kNms/rad
Roll	B_{55}	3.54×10^6	2%	7.08×10^4	kNms/rad
Yaw	B_{66}	–	–	–	kNms/rad

4.3.4. Second-Order Wave Effects

When a floating structure is exposed to waves, it experiences wave loads that can be decomposed into first and second-order components. The first-order loads generate motions at the wave frequency and are modelled in OrcaFlex using RAOs to define either the vessel motions or wave loads. The second-order loads are generally smaller in magnitude. However they include low and high frequency components that can significantly influence the vessel response.

The low frequency second-order terms, commonly referred to as wave drift loads, can excite slow-drift motions when their frequencies are close to the natural frequencies of the structure. This is particularly important for moored systems, where the natural frequencies in surge, sway, and yaw are typically very low. In such cases, second-order drift loads may generate large low-frequency excursions.

The inclusion of second-order wave effects is normally performed through the calculation of Quadratic Transfer Functions (QTFs). However, including both difference and sum frequency effects significantly increases the computational cost and simulation time.

An alternative approach is Newman's approximation method, which attempts to balance computational efficiency and modelling accuracy. This method approximates the slow-varying drift loads directly from the mean wave drift loads, reducing the computational effort considerably since only first-order quantities are required.

In order to investigate the required modelling accuracy for the soft-moored GBF, a comparative study with different levels of second-order wave load modelling was performed. The full QTF diffraction problem was solved for the GBF in order to obtain the mean drift loads, presented in Figure 4.8.

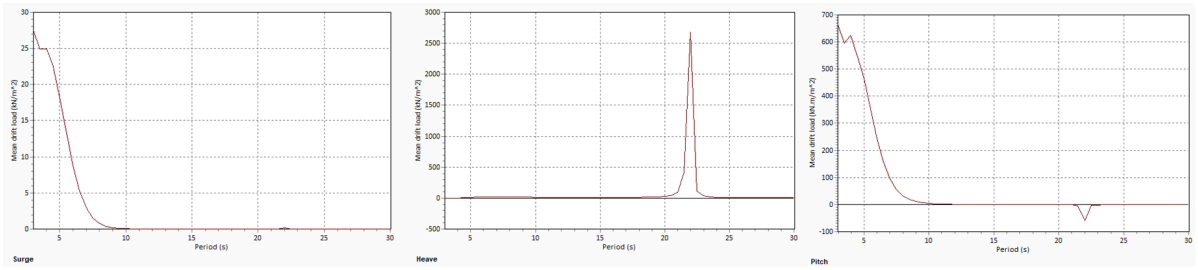

Figure 4.8: Mean wave drift loads obtained from the QTF diffraction analysis

The following modelling approaches were then simulated for two different sea states and their response statistics were compared:

- **QTF+sum:** Inclusion of both difference and sum frequency second-order effects.
- **QTF:** Inclusion of only difference frequency effects (wave drift loads).
- **Newman:** Simplified inclusion of second-order wave effects using Newman's approximation.
- **1st order:** Neglecting all second-order wave effects.

The QTF+sum case is considered the most accurate representation and is therefore used as the benchmark solution. The comparison of the resulting 3-hour Most Probable Extreme (MPE) responses for the degrees of freedom of interest is presented in Table 4.3.

From the comparison of the response statistics, it is observed that the QTF model reproduces the benchmark solution with excellent accuracy, while reducing the simulation time by approximately

Table 4.3: Comparison of simulation models for different sea states

Sea State: $H_s = 1$ **m,** $T_p = 6$ **s**								
Model	**Clock time [sec]**	**Diff.**	**Surge 3 h MPE [m]**	**Diff.**	**Heave 3 h MPE [m]**	**Diff.**	**Pitch 3 h MPE [°]**	**Diff.**
QTF+sum	2877	–	2.09	–	0.36	–	0.70	–
QTF	1720	-40%	2.10	0%	0.36	0%	0.70	0%
Newman	35	-99%	2.05	-2%	0.23	-38%	0.72	2%
1st order	25	-99%	0.78	-63%	0.15	-59%	0.33	-52%
Sea State: $H_s = 1$ **m,** $T_p = 12$ **s**								
Model	**Clock time [sec]**	**Diff.**	**Surge 3 h MPE [m]**	**Diff.**	**Heave 3 h MPE [m]**	**Diff.**	**Pitch 3 h MPE [°]**	**Diff.**
QTF+sum	3164	–	0.86	–	0.52	–	0.78	–
QTF	1960	-38%	0.86	0%	0.52	0%	0.78	0%
Newman	42	-99%	0.87	1%	0.41	-21%	0.55	-30%
1st order	26	-99%	2.22	158%	0.53	2%	0.50	-36%

40%. Newman's approximation, on the other hand, shows noticeable deviations in heave and pitch motions. This is consistent with the observations reported in [17], where Newman's approximation is shown to underestimate second-order wave loads in shallow water conditions and is mainly applicable to horizontal degrees of freedom.

Furthermore, neglecting second-order wave effects entirely leads to significant discrepancies in the predicted responses. Consequently, second-order wave loads were included in the present study using the QTF approach, while excluding sum frequency effects in order to achieve a balance between computational efficiency and modelling accuracy.

4.4. Tugboat Sensitivity Study

Tugboat selection was investigated to identify the most appropriate vessel type for the installation method. Tugboat selection is typically based on the required bollard pull (BP) needed to maintain operational control under the specified environmental conditions. In general, harbour tugboats (HT), with a BP of up to $80\,\mathrm{t}$, are preferred for installation operations due to their lower cost and wider availability. However, the desired installation accuracy imposes increased station-keeping requirements, which standard harbour tugboat capability alone may not satisfy. To address this, the use of pre-laid anchors in combination with harbour tugboats is recommended, as outlined in [15], and was selected as the most representative configuration to simulate. The key parameters of the selected tugboat type are summarised in Table 4.4, with hydrodynamic properties retained from an internal company library.

Table 4.4: Harbour tugboat technical specifications.

Parameter	**Value**	**Units**	**Notes**
Bollard pull	80	t	
LOA	50	m	
Displacement	9020	t	

4.4.1. Tow Configuration

Regarding the favourable tugboat fleet arrangement for installation, the star configuration was selected, employing three tugboats as illustrated in Figure 4.9. This configuration has been demonstrated in practice in the BOD project and keeps the number of vessels at a minimum, which is consistent with a typical project execution approach.

A sensitivity study was conducted to determine the optimal orientation of the tugboat arrangement relative to the predominant wave direction, as this can significantly affect the maximum loading and

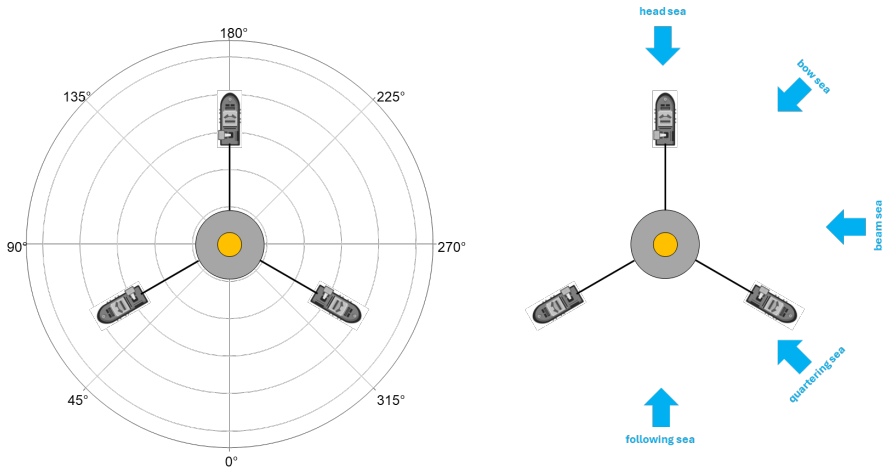

Figure 4.9: Installation spread arrangement and wave headings.

structural response, and consequently the overall operability of the method. Results of the directionality study are presented in Figure 4.10 for a range of wave periods, showing the heave motion of the structure and the maximum towing line tension in the form of most probable extreme (MPE) values from 3-hour simulations.

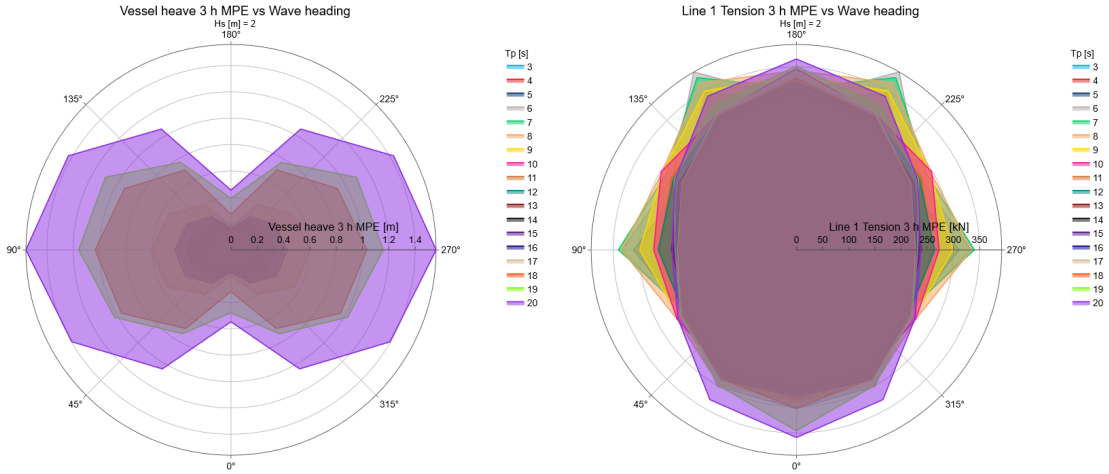

Figure 4.10: Heave (left) and line tension (right) 3 hour MPEs per wave heading.

It is observed that no single worst direction or wave period governs the response, as the structure behaves differently depending on the prevailing environmental conditions. For this reason, the investigation could not be reduced to a single wave direction and instead required examination of a range of headings, from head seas to following seas. However, the number of cases can be reduced by accounting for layout symmetries.

During installation, tugboats are moored to pre-laid anchors on the seabed to ensure sufficient holding capacity. The orientation of the pre-laid anchors can be engineered prior to installation to maximise the operability of the operation. Similarly, in the case of free-floating tugboats, the orientation of the installation spread relative to the wave heading can significantly affect overall operability.

4.4.2. Simulation Approach

An additional sensitivity study was carried out to determine the most appropriate approach for tugboat modelling. The study addressed two questions. First, does simulating the tugboats as fixed points yield response results comparable to modelling them as free-floating vessels with three degrees of

freedom (3-DOF)? Second, can the fixed-point approach be justified as a simplification that reduces computational effort?

Two model variants were compared: one in which the tugboats were simulated as fixed nodes, and one in which they were modelled as moored floating vessels with full hydrodynamic properties. Figure 4.11 presents a comparison of the results for two of the monitored response metrics, pitch motion and towing line tension. Table 4.5 provides a more detailed comparison between the two approaches for a specific wave condition.

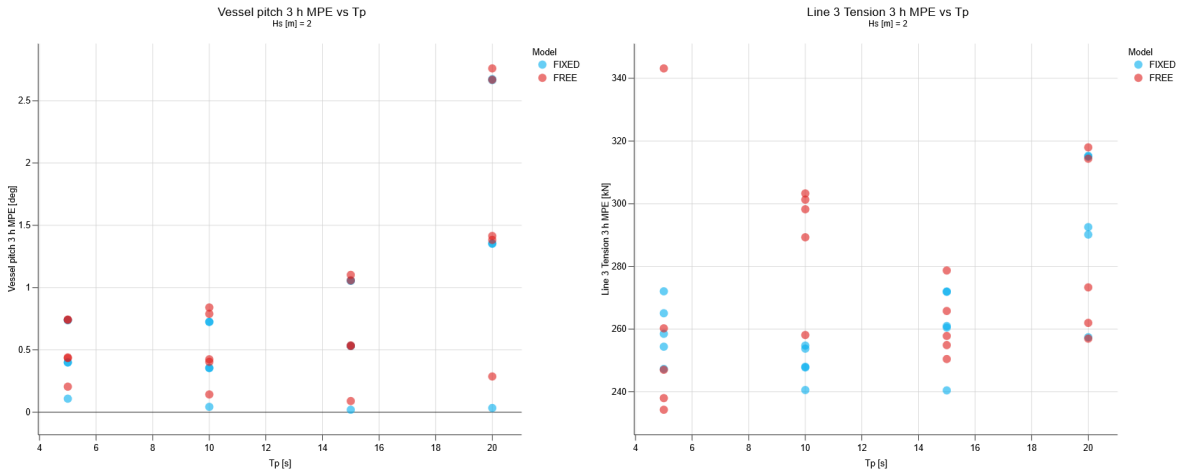

Figure 4.11: Comparison of GBF's pitch (left) and line tension (right) response for different tugboat simulation approaches.

Table 4.5: Comparison of 3-hour MPE responses for fixed and free tugboat modelling approaches ($H_s = 2$ m, $T_p = 15$ s, wave heading = 45°).

Model	**Clock time** [min]	**Surge** [m]	**Sway** [m]	**Heave** [m]	**Roll** [deg]	**Pitch** [deg]	**Yaw** [deg]	**Line 1** [kN]	**Line 2** [kN]	**Line 3** [kN]
Fixed	54.14	1.66	0.01	0.37	0.00	0.53	0.02	288.00	260.63	260.50
Free	61.23	2.39	1.13	0.33	0.10	0.53	1.44	274.68	247.49	278.70
Difference	+13%	+44%	–	−10%	–	0%	–	−5%	−5%	+7%

Modelling the tugboats as free-floating vessels generally resulted in higher system responses, indicating that neglecting their dynamics could lead to an overestimation of operability. Furthermore, as evident from Table 4.5, the fixed-node simplification produced near-zero structural responses in sway, roll, and yaw, which was considered physically unrealistic, while in parallel simulation time is only increased by 13 %. For these reasons, explicit modelling of the tugboats as moored floating vessels was deemed necessary to capture the actual dynamic behaviour of the system, and this approach was adopted for all subsequent simulations.

5

Workability Evaluation

5.1. Installation Operation

5.1.1. Ballasting

The up-scaled GBF for the IEA 15 MW WTG serves as the baseline design for the installation analysis presented in this chapter. Installation is achieved through controlled seawater ballasting, progressively increasing the structural draft until the foundation reaches the seabed. The process comprises two distinct phases, depicted in Figure 5.1:

- **Controlled lowering operation.** Seawater is used to ballast the structure and achieve seabed mating within the required installation accuracies (Figure 5.1, steps 1–4).
- **Design ballast installation.** Sand ballast is installed (Figure 5.1, step 5) to achieve the operational dead weight required for the in-place GBF to support the WTG.

The two phases are distinct and need not be performed consecutively, provided that the water-ballasted GBF can be demonstrated to maintain position under the expected sea states. This creates an intermediate phase (Figure 5.1, step 4) in which the foundation rests on the seabed but is not yet ready to support the WTG. Recommended practice is to continue water ballasting beyond seabed mating, filling the compartments to capacity to maximise the dead weight available during this intermediate phase and thereby increase the safety margin against environmental loading. The controlled lowering operation is considered the most critical phase of the installation process and is therefore the primary focus of the subsequent analysis.

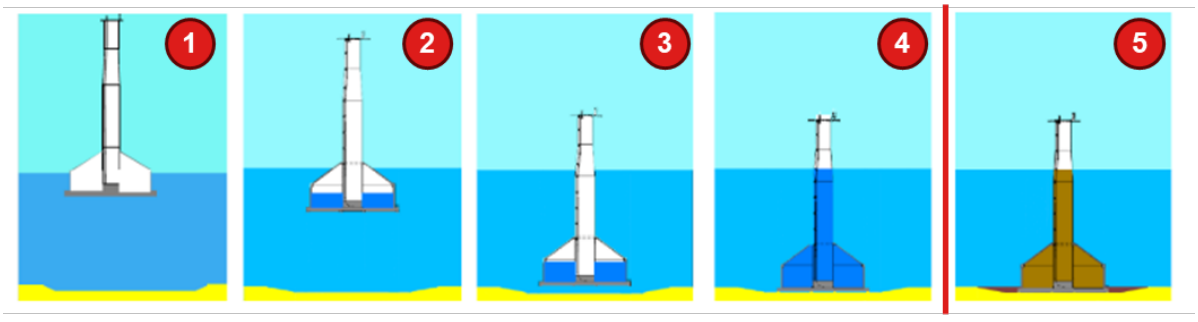

Figure 5.1: Sub-phases of the GBF ballasting operation [32].

The ballasting system is sized to satisfy the DNV-ST-N001 requirement that the ballast tank can be fully filled or emptied within $4\,\mathrm{hrs}$ for an unmanned tow [15]. The system must additionally provide precise ballast control to allow repeated mating attempts if the required positioning accuracy is not achieved on the first attempt. Subject to these requirements and the constraints imposed by the maximum manifold diameter and pumping velocity, a configuration of four pumps is found to satisfy the specified criteria. The adopted system parameters are presented in Table 5.1.

Parameter	Value	Units	Notes
Touchdown ballast	7500	t	Achieved at step 3
Maximum ballast	12900	t	Achieved at step 4
Number of pumps	4	–	Assumption
Pump capacity	1000	m^3/hr	Project data
Manifold diameter	0.4	m	Project data
Pumping velocity	3.0	m/s	Assumption

Table 5.1: Ballasting system parameters.

Figure 5.2 presents the evolution of structural draft over time during the controlled lowering phase at full pumping capacity. Seabed mating is achieved within approximately $2\,\mathrm{hrs}$, after which an additional $1.5\,\mathrm{hrs}$ is required to fill the ballast compartments to capacity, giving a total operation duration of approximately $3.5\,\mathrm{hrs}$. The initial immersion phase is relatively slow, with the first $10\,\mathrm{m}$ of draft requiring approximately $1.5\,\mathrm{hrs}$. This is followed by a rapid descent from $20\,\mathrm{m}$ to $40\,\mathrm{m}$ draft in under $20\,\mathrm{min}$, which requires careful operational control and likely a reduction in pumping capacity over this sub-phase.

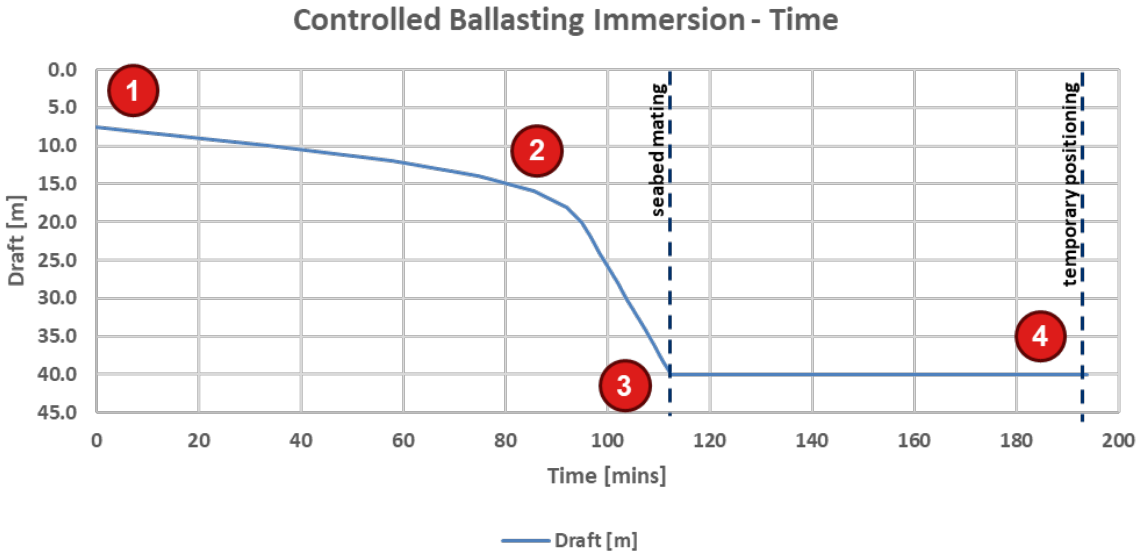

Figure 5.2: Evolution of structural draft during controlled ballasting immersion.

Ballasting, for both water and sand phases, is carried out using a specialised vessel or barge equipped with integrated storage, mixing, pumping, and monitoring systems. The pumping capacity of such vessels can be readily scaled to the project requirements, making the system parameters adopted here directly adjustable to support a faster or slower immersion rate.

5.1.2. Stability

Monitoring the structure's static stability during immersion is essential to ensure a safe and controlled installation. Figure 5.3 presents the evolution of the metacentric height (GM) of the baseline configuration. The GM is the primary measure of a floating structure's initial static stability.

The GM evolves non-monotonically, driven by the continuously changing mass and hydrostatic properties of the structure. It decreases sharply during the early immersion sub-phases. A minimum occurs in the 15–25 m draft range, after which the GM recovers. Within this range the available GM reserve is markedly reduced, yet it remains above the DNV minimum of $GM > 0.5$ m [15]. The initial and final installation sub-phases retain a sufficient stability margin, well clear of this limit.

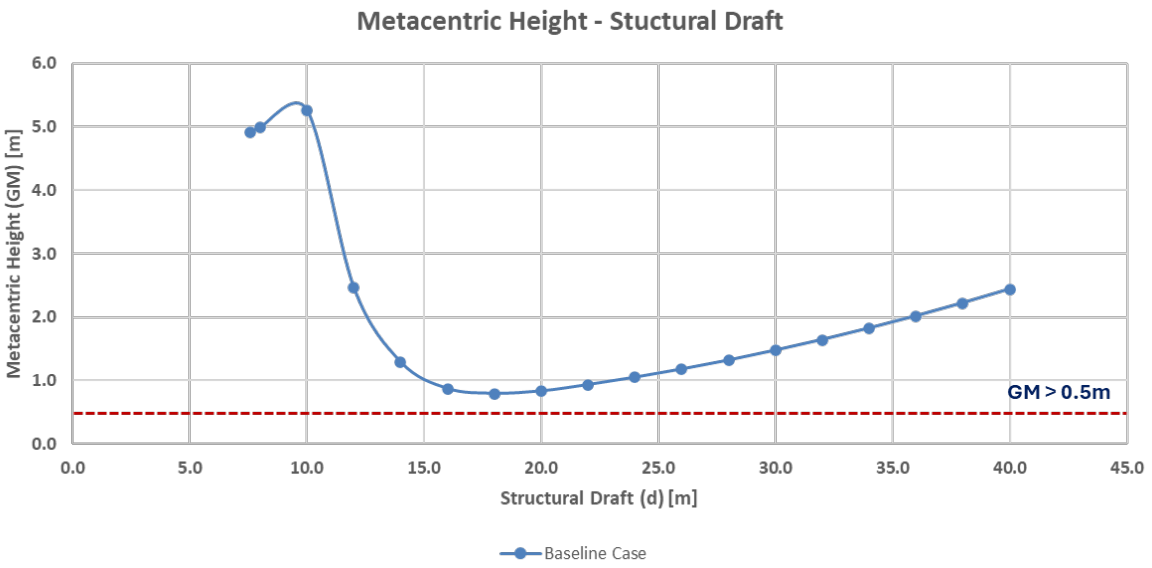

Figure 5.3: Evolution of the metacentric height (GM) with structural draft for the baseline case during immersion.

5.2. Critical Installation Sub-phases

The analysis of the installation sequence and of the structural behaviour during immersion reveals the operation's main bottlenecks. Two sub-phases pose the highest risk of reducing the overall workability:

1. **Station-keeping**, when the foundation arrives at its installation location and holds position. This sub-phase is important for two reasons. First, it is almost 80% of the immersion duration, lasting $1.5\,\mathrm{hrs}$. Second, station-keeping sub-phase duration may grow substantially when waiting for appropriate conditions for immersion, directly impacting the achievable workability.
2. **Landing**, when the structure floats in close proximity to the seabed but has not yet touched down. Stricter operational criteria apply, since the structure risks seabed collision and must achieve the targeted installation accuracy. The structural response is also excited by the wave spectrum at this draft. This sub-phase is therefore expected to yield the lowest operability.

The simulation consequently focuses on two representative drafts, 10 m for station-keeping and 38 m for landing, and evaluates the structural response to establish the operability of each sub-phase. The two examined drafts are summarised in Table 5.2. The assessment targets the dynamic response, while for the static stability only mitigation measures are proposed. The corresponding model set-ups are presented in Figure 5.4.

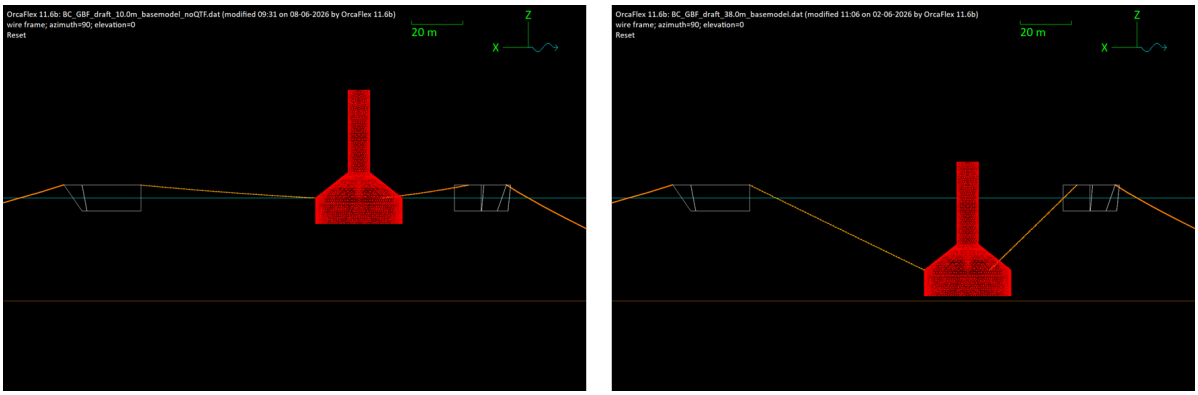

Figure 5.4: OrcaFlex simulation model set-ups for the two critical installation sub-phases: station-keeping at 10 m draft and landing at 38 m draft (2 m seabed clearance).

Table 5.2: Installation sub-phases and corresponding structural drafts examined in the workability evaluation.

Sub-phase	Draft d [m]
Station-keeping	10
Landing	38

5.3. Operability Criteria

The operability of the method is evaluated against a set of response-based criteria, as discussed earlier in this report. Different criteria constrain the two sub-phases of focus, reflecting their distinct governing responses. To monitor these criteria, a set of points of interest (POIs) is defined on the model. POIs 1–4 are located at the base of the foundation, where the seabed clearance and the touchdown velocity are evaluated, while the global position, heading, and inclination are referred to the centre of gravity (CoG). The towing points mark the connections to the three tugboats, where the line tensions are tracked. The complete arrangement is shown in Figure 5.5.

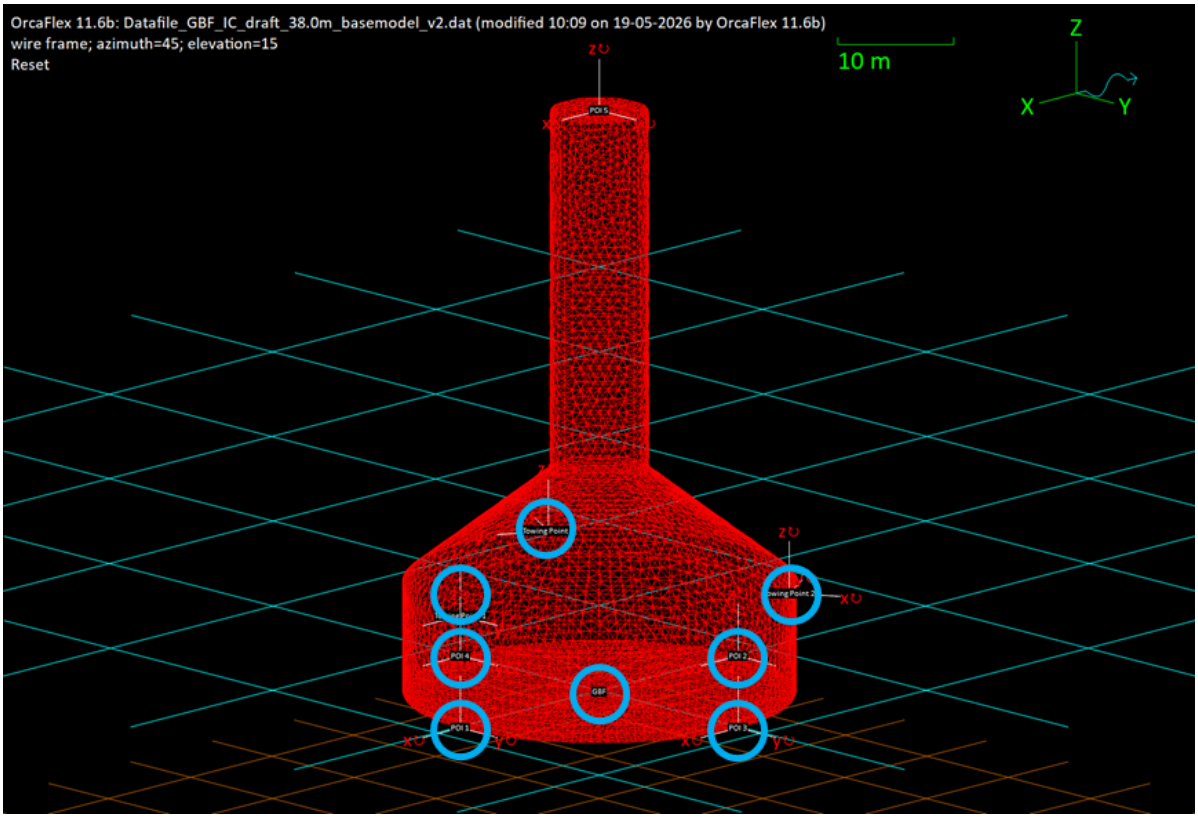

Figure 5.5: Points of interest (POIs) and towing points defined on the GBF model for monitoring the operability criteria.

Station-Keeping

In this sub-phase the structure floats at a shallow draft, held on station while it waits for the controlled lowering to begin. The governing criteria derive from marine-operation standards and equipment limits, and are listed in Table 5.3. The inclination limit caps the heel of the floating structure, while the line-tension limit keeps the towing lines within half of their breaking load, as per DNV [16]. The selected towing lines for the model have MBL = $1700\,\mathrm{kN}$, thus the limit was set accordingly.

Landing

In this sub-phase the structure floats approximately 2 m above the seabed, immediately before touch-down. The seabed proximity and the required placement accuracy activate the full set of criteria, which

Table 5.3: Operability criteria for the station-keeping sub-phase of the F&S method.

No.	Criterion	POI(s)	Limit	Note
1	GBF inclination	CoG	$< \pm 5°$	Maximum allowable heel/trim
2	Line tension	Towing points	< 850 kN	MBL/2

are listed in Table 5.4. Position and heading accuracy ensure correct placement. The seabed clearance prevents premature impact, the landing velocity limits the touchdown load, and the line-tension limit safeguards the towing lines.

Table 5.4: Operability criteria for the landing sub-phase of the F&S method.

No.	Criterion	POI(s)	Limit	Note
1	Position accuracy	CoG	$< \pm 2$ m	Targeted positioning accuracy
2	Heading accuracy	CoG	$< \pm 5°$	Targeted heading accuracy
3	Seabed clearance	POI 1–4	> 0 m	Avoid seabed impact
4	Landing velocity	POI 1–4	< 0.3 m/s	Structural integrity
5	Line tension	Towing points	< 850 kN	MBL/2

5.4. Baseline Operability

The operability is evaluated from the criteria established above and from a set of 3-hour simulations spanning the design matrix of sea states given in Table 5.5.

Table 5.5: Design matrix of sea states used for the baseline operability evaluation.

Parameter	Symbol	Range	Step	Units
Significant wave height	H_s	0.5–2.5	0.5	m
Peak period	T_p	2–20	1	s
Wave heading	WH	0–180	45	deg

For the wave heading, the worst case of each H_s–T_p pair is retained for the operability evaluation, which reduces the number of variables. This choice rests on two reasons. First, the pre-laid anchors are selected *a priori* and cannot be repositioned during the operation. Second, the wave direction changes more frequently than the H_s–T_p condition, so the tugboat arrangement faces several wave headings within a typical 3-hour sea state.

The workability evaluation focuses on the two sub-phases that govern the operability of the installation: station-keeping and landing. Each sub-phase is represented by a single characteristic draft, at which the structural response is simulated. Station-keeping corresponds to the floating draft maintained before controlled immersion. Landing corresponds to the near-seabed draft just before mating, which leaves a 2 m clearance above the 40 m-deep seabed.

5.4.1. Station-Keeping

Figure 5.6 presents the operability envelope of the station-keeping sub-phase under the criteria governing this sub-phase. The operability collapses for sea states with $T_p > 8$ s. This reduction is driven primarily by the maximum-inclination criterion and is followed by the line-tension criterion. The behaviour stems from system resonance, as the roll natural period ($T_{\text{roll}} = 12.5$ s) lies within the wave spectrum, which strongly reduces the operable envelope of this sub-phase.

5.4.2. Landing

For the landing sub-phase, the set of operability criteria is larger, owing to the seabed proximity. Figure 5.7 presents the corresponding operability envelope. Different sets of criteria limit the operability

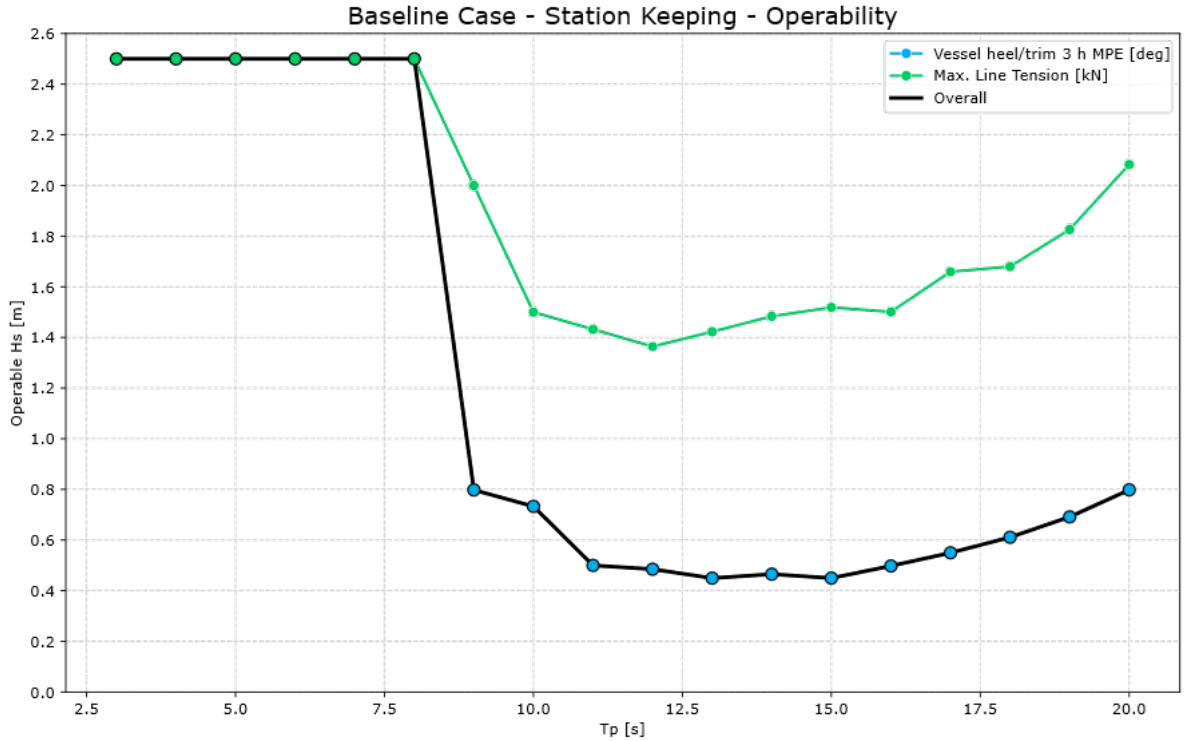

Figure 5.6: Operability envelope of the baseline case (BC) for the station-keeping sub-phase.

across different sea-state ranges. The wind-sea range ($3 < T_p < 12$ s) is governed by the positioning-accuracy criteria, mainly location and then heading. The swell range ($12 < T_p < 20$ s) is governed by the maximum-velocity and minimum-clearance criteria.

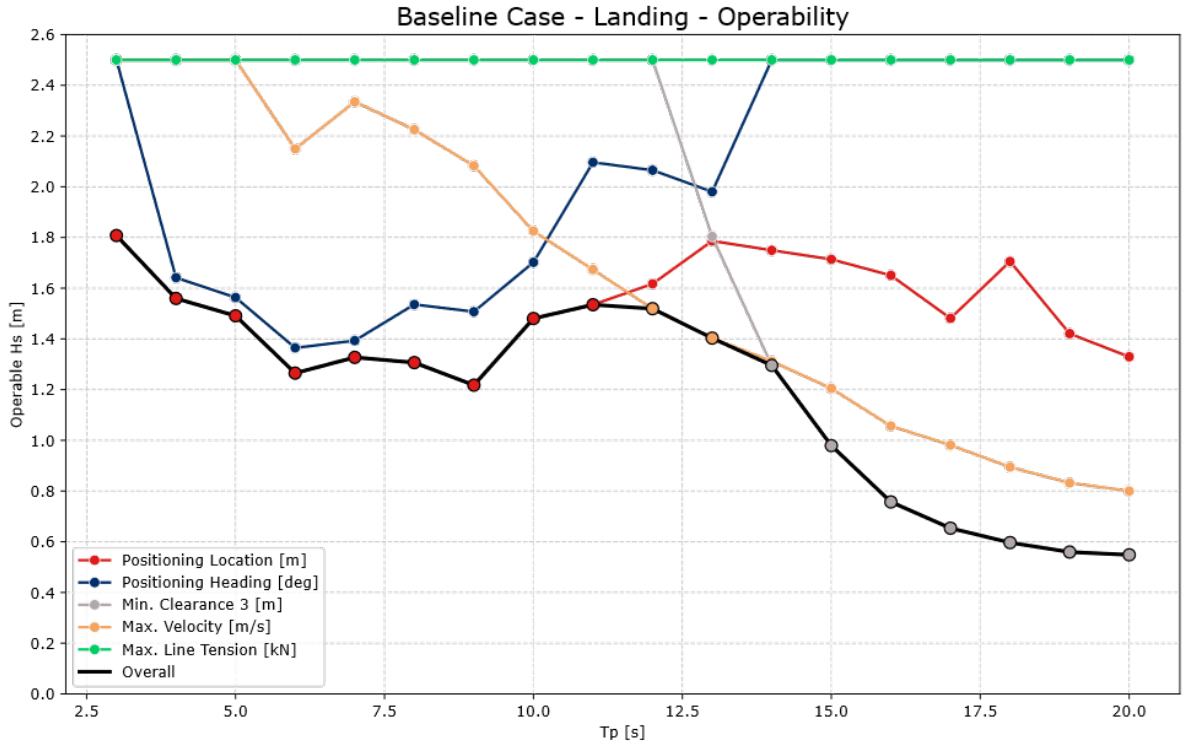

Figure 5.7: Operability envelope of the baseline case (BC) for the landing sub-phase.

5.5. Environmental Conditions

To evaluate the workability of the installation method, a suitable location was selected to provide representative metocean data for benchmarking against the operability criteria. The Noirmoutier offshore wind farm, in the Bay of Biscay, France, was selected as a potential deployment site for the GBF concept (Figure 5.8). Its challenging soil conditions could favour GBFs over monopiles.

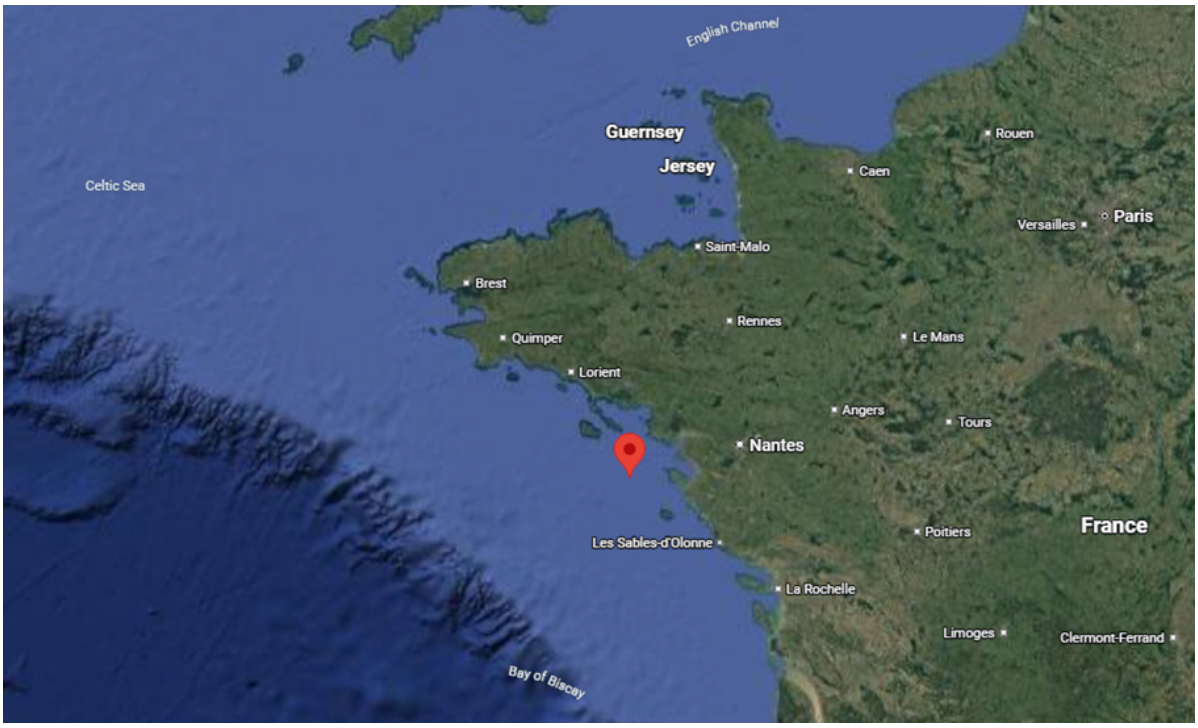

Figure 5.8: Selected location for workability evaluation in the Bay of Biscay.

Wave scatter data were extracted for the location using the Wave Climate database [42] and are presented in Figure 5.9. These data were subsequently used to evaluate the workability of the installation method and to quantify the improvements proposed later in this study. The wave climate contains distinct wind-sea and swell sea states, being representative for evaluation under both conditions.

5.6. Baseline Workability

Workability represents the environmental component of operability. It is defined as the fraction of time during which the environmental conditions at the site remain within the operational limits of the system, so that the operation is executed safely. It is quantified through the Operability Robustness Index (ORI), the ratio of operable to total sea states in the scatter diagram, evaluated at the industry-standard 3-hour resolution. A distinction is drawn between total and conditional workability. The total workability normalises the operable sea states over the whole scatter diagram. The conditional workability normalises them only over the sea states that lie within the harbour-tugboat operational limit ($H_s \leq 3.0$ m), and thus isolates the limitation of the installation system from that imposed by the tugboats. Benchmarking the operability envelopes of the two phases against the H_s–T_p scatter diagram of the selected site (Figure 5.9) yields the values summarised in Table 5.6. Workability scatters for both station-keeping and landing sub-phases are shown in Figure D.1 and Figure D.2 in Appendix D.

Table 5.6: Baseline case total and conditional workability of the two installation phases at the selected site.

Installation phase	Overall Workability [%]	Conditional Workability [%]
Station-keeping	24.4	29.5
Landing	37.7	45.7

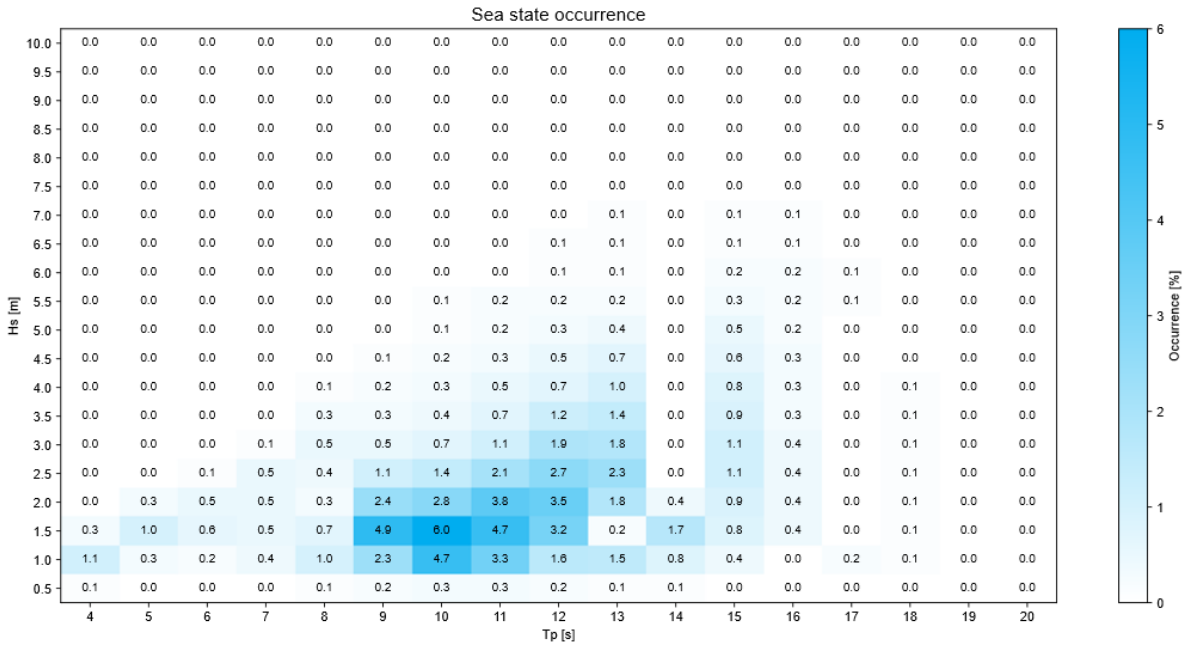

Figure 5.9: Sea-state ($H_s - T_p$) occurrence scatter diagram of the selected location.

Both the total and the conditional workability remain low for the two phases, which underlines the need for improvement. The station-keeping phase is the less workable of the two, despite being constrained by fewer criteria. This counter-intuitive result is driven by resonance: the roll natural period ($T_{\text{roll}} = 12.5$ s) renders the system inoperable around $T_p \approx 12$–14 s, removing many of the most frequently occurring sea states at the site from the operable set. The landing phase, by contrast, remains operable over a broader period range, and therefore captures a larger share of the site's sea states.

6

Workability Improvement

6.1. Operability Improvement Methods

The ultimate goal of this work is to improve the overall workability of the installation method. The baseline evaluation presented in the previous chapter revealed that the two governing sub-phases are limited by distinct response groups: the station-keeping sub-phase is constrained primarily by the resonant amplification of the vertical motions (heave, roll and pitch), whereas the landing sub-phase is constrained by the positioning accuracy, which is governed by the horizontal motions (surge, sway and yaw). Any effective improvement must therefore act on one, or both, of these response groups. To this end, three concepts were initially considered as potential means of enlarging the operational envelope of the Float-out & Submerge (F&S) method, each acting through a different physical mechanism, as presented in Figure 6.1. All three aim to improve the response of the tugboat-structure system. More specifically:

- **Smart ballasting.** This approach retains the outer dimensions of the structure (and thus its hydrodynamic behaviour) while modifying its internal layout to accommodate separate ballast compartments. By controlling the sequence in which these compartments are flooded, the inertial properties (and hence the natural periods) of the structure can be manipulated, thereby targeting the vertical response that governs the station-keeping sub-phase.
- **Mooring configuration.** This approach modifies the arrangement and stiffness of the mooring and towing lines connecting the structure to the tugboat spread, without altering the foundation itself. By increasing the horizontal restoring stiffness of the system, the surge, sway and yaw motions are constrained, thereby improving the positioning and heading accuracy that governs the landing sub-phase. A bridle arrangement is investigated as the specific realisation of this concept later in this chapter.
- **Flotation aids.** This concept involves the use of external floating aids to increase the buoyancy and static stability of the structure, which simultaneously shifts its natural periods further from the wave-energy range. Such devices must be compatible with both the transportation phase and the controlled immersion of the structure at the installation site. At this scale, this could be realised by means of a reusable lattice steel structure, a concept that has been successfully employed in previous T&I operations.

All three concepts were evaluated in terms of feasibility and expected improvement potential, and two were selected for further investigation: smart ballasting and a modified mooring configuration. They were preferred as the most practical and cost-effective options, requiring no additional equipment or specialised vessels. The smart-ballasting modifications are limited to the internal compartmentalisation and can be incorporated during fabrication, while the mooring modification relies entirely on the existing towing and anchoring infrastructure. Equally important, the two approaches are complementary. Smart ballasting targets the vertical response that limits the station-keeping sub-phase, by shifting the natural periods of the structure away from the dominant wave-energy range, thereby reducing excitation and the resulting dynamic response. The mooring configuration targets the horizontal response that limits

the landing sub-phase, by increasing the positioning stiffness of the system. The flotation-aid concept was not pursued at this stage, as it would introduce additional equipment, greater operational complexity and increased wave exposure; it nevertheless remains a promising direction and is revisited among the recommendations of this work. The smart-ballasting approach is examined first, followed by the mooring configuration.

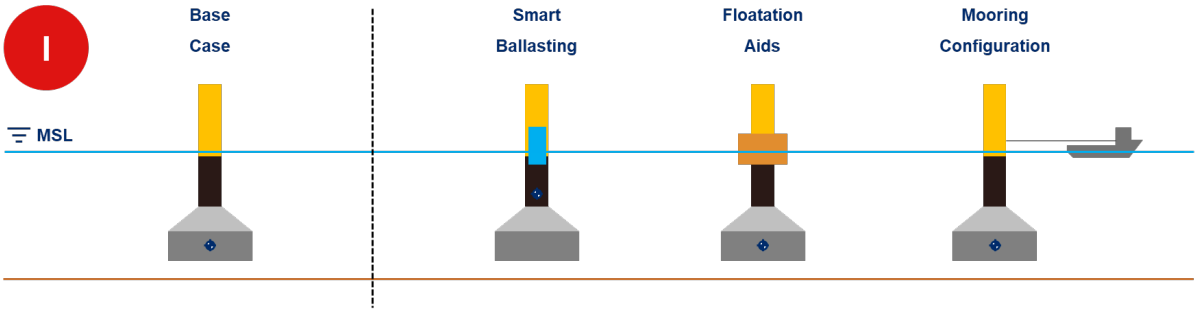

Figure 6.1: Installation operability improvement concepts.

6.2. Smart Ballasting

6.2.1. Smart-Ballasted Design

To enable smart ballasting during installation, an additional tank is incorporated in the upper section of the structure. This requires modifying the internal layout to accommodate both the tank and the associated piping for the controlled ballasting operation. Figure 6.2 illustrates the updated design configuration, while Table 6.1 presents the main dimensions. This design is hereafter referred to as the smart-ballasted (SB) case, compared to the baseline case (BC) design, without the additional ballast tank.

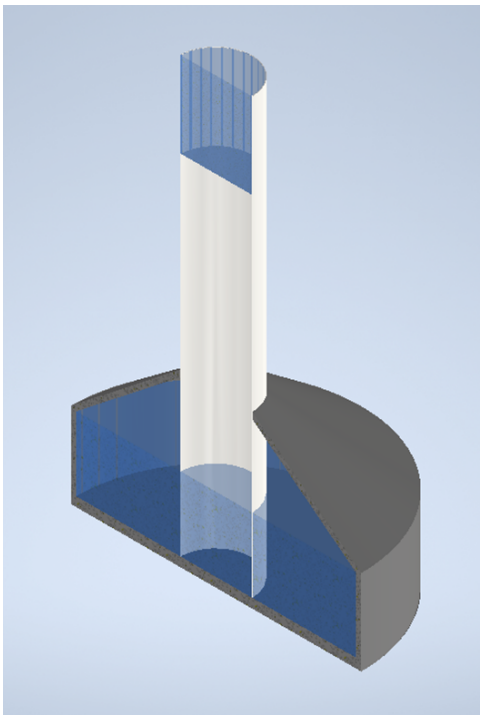

Figure 6.2: Cross-section of the smart-ballasted (SB) GBF design, showing the upper ballast tank configuration.

As established in the ballasting operation analysis presented earlier, the total ballasting time remains unchanged, since the total ballast volume required to achieve the target draft remains unchanged. In

addition, based on the maximum pumping capacity of the adopted system, the tank can be filled or emptied in under 5 minutes, providing considerable operational flexibility.

Table 6.1: Ballast tank design parameters.

Parameter	Value	Unit
Diameter	8.32	m
Height	5.00	m
Ballast water mass	280	t
Fill/empty time	250	s

6.2.2. Static Stability

Continuous ballasting during the installation phase causes the hydrostatic properties of the structure to vary with draft, as presented earlier for the baseline case (BC) design. DNV recommends a metacentric height above 0.5 m ($GM > 0.5$ m) for similar marine operations [16]. Figure 6.3 illustrates the evolution of GM with draft for both designs.

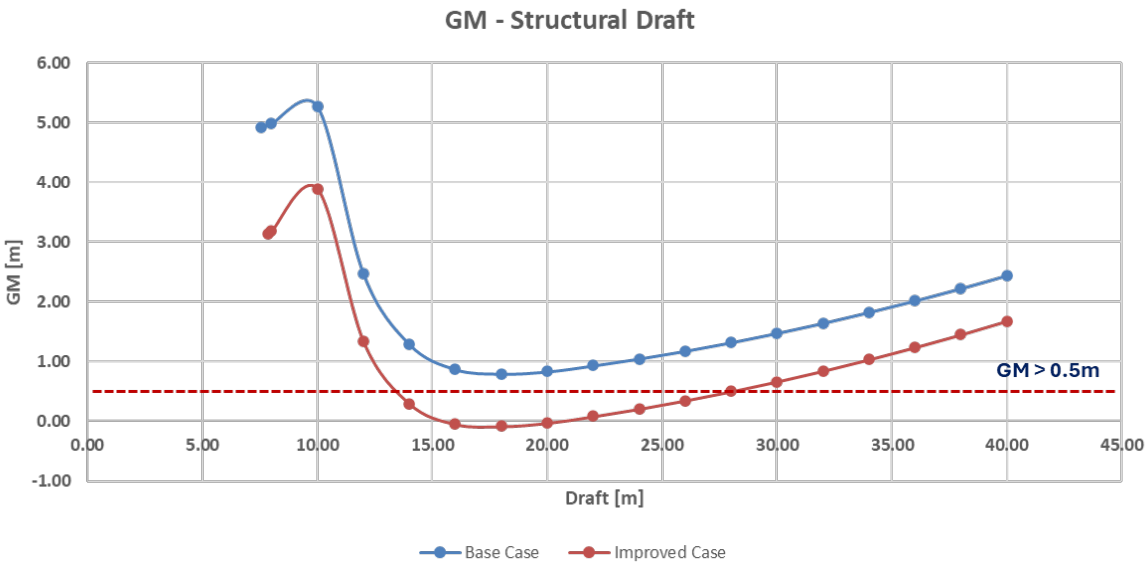

Figure 6.3: Comparison of the evolution of GM with structural draft for base (BC) and smart-ballasted (SB) GBF designs.

The criterion is satisfied by the BC throughout the entire immersion process. The SB, in contrast, exhibits a range of instability during immersion, between 15 m and 20 m draft, which is acknowledged by DNV for this type of operation [16]. A wider draft range, from 13 m to 28 m, falls below the DNV threshold of $GM > 0.5$ m. The assessment accounts for free surface correction (FSC) effects, as discussed in Section 4.3.1.

6.2.3. Hydrodynamic Analysis and Natural Period

Together with the hydrostatic properties, the hydrodynamic properties of the GBF also evolve continuously during immersion, driven by the changing submerged volume and geometry of the structure. The roll natural period is monitored, as it is the main parameter affected by the smart-ballasting approach. Owing to the double plane of symmetry of the structure, the roll and pitch natural periods are identical. The roll period is given by Equation 6.1.

$$T_{\text{roll}} = 2\pi \sqrt{\frac{I_{44} + A_{44}}{\rho_w \, g \, GM}} \tag{6.1}$$

The resulting roll natural period is presented in Figure 6.4 as a function of structural draft for both designs.

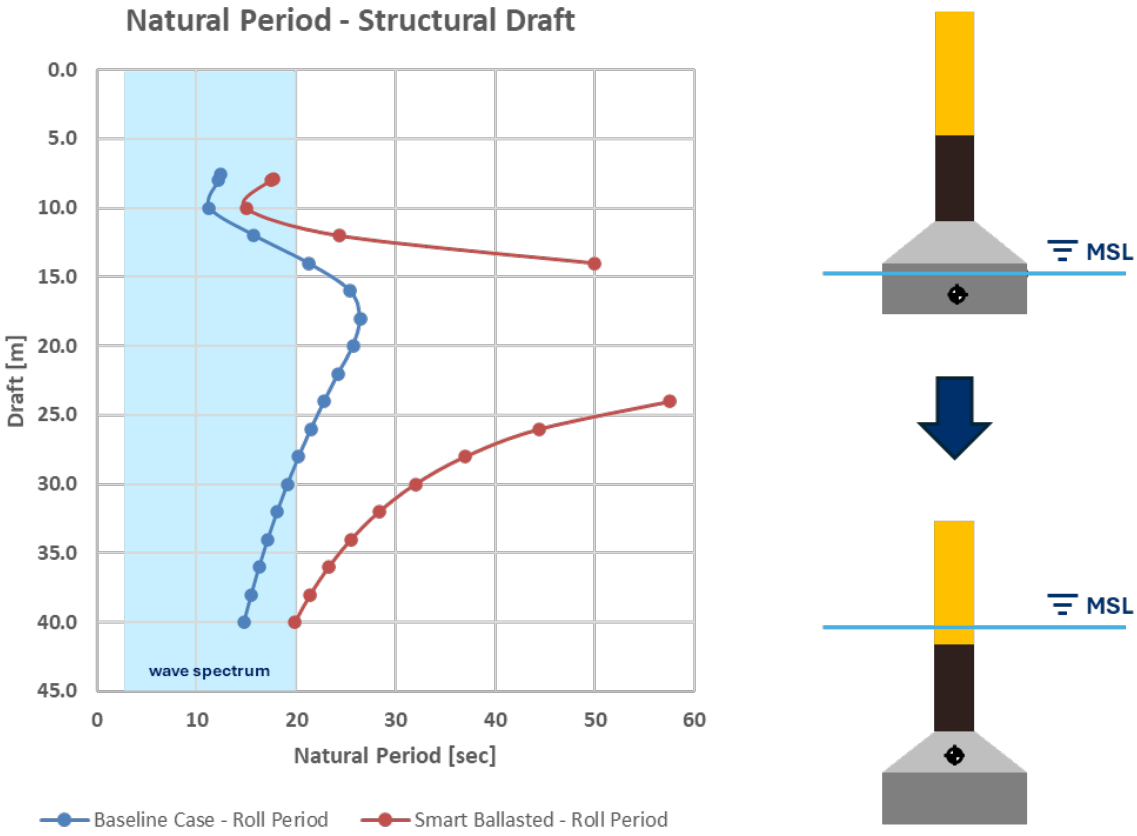

Figure 6.4: Evolution of roll natural period as a function of structural draft, for the baseline case (BC) and smart-ballasted case (SB).

During the initial sub-phases of installation (draft below 15 m), the roll natural period of both configurations falls within the typical wave-energy range. Between 15 m and 28 m draft, the roll natural period of the BC shifts outside this range, which indicates a reduced susceptibility to resonance over this interval. For the SB, the roll natural period is not defined over the same draft range, as the structure is hydrostatically unstable in this region (see Section 6.2.2). Beyond 28 m draft, the roll natural period of the BC configuration returns to the wave-energy range during the final landing sub-phases.

This shift of the roll natural period is the intended outcome of the smart-ballasting technique. It is expected to reduce the structural response and thereby improve the workability of the two examined sub-phases, station-keeping and landing.

6.2.4. Workability Evaluation

The process established for the baseline case is followed here to evaluate the workability of the smart-ballasted design for both examined sub-phases of the installation.

Station-Keeping

Figure 6.5 compares the smart-ballasted (SB) case against the baseline case (BC). The operability envelope of the SB case for the station-keeping condition is given in Figure D.3 in Appendix D.

The operability envelope improves significantly, extending the operable range from $T_p \approx 9$ s up to $T_p \approx 12$ s. This change is owed to the shift of the roll natural period caused by the redistributed mass. The resonant responses that drive the limit exceedances, mainly the maximum-inclination criterion, are shifted towards sea states of higher period. The operability is therefore slightly reduced for $T_p > 15$ s, that is, for swell seas.

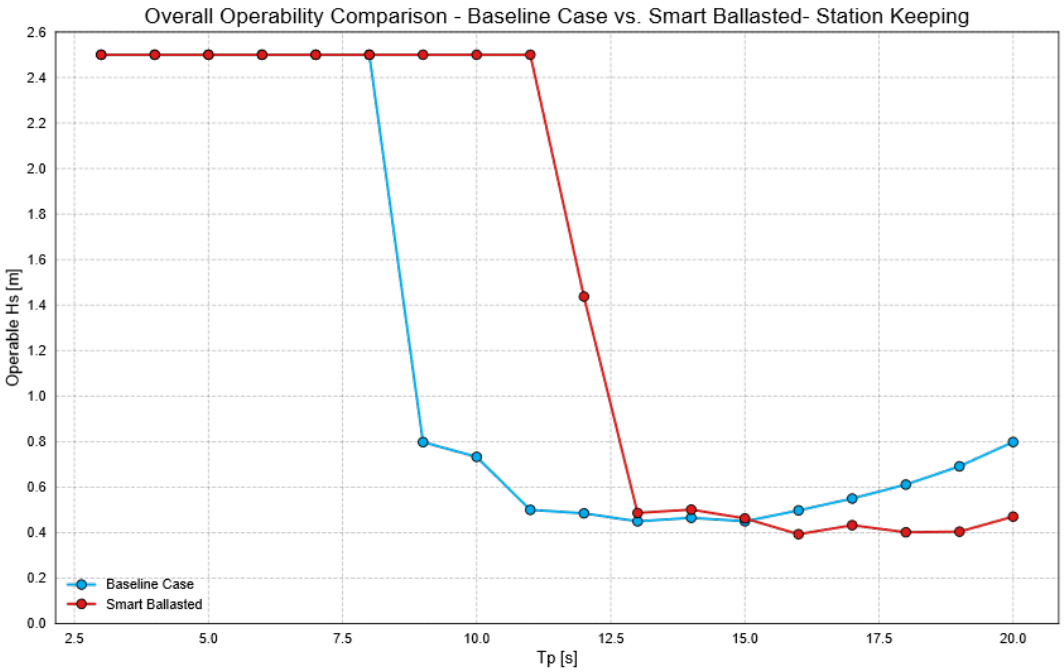

Figure 6.5: Comparison of the station-keeping operability envelopes of the baseline (BC) and smart-ballasted (SB) designs.

In terms of workability, the conditional workability reaches 75.5%, an improvement of 46.0 percentage points over the baseline. This is a substantial gain. The workability scatter is given in Figure D.4 in Appendix D.

Landing

Figure 6.6 compares the smart-ballasted (SB) case against the baseline case (BC) for the landing sub-phase. The operability envelope of the SB case for the landing condition is given in Figure D.5 in Appendix D.

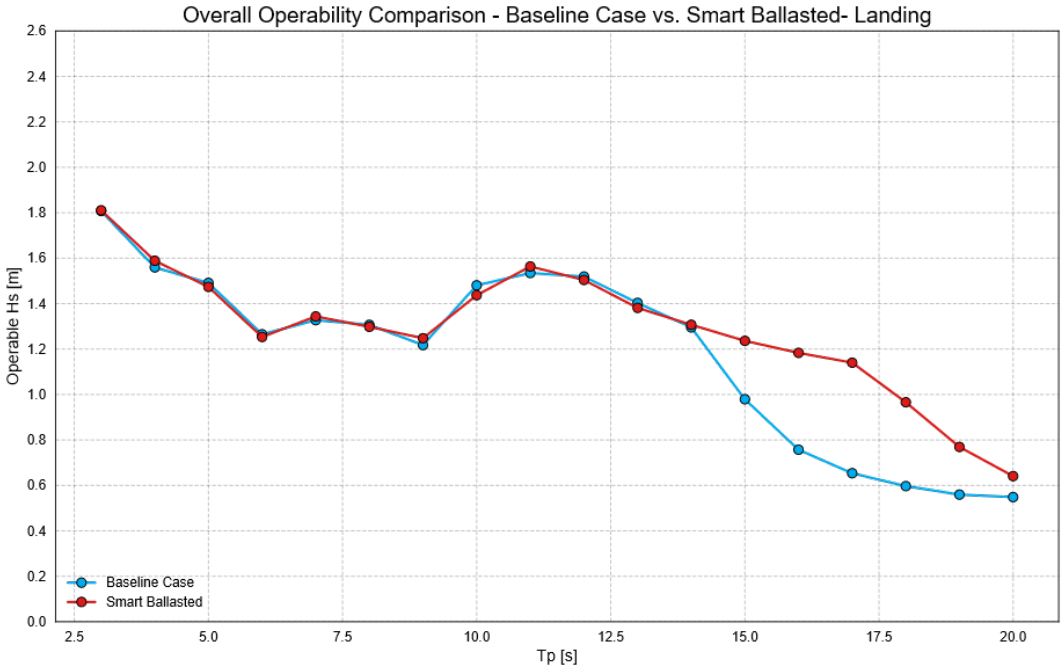

Figure 6.6: Comparison of the landing operability envelopes of the baseline (BC) and smart-ballasted (SB) designs.

The attempted improvement yields additional operability only for sea states with $T_p > 14$ s. The mechanism is similar to the one described for the station-keeping sub-phase. At the large landing draft, however, the roll natural period is already partly detuned from the wave spectrum, so smart ballasting provides only a limited additional benefit.

The conditional workability reaches 46.2%, only 0.5 percentage points above the baseline. This marginal gain is due to the low probability of occurrence of the sea states at which the operability is improved. The workability scatter is given in Figure D.6 in Appendix D.

Table 6.2 summarises the workability improvements of the smart-ballasted design. The method yields a significant benefit for the station-keeping sub-phase, while its effect on the later landing sub-phase is almost negligible.

Table 6.2: Conditional workability of the two installation sub-phases for the baseline case and smart-ballasted designs.

	Conditional Workability [%]		
Sub-phase	Baseline	Smart-Ballasted	Difference [pp]
Station-keeping	29.5	75.5	$+46.0$
Landing	45.7	46.2	$+0.5$

6.3. Bridle Mooring Configuration

The smart-ballasted design improves the workability of the station-keeping sub-phase, but it does not provide any notable improvement for the landing sub-phase, which is the most critical phase of the installation. The reason is that its operability gains occur only for swell seas, which have a low probability of occurrence. The landing operability under the more probable wind-seas remains unchanged. An alternative method is therefore investigated here to increase the operability, and consequently the workability, under wind-sea conditions.

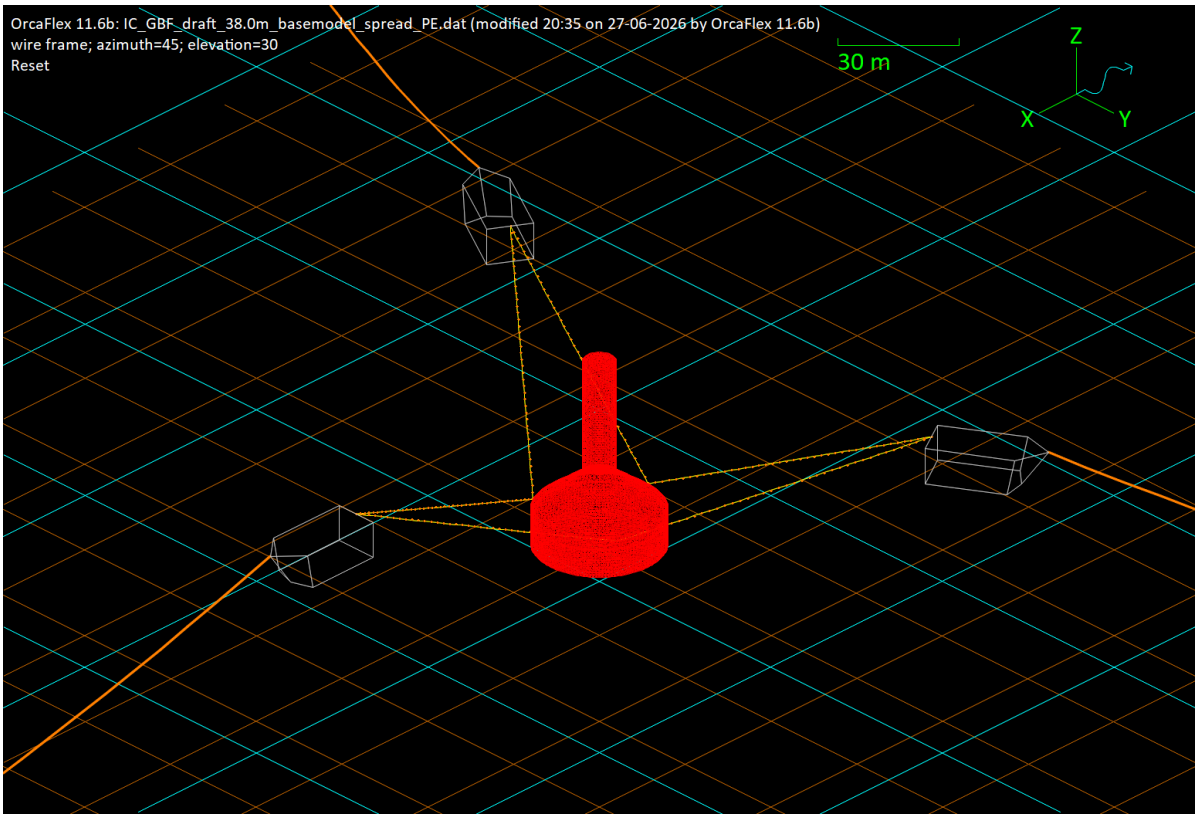

Figure 6.7: Bridle mooring arrangement investigated for the GBF installation.

The baseline analysis shows that the wind-sea response of the landing sub-phase is dominated by the horizontal DOFs (surge, sway, yaw), which are governed by the mooring stiffness. The approach is therefore to improve the positioning and heading accuracy by modifying the mooring configuration, and thus the horizontal-DOF stiffness.

A bridle mooring arrangement, bridle-moored design (BM), shown in Figure 6.7, is investigated in terms of operability and workability.

6.3.1. Workability Evaluation

The process established for the baseline case is followed here to evaluate the workability of the bridle-moored design for both examined sub-phases of the installation.

Station-Keeping

Figure 6.8 compares the bridle-moored (BM) case against the baseline case (BC) for the station-keeping sub-phase. The operability envelope of the BM case for the station-keeping condition is given in Figure D.7 in Appendix D.

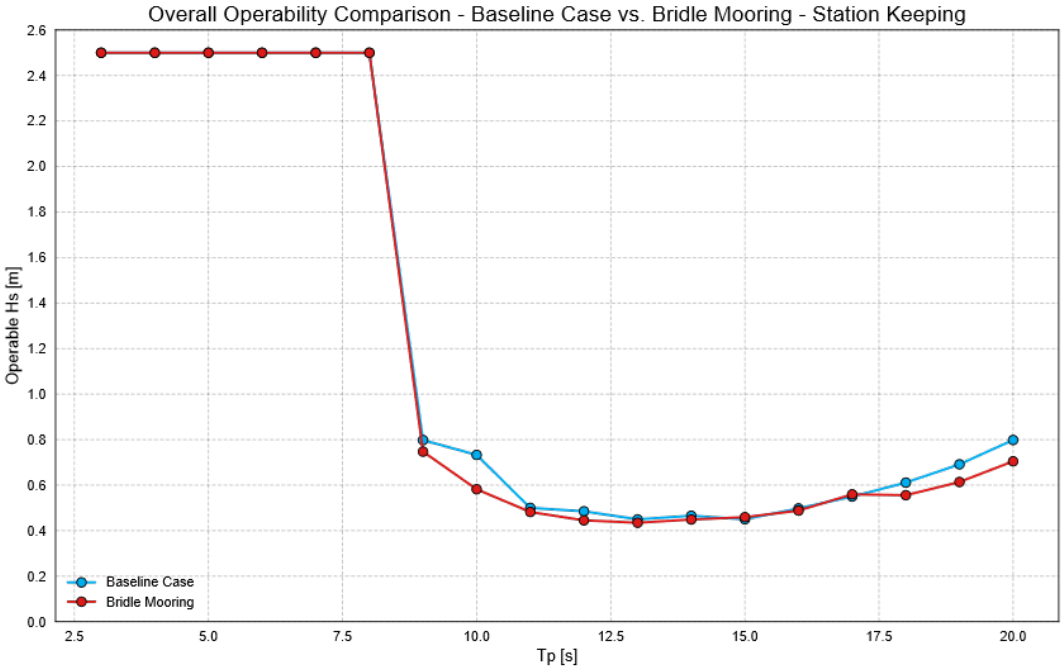

Figure 6.8: Comparison of the station-keeping operability envelopes of the baseline (BC) and bridle-moored (BM) designs.

The two operability envelopes follow the same behaviour, with only minor changes. The BM case shows slightly lower operability over the period range where the resonant response is present. The conditional workability is 27.8%, marginally below the baseline. The workability scatter is given in Figure D.8 in Appendix D.

Landing

Figure 6.9 compares the bridle-moored (BM) case against the baseline case (BC) for the landing sub-phase. The operability envelope of the BM case for the landing condition is given in Figure D.9 in Appendix D.

The operability improves for the wind-sea states, which is the targeted objective. The improvement results from the raised operable limits for positioning location and heading. For swell seas, a slight decrease in operability is observed, following a trend similar to the baseline case. The conditional workability increases to 58.6%, from 45.7% for the baseline. The workability scatter is given in Figure D.10 in Appendix D.

Table 6.3 summarises the workability impact of the bridle-moored arrangement. An important improvement is achieved for the landing sub-phase, while the workability is slightly reduced for the station-keeping sub-phase. This underlines that no single method improves the workability of all installation

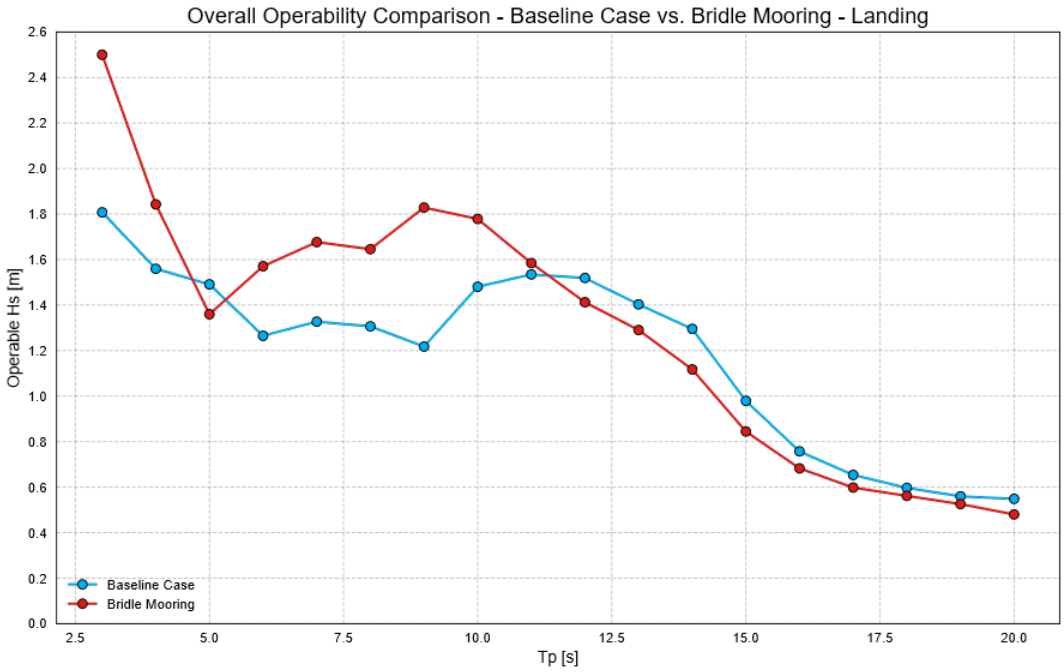

Figure 6.9: Comparison of the landing operability envelopes of the baseline (BC) and bridle-moored (BM) designs.

sub-phases, and that detailed engineering of each sub-phase is required to optimise the workability of the operation.

Table 6.3: Conditional workability of the two installation sub-phases for the baseline and bridle-moored designs.

	Conditional Workability [%]		
Sub-phase	Baseline	Bridle-Moored	Difference [pp]
Station-keeping	29.5	27.8	-1.7
Landing	45.7	58.6	$+12.9$

7

Conclusions & Recommendations

7.1. Conclusions

7.1.1. Research Questions Conclusions

The present research aims to advance the understanding of the Float-out & Submerge method for Gravity Based Foundations. It focuses on foundations suitable for modern $15\,\mathrm{MW}$ offshore wind turbine generators, and proposes improvements to the method. This chapter presents the main conclusions of this work. They are structured to address the research sub-questions defined in the Introduction (Section 1.5) and, ultimately, the main research question.

F&S Compatible Foundation Design

A meaningful evaluation of the F&S method requires a foundation design relevant to the currently installed generation of wind turbines. No suitable GBF design is available for this purpose. Therefore, an automated design algorithm is established. It provides the foundation design used later for the modelling.

The algorithm implements a preliminary design method based on the evaluation of capacity factors. This method is proposed in the literature for GBFs installed with the traditional heavy lift method. The algorithm is further enriched with constraints. These accommodate the specific design parameters of the up-scaled design.

When validated against the realised design (BOD) used as the baseline, the method slightly overestimates the foundation mass by approximately 5%. This overestimation stems from the conservative DLC adopted in the preliminary design method. The DLC combines unidirectional extremes of wind, waves and currents simultaneously.

Another important outcome concerns the full-contact capacity utilisation under the Serviceability Limit State (SLS). This parameter governs the feasible design space. It is the most restrictive design constraint.

Applying the design algorithm to the $15\,\mathrm{MW}$ foundation yields a 30% increase in total foundation mass. This increase is distributed equally between structural weight and ballast. The result is surprising, as it does not follow the trends observed for other foundation types. Nevertheless, it highlights the flexibility of a single GBF outer geometry. The same outer design can host a range of turbines by adjusting only its structural properties (e.g. internal structural members or slab thickness) and its ballast mass. The hydrodynamic properties are thereby preserved.

Finally, it is important to note that the proposed preliminary method produces the optimal design. It minimises the foundation mass while respecting all design requirements. However, the operability evaluation presented later reveals a limitation. The resulting “optimal” design is not necessarily the most suitable one for the F&S installation method.

Simulation Modelling

For the modelling of the installation process, a multibody OrcaFlex model is established. It performs time-domain simulations in line with industry practice. It also captures the investigated non-linear effects, namely second-order waves and viscous damping.

The focus is kept mainly on the phase identified as the most critical, just before seabed mating. This phase is the most critical because it carries the strictest operability criteria. The station-keeping phase is additionally examined to explore potential improvements in the method's operability.

The free-surface effect of the partially filled internal tank is evaluated for its impact on the structure's stability. It is neglected in the dynamic simulations, as permitted by DNV. The stability is monitored throughout the immersion operation. A draft range (15–25 m) exists in which the structure risks instability.

The inclusion of appropriately tuned viscous damping is found to be important. Resonance is observed at certain wave periods. The inclusion of drift loads, both mean and oscillating, is likewise considered important. The mean component accounts for the structure's static load. The oscillating component matters because low-frequency loads can excite the structure's lower modes, mainly the surge, sway and yaw motions.

Finally, and most importantly, the towing-line and mooring configuration, together with their structural properties, are concluded to be of major importance. They largely determine the natural periods of the system's degrees of freedom (DOFs). The natural periods of the vertical DOFs (heave, roll, pitch) are dominated by hydrostatic stiffness. The stiffness provided by the mooring drives the natural periods of the horizontal DOFs (surge, sway, yaw).

For this study, a soft taut mooring is selected, realised with polypropylene lines under a set pretension. This choice handles the risk of snatch loads on the lines. A careful selection of the line type (i.e. line stiffness and MBL) and of the towing arrangement (choice of tugboats and spread configuration) is nonetheless recommended before simulating, to ensure more realistic modelling.

Operability

The operability evaluation of the baseline model indicates the need for distinct operability criteria for each sub-phase of the installation process. The station-keeping sub-phase is governed primarily by DNV guidelines for safe offshore operations, which keep the response within the equipment limits. The landing sub-phase is additionally limited by positioning-accuracy criteria, together with seabed-clearance and maximum potential impact-velocity requirements. The landing sub-phase is considered the most critical in terms of operability, owing mainly to the seabed proximity. The station-keeping sub-phase is also considered significant, as its possible duration directly affects the actual workability of the operation.

The baseline evaluation reveals a reduced operability of the method for both the station-keeping and the landing sub-phases. For station-keeping, resonance arising from the natural period of the floating GBF falling within the wave spectrum ($T_{\text{roll}} = 12.5$ s) significantly reduces the operable sea states. For landing, the increased number and strictness of the operability criteria, both a consequence of the seabed proximity, are the main drivers of the low operability level.

The different operability criteria are governed by distinct sets of degree-of-freedom (DOF) motions. The horizontal DOFs (surge, sway, yaw) are dominated by the mooring stiffness and govern the positioning accuracy and the line loads. The vertical DOFs (heave, roll, pitch) are dominated by the hydrostatic stiffness and govern the inclination, the clearance, and the velocity criteria. A further distinction is that the horizontal-DOF criteria govern under wind-sea conditions ($3 < T_p < 12$ s), whereas the vertical-DOF criteria define operability under swell conditions ($12 < T_p < 20$ s).

The proposed operability-improvement methods exhibit both strengths and weaknesses. The first method, the smart-ballasting approach, targets the roll/pitch natural period in order to detune it and improve the response of the vertical DOFs. In detail, it sacrifices part of the static-stability (GM) surplus to improve the dynamic response of the structure, by pushing its natural roll period outside the wave spectrum. The method yields a notable improvement for the station-keeping sub-phase, while its effect on landing operability is reduced, improving it only for swell sea states. Its principal drawback is the reduced static stability (low GM) of the GBF, which causes an instability range (15–25 m) during immersion and for which mitigation measures must be taken.

The second proposed improvement targets the mooring stiffness, by introducing a different mooring arrangement, in an attempt to improve the response of the horizontal DOFs of the GBF and ultimately the operation operability. It yields a notable improvement for the wind-sea conditions of the landing sub-phase, resulting in better positioning accuracy of the GBF landing. The method resulted in important improvements for the landing sub-phase; however, it proved to slightly worsen the station-keeping sub-phase workability.

Workability
One of the main conclusions of the study is that improving the operability of the method does not automatically improve its workability. The workability depends heavily on the site-specific wave conditions and their probability of occurrence, which vary significantly between locations. An operability gain realised in a region of high occurrence translates into a workability gain. In contrast, an operability gain in rarely occurring sea states has almost no impact on workability. For this reason, the workability is evaluated on a case-by-case basis, as no global optimal workability exists for the method.

The most workable sub-phase of the installation can be altered by the design choices. The smart-ballasted (SB) design improves the workability of both sub-phases. The gain is significant for station-keeping and marginal for landing, which makes station-keeping the more workable sub-phase and allows operation within a wider envelope of conditions. The bridle-moored (BM) design, in contrast, improves the workability only for landing and slightly reduces it for station-keeping, which keeps landing as the more workable sub-phase.

The evaluation of the smart-ballasted (SB) improvement highlights the flexibility offered by integrating an upper tank in the floating GBF. The excess static stability is used to manipulate the roll natural period of the structure and improve its operability. By filling or emptying the tank at specified sub-phases of immersion, the operability is enhanced across the overall installation process.

The evaluation of the bridle-moored (BM) improvement points out the impact of the mooring stiffness on the workability, where high positioning precision is required during the landing sub-phase. The mooring is, however, simulated under simplifying assumptions, which should be relaxed to reveal the actual behaviour of the system.

7.1.2. Main Conclusion
The main research question of this work asks how the workability of the F&S method for modern offshore wind GBFs can be improved. The study shows that the workability can be improved by tuning the dynamic response of the tugboat–structure system to the wave climate of the specific site.

The up-scaling of GBFs to modern turbines makes their design more challenging, since the design must satisfy the structural requirements and, at the same time, remain suitable for installation with the F&S method. A key finding is that the mass-optimal design is not necessarily the most installable one. The inclusion of installation criteria, such as static stability and natural-period targeting, in the design process is therefore significant.

The workability is improved by manipulating the natural periods and the stiffness of the system. The smart-ballasting approach uses the excess static-stability (GM) budget to shift the roll natural period out of the wave spectrum, which improves the vertical-DOF response and the station-keeping workability. A modified mooring arrangement, employing a bridle mooring, raises the horizontal-DOF stiffness, which improves the positioning accuracy and the landing workability under wind-sea conditions. Consequently, no single method benefits both the station-keeping and the landing sub-phases, or both the wind-sea and the swell conditions. Different mitigation strategies should therefore target different sub-phases of the installation.

7.2. Recommendations
This work lays the groundwork for evaluating the workability of the F&S installation method for GBFs. It also proposes a dedicated methodology for this purpose. The methodology relies, however, on a set of assumptions and simplifications. These warrant further investigation. In addition, the insights already gained in this study point towards further improvements to the workability assessment approach.

F&S Foundation Design Approach
In general, the foundation design is recommended to follow a fully DNV-compliant method, as is the industry standard. This method uses the full set of standard DLCs together with site-specific metocean data. The aim is to eliminate the uncertainties and conservativeness of the preliminary design approach adopted in this study.

The slab geometry is normally part of GBF designs. It is excluded here to simplify the calculations and simulations. Its inclusion in the design algorithm is nonetheless recommended. It allows a more accurate evaluation of the utilisation capacities and produces a more realistic design. The inclusion is expected to reduce the utilisation factors. This expands the feasible design space. It also enables feasible designs with a smaller caisson diameter and lower mass.

Most importantly, a discrepancy is observed between the mass-optimal design and the most installable design. For this reason, one of the main recommendations of this work is the establishment of an integrated design procedure. This procedure adds installability requirements, such as stability and natural-frequency targeting, on top of the structural requirements already in place.

Modelling Improvements

An important simplification of this study is the omission of wind and current loads from the simulated environmental conditions. This is a notable deviation from the real case. The large exposed area of the floating GBF makes it prone to substantial wind and current loads. These loads introduce a mean horizontal offset. They therefore govern the horizontal DOFs and the line loads together with imposing heel/trim of the structure, and are expected to reduce the operability of the method. Their effect on the dynamic behaviour of the system also warrants investigation, although a low excitation is expected for both components. In addition, these loads introduce velocity-dependent drag damping on the horizontal DOFs. This damping may partly counteract their excitation. The net effect on operability is therefore not evident a priori, and its inclusion in the model is recommended. The directionality of wind and current relative to the waves is likewise considered when simulating the relevant cases.

When focusing on the landing phase of the installation procedure, the hydrodynamic properties of the GBF are affected by the presence of the seabed. As the structure approaches the seabed, the trapped water layer beneath its base is progressively squeezed out. This cushioning (squeeze-film) effect increases the heave added mass and damping, softening the touchdown. The potential-flow model captures part of the added-mass increase with draft, but it does not resolve the viscous squeeze-film at very small gaps. A reliable representation therefore requires CFD or experimental data, which can then be implemented as gap-dependent added mass and damping in the time-domain model.

Finally, the most probable extreme (MPE) responses are estimated using a Rayleigh-based approach. This approach relies on the assumption of a Gaussian, narrow-band response. Given the strong non-linearities present in the model, a Pareto-based peak-over-threshold method is likely more appropriate for estimating the extremes. Its use is recommended in future analyses.

Operability Recommendations

Several improvements can be proposed, addressing both the operability calculation and the actual operability of the system. With respect to the calculation, a broader set of operability criteria could be included, and the selected criteria could be defined more precisely. The operational limits of the tugboats and of the vessel performing the ballasting could be incorporated as additional criteria. The limits of the selected criteria could also be derived more accurately, for instance by simulating the seabed impact to refine the impact-velocity criterion.

In terms of improving operability, the design of a heave plate, integrated together with the structure's slab, is recommended as a first measure targeting the vertical motions. A heave plate increases the added mass and the damping in heave, and to a lesser extent in pitch and roll, by promoting vortex shedding and viscous drag. Where resonance cannot be avoided, this additional damping limits the resonant response of the structure. A significant improvement is therefore expected for the station-keeping sub-phase, together with a secondary benefit for the landing sub-phase.

The most important measures, however, are those addressing the instability range encountered during immersion, since this hurdle renders the proposed installation method unfeasible. In particular, the use of an external floater or of buoyancy aids could be examined. Such devices restore sufficient static stability across the critical draft interval. A floater can further improve the static stability of the structure while simultaneously pushing its natural period further away from the wave spectrum. This benefit, however, comes at the cost of significantly increased complexity and of higher loads, owing to the larger exposure to the waves. Its adoption should therefore be investigated further to identify the relevant trade-offs.

Finally, sensitivity studies on the tugboat arrangement and the mooring lines are also recommended. The number of tugboats, the line length, and the towing points are the main parameters to be examined. These parameters govern the horizontal response of the system, which is deemed the most limiting factor of the landing sub-phase, and thus the positioning accuracy of the foundation. A significant impact is therefore expected on the landing sub-phase, where positioning accuracy is the governing criterion.

Workability Assessment
The workability is investigated in the present study under assumptions and simplifications, which should be relaxed in future assessments to obtain a result closer to the real observed workability. In particular, a persistence-based approach, using a weather-window analysis on metocean time series, is recommended, in contrast to the static scatter-diagram perspective adopted here.

Since the transport and installation (T&I) operations of the F&S method are performed sequentially, an overall T&I workability evaluation is recommended, together with an investigation of the transportation phase. A detailed design of the immersion operation, including the ballasting sequence, is also suggested.

Finally, the resolution of the historical and forecast metocean data should be investigated. Because the operability improvements are marginal, a sufficient data resolution is required to realise the workability gains. With coarse data, the operational gains are difficult to capture.

A

Offshore Installation Vessels

A.1. Categorisation and Suitability

In this section, a description of the main vessel categories involved in the offshore wind industry for the transport and installation of equipment, meaning WTGs and FOUs, is presented. In more detail, the main vessel categories employed in the industry during the installation phase are:

- **Tugboats**, which are small but powerful vessels used for towing or pushing larger units, such as barges or floating foundation elements. They support positioning, manoeuvring, and general marine operations.

- **Anchor Handling Tug Supply (AHTS) vessels**, which combine towing capability with anchor handling and supply functions. They are essential for setting and recovering anchors, towing large floating structures, and supporting dynamic offshore operations.

- **Crane barges**, which are floating platforms equipped with large cranes capable of heavy lifting. They provide a stable working surface for lifting and installing offshore components, especially when shallow waters or limited manoeuvrability are expected.

- **Dynamic Positioning (DP) vessels**, which maintain their position through automated thruster systems without the need for anchors. They offer high accuracy, making them suitable for heavy lift activities and operations in deeper waters where anchoring is not feasible.

- **Wind Turbine Installation Vessels (WTIVs)**, which are purpose-built units designed specifically for offshore wind turbine installation. They typically feature jack-up legs for elevated working conditions, large cranes, and significant deck space for transporting multiple turbine sets.

- **Semi-submersible Crane Vessels (SSCVs)**, which are large floating platforms with very high lifting capacities. Their semi-submersible design gives them excellent stability during heavy lifts, making them suitable for installing massive structures or deep-water components.

Of these vessels, some are purpose built, such as WTIVs that are specifically employed in the offshore wind industry, while others, like tugboats, are used in many different marine operations. Moreover, vessel types from more than one category are normally involved in the installation of an OWF.

Figure A.1: Vessels operating in the offshore wind industry: Tugboat (upper left) [35] , AHTS (upper right) [47], crane barge (middle left) [44], dynamic positioning heavy lift vessel (middle right) [28], jack-up WTIV (lower left) [4] and SSCV (lower right) [9].

Furthermore, dredging vessels, normally trailing suction hopper dredgers (TSHD), are employed in the seabed preparation phase, and fall pipe vessels (FPV) are used for the application of scour protection after the installation of foundations.

Because monopiles have dominated the offshore wind foundation market, most vessels deployed in the sector are specifically designed for this purpose [29]. Installation activities are typically executed with vessels operating in a shuttle mode between a marshalling port, where components are delivered by manufacturers, and the project site. Contemporary state-of-the-art vessels can transport up to six XXL monopile foundations per trip, with crane lifting capacities of approximately 3000 t [56].

Since for WTGs of the 10 MW scale founded on GBFs the foundation net weight might exceed 5000 t, it is clear that different T&I approaches must be followed. Most purpose-built offshore wind vessels cannot lift these structures. Only about ten heavy-lift (HLV) and semi-submersible crane (SSCV) vessels worldwide are capable of such operations, and these are owned by a small number of contractors.

A.2. Availability and Daily Rates

In general, vessel availability has been one of the most significant bottlenecks in the offshore wind industry in recent years [19]. The combination of low vessel availability and high demand, with many projects entering their construction phase, has led to increased day charter rates. This trend is further reinforced by the fact that the lead time for new-build vessels, or for repurposing existing ones, is typically 3 to 4 years [18].

Deployment of these vessels for the installation of an OWF is normally in the form of a time chartering agreement between the developer and the vessel owner. An estimation of the chartering cost of different vessel categories is presented in Table A.1.

Table A.1: Estimated day rates per vessel category employed in offshore wind industry [35] [50].

Vessel Type	Specifications	Day Rate [USD]
Harbour Tugboat	• Bollard pull up to 80 t • High availability	1k–5k
AHTS	• Bollard pull up to 300 t • Higher operational limits offshore	40k–65k
Crane barge	• Crane capacity 1000–4000 t • Limited operation offshore	80k–100k
DP HLV	• Crane capacity up to 5000 t • Dynamic positioning	100k–250k
WTIV	• Crane capacity up to 3000 t • Jacking system	150k–250k
SSCV	• Crane capacity 3000–20000 t • Self-propelled and dynamic positioned	280k–500k

For HLVs and SSCVs, competition with demand from the oil and gas sector, especially due to extensive decommissioning activities, further affects availability and pricing. Considering the general scarcity of these vessels, combined with their limited suitability, the very high day rates can be justified.

A.3. Operational Limits

Each of the aforementioned vessel categories offers different advantages and limitations regarding their operational limits. By operational limits it is meant the maximum sea states under which the transit or operation of the vessel can be executed safely and successfully. Although these limits may vary significantly within a category of vessels, considering their year of build and onboard technology (i.e. DP systems), an overview of the operational limits is given in Figure A.2.

Vessel type	Operating equipment	Capacity	Transit condition		Operating condition	
			Speed (knots)	Wave height (Hs, m)	Wave height (Hs, m)	Wind speed (m/s)
WTIV	Jack up/down + crane	Crane capacity: 800−1500 ton	12	3.0	2.5	16
Jack-up barge	Jack up/down + crane	Crane capacity: 800 ton	4	2.5	1.65	16
Crane barge	Shear crane	3000 ton	4	1.5	1.0	10
Cargo barge	Stacking (without crane)	2000−5,000p	4	1.5	1.5	14
Tug boat	Towing	750 hp, 1000 p	13	2.5	1.0−1.65	14

Figure A.2: Operational limits for transit and operations for different categories of offshore vessels [27].

It is observed, as expected, that the transit limits are lower compared to the operational limits for all vessels, while the operation itself is normally constrained by other factors, such as the desired accuracy of an offshore installation or the design limits of a lifted structure. Furthermore, operation is also limited by the wind speed on site, especially when a heavy lift is performed. For HLVs and SSCVs, which are not included in the table, higher operational limits are generally expected, as mentioned in the literature, although these must again be considered in parallel with other limiting factors of each specific operation.

More specifically, for the T&I of GBFs, considering the two main approaches, an upper limit of $H_s \approx 1.0-2.5$ m is established for heavy lift (HL) transportation, while for towing in the F&S method, $H_s \approx 2-3$ m is expected to be the limiting factor. Regarding the installation phase, the HL approach is limited at $H_s \approx 1-2$ m, while F&S can be executed up to $H_s \approx 1.5-2.5$ m [38].

When designing and planning an offshore operation, a general value of about 1.5 or 2 m of significant wave height can be adopted for preliminary studies. In practice, a detailed time weather window analysis must be developed for both the transportation and installation phases [44]. For HL operations, the required weather operational window (WOW) is estimated at approximately 24 hours, while for F&S a range of 12–24 hours is expected, depending on the site conditions and the specifications of the installed structure [38].

B

Gravity Based Foundations

B.1. Development

Gravity based structures (GBSs) are large-mass structures that rely on their own dead weight to ensure stability and load-carrying capacity, without the need for piling. The concept originates from the extensive experience accumulated in the North Sea oil and gas (O&G) industry, most notably the Condeep (Concrete Deep-Water Structure) concept. Condeep was developed to support O&G platform developments and to provide internal volume for storing produced hydrocarbons [1, 22].

GBSs were subsequently adopted during the early development of the offshore wind sector, where they are more commonly referred to as gravity based foundations (GBFs). This adoption directly leveraged the engineering expertise and construction practices established in the O&G industry. The world's first offshore wind farm (OWF), Vindeby (1991) in Denmark, utilised GBFs to support 11 Bonus 450 kW wind turbines in water depths ranging from 2 m to 5 m, approximately 2 km from shore. The farm operated successfully for 25 years before being decommissioned in 2017 [22].

Figure B.1: Historical development of gravity based foundations: the *Condeep* concept in the O&G industry (left) and their early application at the Vindeby offshore wind farm (right).

B.2. Design Generations

GBF designs for offshore wind can be broadly classified into three main generations, each reflecting the progressive response to increasing turbine sizes and project water depths. The structural design and manufacturing method of each generation are strongly influenced by the targeted T&I approach [22]. Notably, all three conventional generations have relied on heavy lift (HL) operations for installation. In more detail:

- **First generation** foundations correspond to the earliest offshore wind developments, primarily in Denmark, including Vindeby (1991) and Middelgrunden (2001). These structures are completely solid, steel-reinforced concrete (RC) caissons deployed in very shallow water depths of 3 m to 7 m. Their installation required barges and cranes of sufficient capacity, with the foundations lowered onto a prepared gravel bed.

- **Second generation** foundations were designed for slightly deeper sites, such as Lillgrund (2007) and Nysted II (2010), in water depths up to 16 m. This was achieved by adopting a hollow slab design, which reduced the net weight while retaining the required dead-weight capacity once the hollow section was filled with ballast material (typically rock) after installation.

- **Third generation** foundations, as deployed at Thornton Bank (2009, ∼17 m depth) and Fécamp (2022, ∼30 m depth), feature a conical lower section and a vertical upper shaft, with a hollow interior filled with sand and water ballast after positioning on the seabed. The increased water depth and turbine size required the use of heavy lift vessels (HLVs) and semi-submersible crane vessels (SSCVs) for installation.

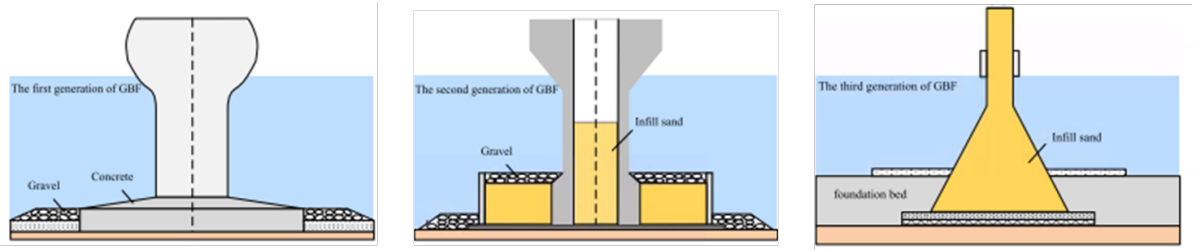

Figure B.2: Design generations of GBFs used in the offshore wind industry [51].

B.3. Novel Concepts

The growing mass of modern GBFs and the limited availability of heavy lift vessels have motivated the development of a number of novel self-buoyant T&I concepts in recent years, most of them explored during the 2010–2020 period [38]. These concepts share the common objective of enabling foundation installation without reliance on specialised heavy lift equipment, by designing the structure to float and be towed to site using standard tugboats. Two of the most relevant active concepts are briefly described below.

The **Cranefree®** concept by Seatower is a hybrid concrete-steel self-floating GBF installed using a floated-to-fixed (F2F) method, designed for cost-effective mass production. By enabling the structure to float, the dependence on heavy lift vessels is fully eliminated, with standard tugboats sufficient for both transport and positioning. The concept was successfully demonstrated at the Fécamp OWF in approximately 30 m of water depth, where an offshore meteorological mast was installed by towing the hollow structure to site and submerging it through controlled seawater flooding [5].

The **ELISA/ELICAN** concept, developed by Esteyco, takes the integrated approach a step further. It enables the complete wind turbine system (foundation, telescopic tower, and rotor-nacelle assembly) to be fully assembled and commissioned onshore, then floated out as a single unit [23]. The self-buoyant concrete caisson is towed to the installation site using standard tugboats and submerged through controlled ballasting. Once the foundation is stabilised on the seabed, the telescopic tower is extended to its operational height using hydraulic or strand-jack systems. The concept has been demonstrated at full scale through a 5 MW prototype at Gran Canaria, Canary Islands, validating the approach for intermediate water depths [24].

Both concepts illustrate the broader industry direction towards self-buoyant GBF designs that decouple the installation process from the constrained global fleet of heavy lift vessels, offering a more accessible and potentially more economical path to offshore foundation deployment.

Figure B.3: ELISA/ELICAN concept by Esteyco (left) [23]. Cranefree concept in its final installed position (right) [5].

B.4. Advantages & Challenges

A structured understanding of the advantages and limitations of GBFs, relative to the current industry standard of monopiles and jacket foundations, is essential before evaluating their potential role in future offshore wind projects. The following discussion is organised by category, and summarised in Table B.1.

Design. GBFs are applicable to a broader range of seabed conditions than pile foundations, including rocky or hard seabeds where pile driving is technically demanding and costly [1]. Furthermore, concrete offers improved resistance to ice loading compared to steel, making GBFs well suited to cold-climate sites such as those in the Baltic Sea [39]. On the other hand, foundation masses for modern 15 MW-class turbines can exceed $15\,000\,\mathrm{t}$, imposing significant challenges during manufacturing and T&I operations. Their large submerged volume also increases hydrodynamic loading, which must be accounted for during the floating phases of installation [1]. The design is inherently more complex compared to monopiles, particularly for hybrid steel-concrete configurations.

Material. The predominant use of concrete reduces exposure to steel price volatility, which has become one of the most significant cost risk factors in offshore wind CAPEX [46]. Concrete prices are generally more stable and less susceptible to global supply chain disruptions [46]. The main material limitation is the poor tensile strength of concrete, which must be compensated by steel reinforcement, requiring very large material volumes per foundation unit. Hybrid design concepts have emerged specifically to seek an optimal trade-off between the properties of concrete and steel within the same foundation [39].

Manufacturing. GBF fabrication relies heavily on local industries, particularly for concrete supply and construction works. This supports local content requirements and can ease the permitting process or increase eligibility for local subsidies in certain regions [1]. The principal manufacturing challenge is the need for large port quayside areas or dry dock facilities in proximity to the project site, which may not be readily available. The bespoke and labour-intensive nature of concrete construction also makes it considerably harder to industrialise compared to the serial production of steel monopiles.

Transport & Installation. The very large mass of GBFs represents the primary challenge for their adoption in the offshore wind industry. Two main approaches exist for installation: the conventional heavy lift (HL) method and the float-out & submerge (F&S) method. The scale and mass of GBF structures significantly limit the available weather windows for marine operations [38]. Conventional HL methods further depend on a limited number of HLVs and SSCVs with sufficient crane capacity [39]. Additional challenges common to both methods include the requirement for thorough seabed preparation prior to installation and the need for extensive scour protection after placement [21].

Operation & Lifetime. Reinforced concrete structures are designed for operational lifetimes exceeding 50 years, requiring minimal maintenance once installed [41]. The possibility of repowering an offshore wind farm by replacing the turbines while retaining the existing foundation represents a significant long-term economic advantage [39]. The primary operational concern is the need for ongoing monitoring of foundation settlement and tilt, given that GBFs rely on seabed contact rather than structural embedment for their stability.

Decommissioning. GBFs can in principle be decommissioned by reversing the installation process, offering a relatively straightforward end-of-life strategy compared to pile-based foundations. Depending on the installation method adopted, heavy lift equipment may still be required for removal. In addition, the large mass and volume of the concrete structure necessitate access to suitable demolition yards in the vicinity of the project site.

Environmental. GBF installation eliminates the underwater percussive noise associated with pile driving, which is one of the primary environmental objections to monopile installation and a common constraint in the permitting process [1]. There is also a reported potential to reduce CO_2 emissions by up to 50% compared to equivalent steel foundations [45]. The main environmental limitation is the extensive seabed interference caused by the large foundation footprint and the associated seabed preparation and scour protection works [39].

Table B.1: Summary of advantages and limitations of GBFs compared to steel foundations, i.e. monopiles and jackets.

Category	Advantages	Limitations
Design	• Soil flexibility • Ice endurance	• Enormous mass • Hydrodynamic loading • Complex design
Material	• Steel price independency • Concrete price stability	• Poor tensile strength • Large material volume
Manufacturing	• High local content • Supports permitting & subsidies	• Large port infrastructure required • Industrialisation difficulty
Transport & Installation	• F&S methods scalability	• Limited weather windows • Seabed preparation • Scour protection
Operation & Lifetime	• Extended lifespan • Low maintenance • Repowering possibility	• Settlement and tilt monitoring
Decommissioning	• Reversible installation process	• May require heavy lift • Large demolition yards required
Environmental	• Noiseless installation • Lower CO_2/MWh	• Extensive seabed interference

C

Foundation Design

C.1. Foundation Design Guidelines

In the offshore wind energy sector, foundations (FOUs) are designed to withstand the loads imposed by the turbine and environment. Loads acting on the structure can be categorised as vertical and lateral, with the former corresponding to the weights of the WTG and foundation, and the latter including shear forces and overturning moments. Another common categorisation distinguishes between static and cyclic loads, with vertical weights considered static, and varying lateral loads due to wind, waves, and currents considered cyclic. Cyclic loading is the main design driver for offshore foundations, as it governs the desired operational lifetime of 25–30 years for modern WTGs [1].

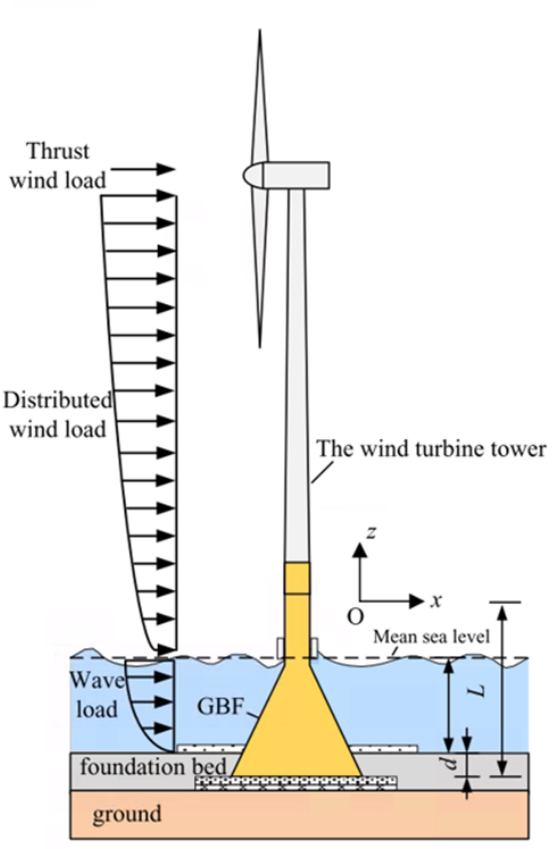

Figure C.1: Loads on an offshore wind turbine and its foundation [51].

DNV (Det Norske Veritas) and IEC have published design standards to evaluate the limit states of offshore wind turbines and their foundations. According to DNV-OS-J101 [11], the following design criteria must be met:

- Ultimate Limit State (ULS): The condition corresponding to the maximum load-carrying resistance of the structure. Exceeding the ULS may result in structural failure, such as yielding, buckling, or collapse.
- Fatigue Limit State (FLS): The condition associated with possible failure due to cyclic loading over time, ensuring that repeated load cycles do not lead to fatigue fracture or unacceptable damage.
- Serviceability Limit State (SLS): Conditions that ensure proper functionality and performance under normal operating loads.
- Accidental Limit State (ALS): The condition corresponding to damage caused by accidental or extreme events, such as impacts, drops, collisions, or loss of components. The structure must maintain integrity, possibly with limited damage, rather than total collapse.
- Target Natural Frequency: The design must ensure that the first bending mode, or relevant modes, do not coincide with excitation from rotor frequencies (1P) or blade passing frequencies (3P).

Additional factors affecting foundation design, such as marine growth, earthquakes, ice loading, and transport and installation (T&I) loads, are included in relevant published documents and recommended practices, such as DNV-RP-N103 [13].

Design objectives differ between MPs and GBFs, influencing their dimensions, manufacturing, and the chosen T&I methods. For example, FLS requirements are generally easier to satisfy for GBFs than MPs due to the superior fatigue resistance of concrete. On the other hand, ULS and floating stability are more critical design considerations when a float-out & submerge (F&S) method is applied [45].

C.2. GBF Preliminary Design Calculations

The design method followed can be found in detail in the relevant sources [31] [1] [12]. Hereby, a set of the most important equations used is presented along with the selected parameter values in Table C.1.

Parameter	Symbol	Value	Units
friction angle - gravel	ϕ_d	38	deg
effective submerged soil unit weight - gravel	γ'	12	$\mathrm{kN\,m^{-3}}$
embedment depth	D_f	0.2	m
soil friction reduction factor	r	0.7	-

Table C.1: Capacities calculation parameters

Eccentricity is defined as the distance from the foundation centreline where the resulting loads will be applied. It is defined as:

$$e = \frac{M}{V} \tag{C.1}$$

where M stands for total moment at mudline and V for the total vertical load.

The effective foundation area, as depicted in Figure C.2 is calculated as:

$$A_{\text{eff}} = 2\left[R^2 \arccos\left(\frac{e}{R}\right) - e\sqrt{R^2 - e^2}\right] \tag{C.2}$$

The effective dimensions, width and length, of a rectangle equivalent to the effective foundation area are calculated:

$$b_{\text{eff}} = \frac{l_{\text{eff}} b_e}{l_e} \qquad l_{\text{eff}} = \sqrt{A_{\text{eff}} \frac{l_e}{b_e}} \tag{C.3}$$

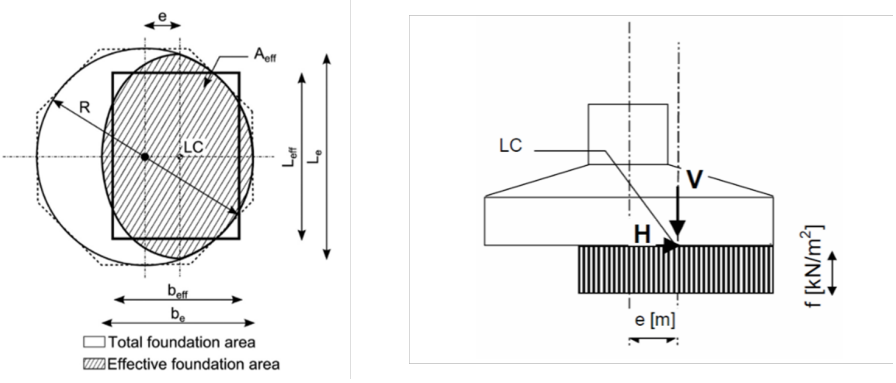

Figure C.2: Foundation effective area definition.

Bearing resistance capacity

$$p_u = \gamma' D_f, \tag{C.4}$$

$$q_u = \frac{1}{2}\gamma' b_{\text{eff}} N_\gamma s_\gamma i_\gamma + p_0' N_q s_q i_q, \tag{C.5}$$

where:

- γ' = effective submerged unit weight of soil;
- D_f = embedment length
- b_{eff} = effective foundation width;
- p_0' = effective overburden pressure at foundation–soil interface;
- N_γ, N_q = bearing capacity factors;
- s_γ, s_q = shape factors;
- i_γ, i_q = load inclination factors.

$$N_\gamma = \frac{3}{2}(N_q - 1)\tan\phi_d \qquad N_q = e^{\pi \tan\phi_d}\left(\frac{1+\sin\phi_d}{1-\sin\phi_d}\right) \tag{C.6}$$

$$s_\gamma = 1 - 0.4\,\frac{b_{\text{eff}}}{l_{\text{eff}}} \qquad s_q = 1 + 0.2\,\frac{b_{\text{eff}}}{l_{\text{eff}}} \tag{C.7}$$

$$i_\gamma = i_q^2 \qquad i_q = \left(1 - \frac{H_d}{V_d + A_{\text{eff}} \cdot c_d \cdot \cot\phi_d}\right)^2. \tag{C.8}$$

Sliding resistance capacity

$$H_d = r(A_{eff}\ c_d + V\ tan\phi_d) \tag{C.9}$$

Tipping resistance capacity

$$M_{st} = V \cdot \frac{D_{slab}}{2} \tag{C.10}$$

Full-contact resistance capacity

$$e_{max} = \frac{D_{slab}}{6} \tag{C.11}$$

D

Operability - Workability Figures

D.1. Baseline Case Design

Station-Keeping - Workability

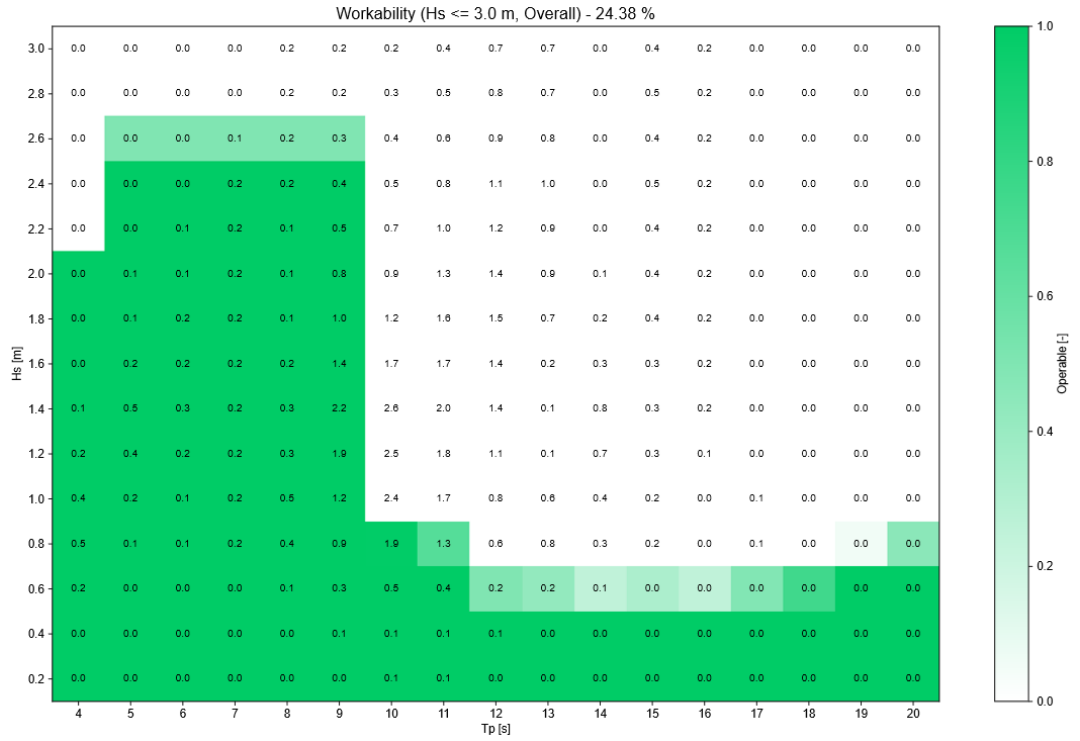

Figure D.1: Workability scatter of the baseline case (BC) for station-keeping installation sub-phase (overall workability: 24.4%).

Landing - Workability

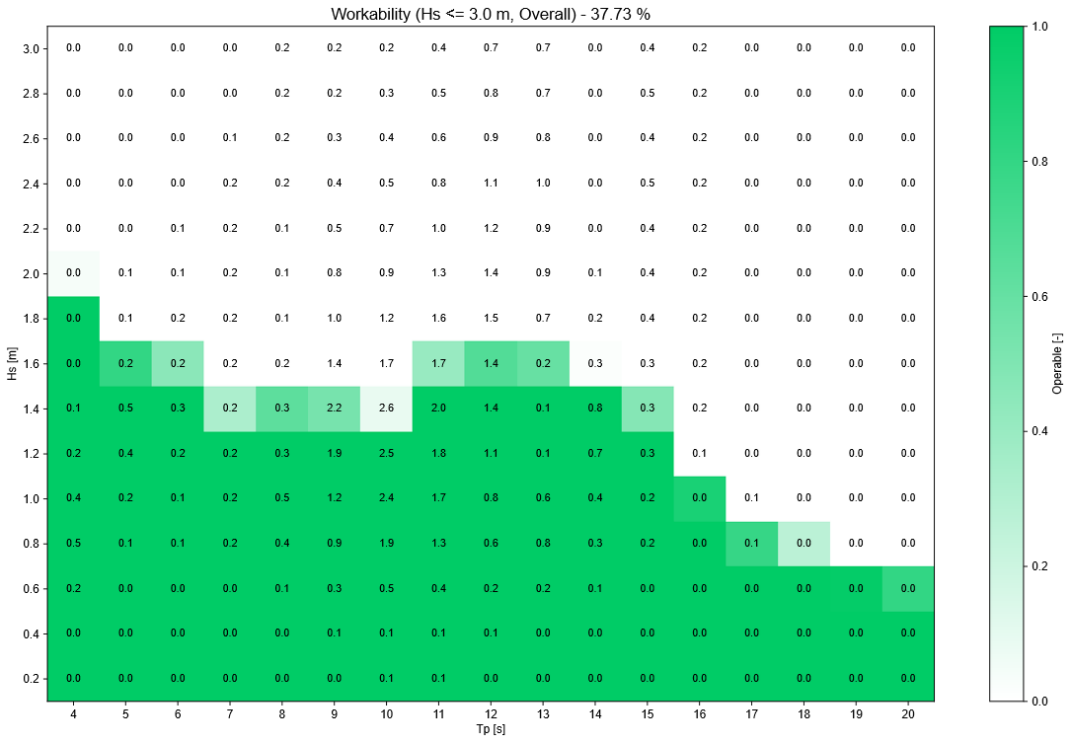

Figure D.2: Workability scatter of the baseline case (BC) for landing installation sub-phase (overall workability: 37.7%).

D.2. Smart-Ballasted Design

Station-Keeping - Operability

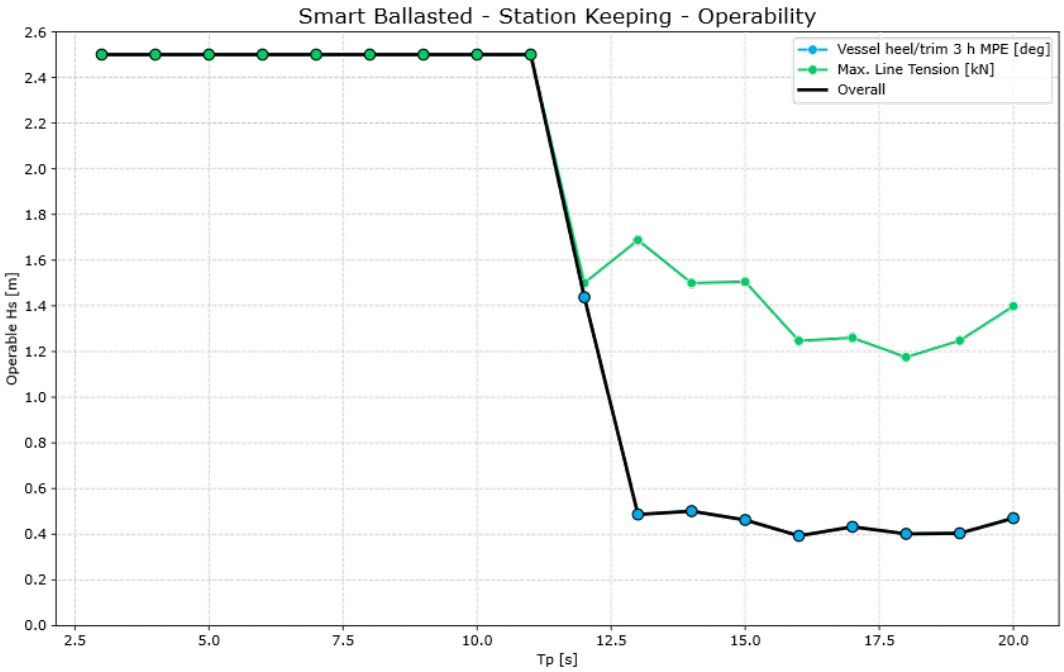

Figure D.3: Operability envelope of the smart-ballasted (SB) case for station-keeping sub-phase.

Station-Keeping - Workability

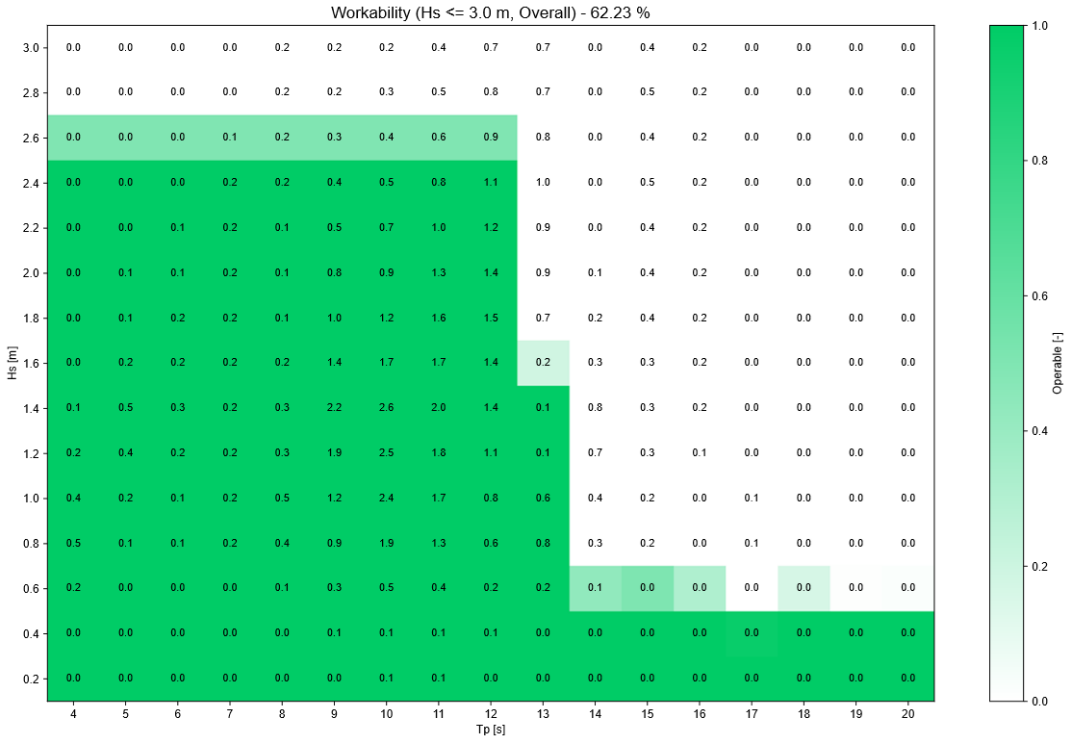

Figure D.4: Workability scatter of the smart-ballasted (SB) design for station-keeping installation sub-phase (overall workability: 62.2%).

Landing - Operability

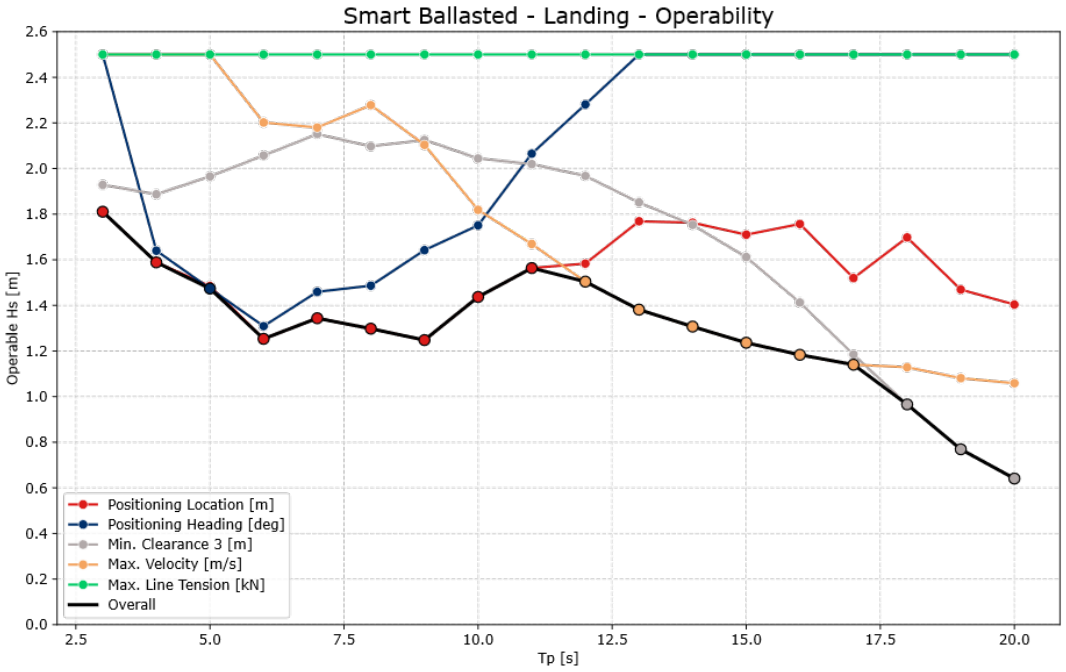

Figure D.5: Operability envelope of the smart-ballasted (SB) case for landing sub-phase.

Landing - Workability

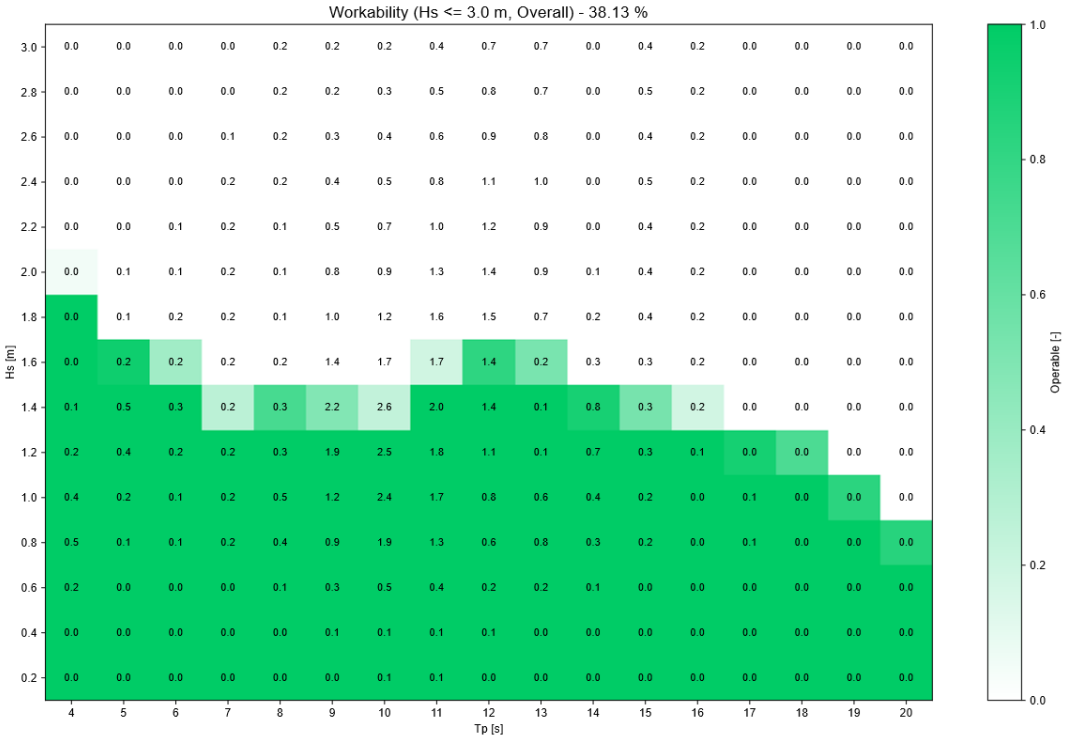

Figure D.6: Workability scatter of the smart-ballasted (SB) design for landing installation sub-phase (overall workability: 38.1%).

D.3. Bridle Mooring Design

Station-Keeping - Operability

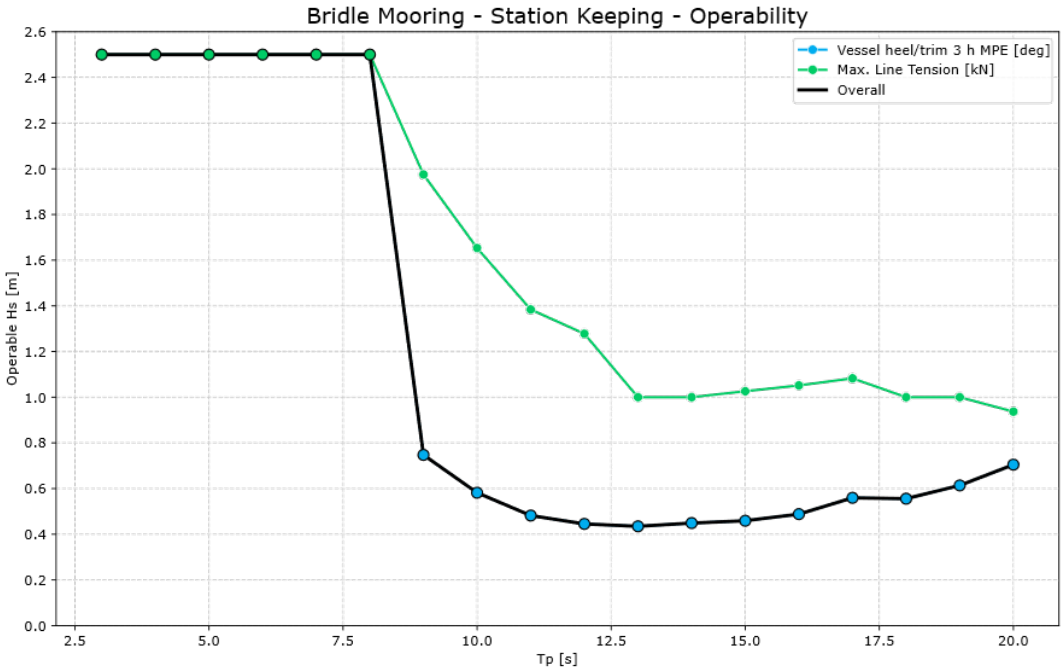

Figure D.7: Operability envelope of the bridle-moored (BM) case for station-keeping sub-phase.

Station-Keeping - Workability

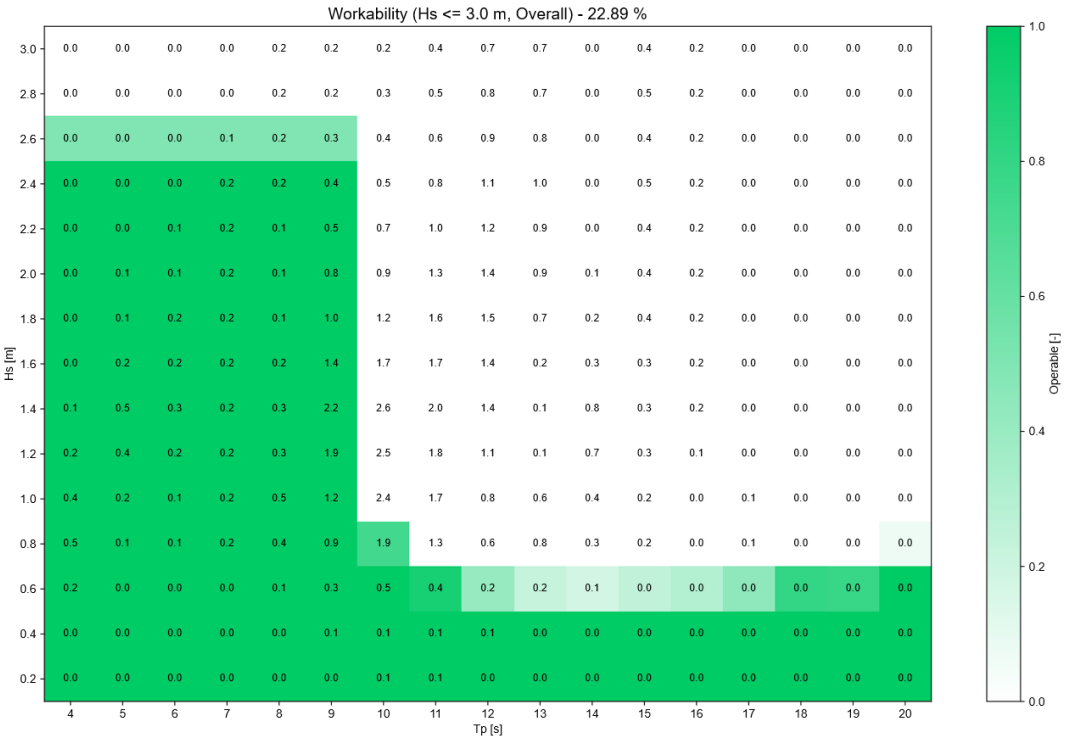

Figure D.8: Workability scatter of the bridle-moored (BM) case for station-keeping installation sub-phase (overall workability: 22.9%).

Landing - Operability

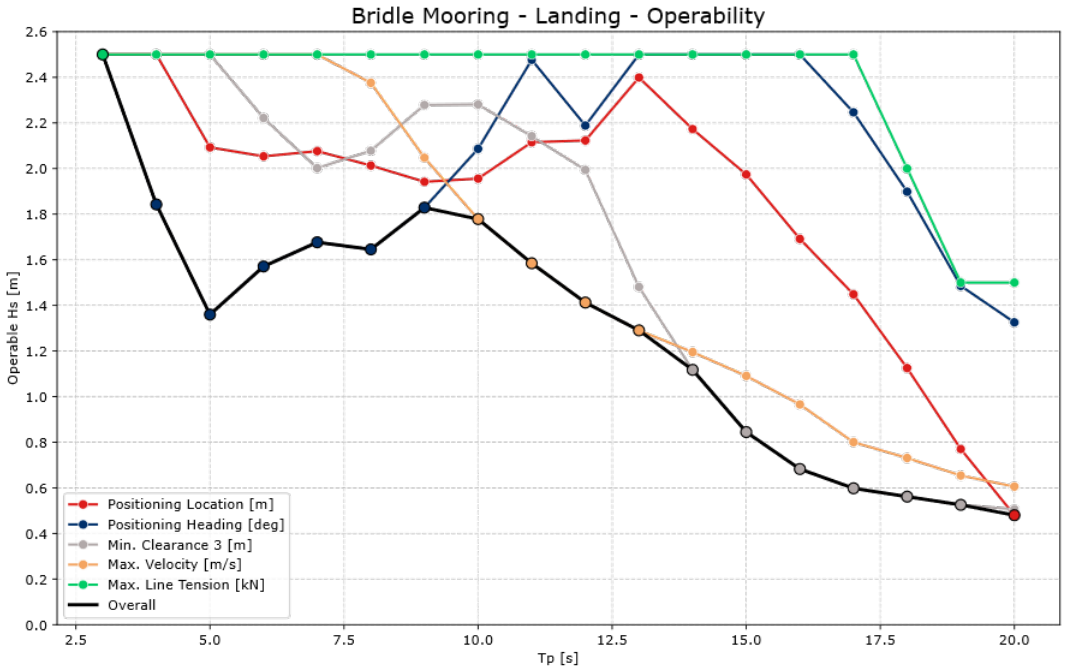

Figure D.9: Operability envelope of the bridle-moored (BM) case for landing sub-phase.

Landing - Workability

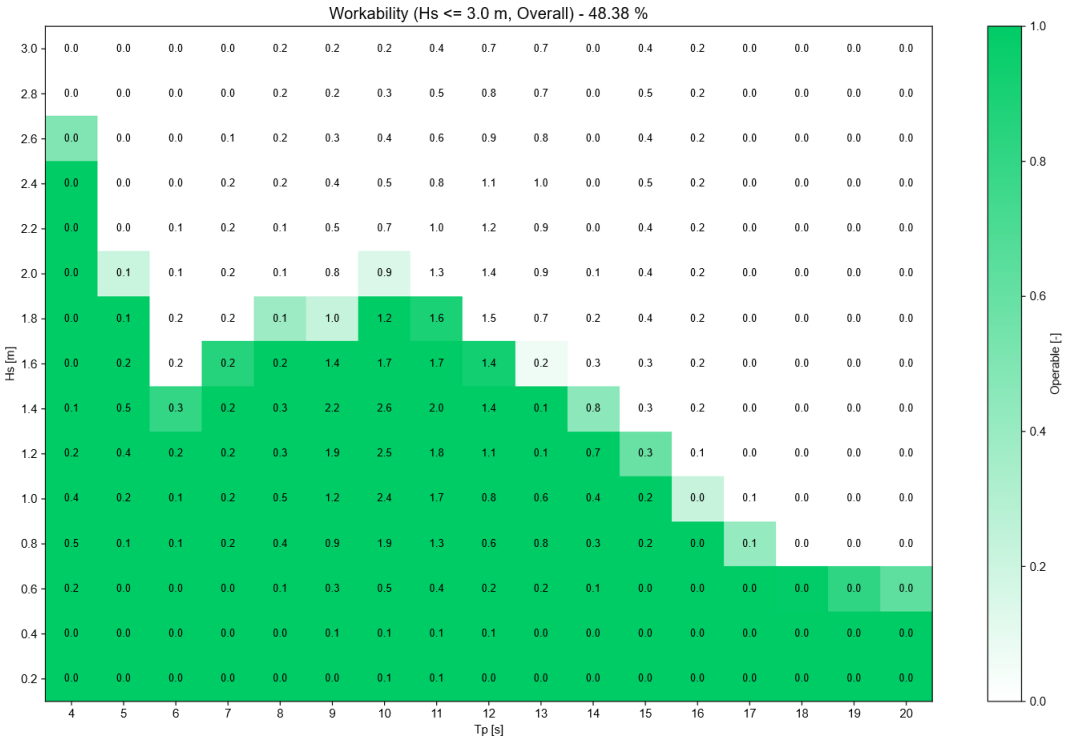

Figure D.10: Workability scatter of the bridle-moored (BM) case for landing installation sub-phase (overall workability: 48.4%).

References

[1] Muhammad Aleem et al. “Gravity-based foundation for offshore wind turbines”. In: *Wind Energy Engineering: A Handbook for Onshore and Offshore Wind Turbines*. Elsevier, Jan. 2023, pp. 383–396. ISBN: 9780323993531. DOI: 10.1016/B978-0-323-99353-1.00014-1.

[2] Carlos Andres Parra Muk Chen Ong Muk Chen Ong, Lin Li, and Xinying Zhu. *Numerical Study on Offshore Lifting Operations of a Subsea Spool*. Tech. rep. University of Stavanger, 2018.

[3] Laszlo Arany et al. “Design of monopiles for offshore wind turbines in 10 steps”. In: *Soil Dynamics and Earthquake Engineering* 92 (Jan. 2017), pp. 126–152. ISSN: 02677261. DOI: 10.1016/j.soildyn.2016.09.024.

[4] CADELER AS. URL: https://www.cadeler.com/ (visited on 12/11/2025).

[5] Seatower AS. *Seatower AS*. 2025. URL: https://www.seatower.com/ (visited on 09/29/2025).

[6] Bas van Wuijckhuijse et al. *Transforming Installation Methods by Reducing Crane Dependency Buoyancy-Assisted Monopile Installation W h i t e Pa p e r*. Tech. rep. TWD, 2024.

[7] Guy Brindley et al. *Wind energy in Europe TEXT AND ANALYSIS: Giuseppe Costanzo*. Tech. rep. 2026.

[8] Bouygues Construction. URL: https://www.bouygues-construction.com/ (visited on 12/06/2025).

[9] Heerema Marine Contractors. URL: https://www.heerema.com/heerema-marine-contractors/fleet (visited on 12/11/2025).

[10] Danish Energy Agency. *Technology Data for Energy Plants for Electricity and District heating generation*. Tech. rep. ENERGINET, Mar. 2018. URL: www.ens.dk.

[11] Det Norske Veritas. *OFFSHORE STANDARD DET NORSKE VERITAS AS Design of Offshore Wind Turbine Structures*. Tech. rep. Det Norske Veritas, 2013. URL: http://www.dnv.com.

[12] DNV. *DNV-RP-C212 - Offshore soil mechanics and geotechnical engineering*. Tech. rep. DNV, 2021.

[13] DNV AS. *DNV-RP-N103 - Modelling and analysis of marine operations*. Tech. rep. 2017.

[14] DNV AS. *DNV-ST-0437 Loads and site conditions for wind turbines*. Tech. rep. 2024.

[15] DNV AS. *DNV-ST-N001 Marine operations and marine warranty*. Tech. rep. 2023.

[16] DNV GL. *Marine Operations and Marine Warranty*. Tech. rep. DNV-ST-N001. Standard for marine operations and marine warranty, including alpha-factor methodology for weather-restricted operations. DNV GL, 2020.

[17] Marie-Laure Ducasse, Damiano Soulat, and Florent Vertallier. *INVESTIGATION OF HYDRODYNAMIC BEHAVIOUR OF WIND TURBINE GBS DURING OFFSHORE INSTALLATION AND ENGINEERING DESIGN OUTCOMES*. Tech. rep. 2018. URL: http://asmedigitalcollection.asme.org/OMAE/proceedings-pdf/OMAE2018/51319/V010T09A057/2536932/v010t09a057-omae2018-77619.pdf.

[18] Adnan Durakovic. *New NOV Crane for Cadeler’s Wind Osprey*. 2021. URL: https://www.offshorewind.biz/2021/08/03/new-nov-crane-for-cadelers-wind-osprey/ (visited on 10/12/2025).

[19] Rystad Energy. *Shortage of Heavy Lift Vessels for the Offshore Wind Industry Post 2025*. 2020. URL: https://oceannews.com/news/energy/shortage-of-heavy-lift-vessels-for-the-offshore-wind-industry-post-2025 (visited on 10/12/2025).

[20] Erik-Jan de Ridder. *Final Report End report of the GBS WIND JIP*. Tech. rep. 2019.

[21] M. D. Esteban et al. *Gravity based support structures for offshore wind turbine generators: Review of the installation process*. Dec. 2015. DOI: 10.1016/j.oceaneng.2015.10.033.

[22] M. Dolores Esteban, José Santos López-Gutiérrez, and Vicente Negro. *Gravity-based foundations in the offshore wind sector*. 2019. DOI: 10.3390/jmse7030064.

[23] Esteyco. *ELICA Project*. 2025. URL: https://esteyco.com/projects/elisa/index.html (visited on 09/29/2025).

[24] ESTEYCO S.A. *Self-installing concrete gravity-base substructure (ELISA Technology). Sizing for 15 MW turbine and holistic approach for its implementation in the*. Tech. rep. ESTEYCO; NREL, 2024.

[25] Femern A/S. *Fehmarnbelt Fixed Link*. Project documentation and press releases. World's longest immersed tunnel, under construction between Denmark and Germany. 2024. URL: https://femern.com.

[26] Evan Gaertner et al. *Definition of the IEA Wind 15-Megawatt Offshore Reference Wind Turbine Technical Report*. Tech. rep. 2020. URL: www.nrel.gov/publications..

[27] Zhen Gao et al. *A SUMMARY OF THE RECENT WORK AT NTNU ON MARINE OPERATIONS RELATED TO INSTALLATION OF OFFSHORE WIND TURBINES*. Tech. rep. NTNU, 2018.

[28] DEME Group. URL: https://www.deme-group.com/ (visited on 12/11/2025).

[29] H-BLIX. *Offshore wind vessel availability until 2030: Baltic Sea and Polish perspective*. Tech. rep. 2022. URL: www.h-blix.com.pl.

[30] Henno Smaling. *Hydrodynamic loading on the shaft of a gravity based offshore wind turbine*. Tech. rep. 2014.

[31] Joey Hu. *Preliminary Design Methodology Of Concrete Gravity-Based Foundations For Offshore Wind European Wind Energy Master*. Tech. rep. 2022.

[32] IMMONTEC. *Transport and installation of 5 Gravity Based Foundations - Blyth Offshore Wind Demonstrator*. 2017. URL: https://immontec.com/blog/artikel/blyth-offshore-wind-demonstrator/ (visited on 12/06/2025).

[33] IMMONTEC B.V. *Project information description of the activities Blyth Offshore Wind Demonstrator*. Tech. rep. IMMONTEC B.V., 2017.

[34] Saleh Jalbi and Subhamoy Bhattacharya. *Concept Design of Jacket Foundations for Offshore Wind Turbines in 10 Steps*. Tech. rep. University of Surrey, 2020.

[35] Zhiyu Jiang. "Installation of offshore wind turbines: A technical review". In: *Renewable and Sustainable Energy Reviews* 139 (Apr. 2021), p. 110576. ISSN: 1364-0321. DOI: 10.1016/J.RSER.2020.110576. URL: https://www.sciencedirect.com/science/article/pii/S1364032120308601.

[36] Yun jae Kim et al. *A comprehensive review of foundation designs for fixed offshore wind turbines*. Jan. 2025. DOI: 10.1016/j.ijnaoe.2025.100643.

[37] Kuehne Climate Center. *Logistics' Role in Scaling Offshore Wind Energy to Climate Targets A scenario study on installation vessel requirements In collaboration with*. Tech. rep. Kuehne Climate Center, Dec. 2025.

[38] Marc Costa Ros. *Carbon Trust - Offshore wind industry review of GBSs*. Tech. rep. Carbon Trust, 2015.

[39] Alexandre Mathern, Christoph von der Haar, and Steffen Marx. *Concrete support structures for offshore wind turbines: Current status, challenges, and future trends*. Apr. 2021. DOI: 10.3390/en14071995.

[40] Anders Myhr et al. "Levelised cost of energy for offshore floating wind turbines in a life cycle perspective". In: *Renewable Energy* 66 (June 2014), pp. 714–728. ISSN: 0960-1481. DOI: 10.1016/J.RENENE.2014.01.017. URL: https://www.sciencedirect.com/science/article/pii/S0960148114000469.

[41] offshoreWIND.biz. *EDF Performs Autonomous Foundation Inspection at Blyth Offshore Wind Farm*. 2022. URL: https://www.offshorewind.biz/2022/05/23/edf-performs-autonomous-foundation-inspection-at-blyth-offshore-wind-farm/ (visited on 10/09/2025).

[42] Info Plaza. *Wave Climate*. 2026. URL: https://www.waveclimate.com/ (visited on 05/10/2026).

[43] Charalampos Romanidis. *Gravity Based Foundations for Offshore Wind Energy*. Specialisation Project Report, TMR4590. European Wind Energy Master. NTNU – Norwegian University of Science and Technology, 2025.

[44] Ismael Ruiz et al. *GRAVITY BASE FOUNDATIONS FOR OFFSHORE WIND FARMS MARINE OPERATIONS AND INSTALLATION PROCESSES*. Tech. rep. 2013.

[45] Samanthia Fred ; Desen Ozkan ; Katarina Hallden ; Bridget Moynihal ; John DeFrancisci ; Dan Kuchma ; Chris Bachant ; Eric Hines. “Low-Carbon, Nature-Inclusive Concrete Gravity-Based Foundations for Offshore Wind Turbines”. In: OSPRE - Offshore Power Research & Education Collaborative (2022).

[46] Petter Osmundsen Sindre Lorentzen. *Cost Development and Cost Drivers in UK Offshore Wind Farms*. 2025. URL: https://onlinelibrary.wiley.com/doi/10.1002/we.70048?af=R (visited on 12/12/2025).

[47] John Snyder. *Eager buyers scoop up valuable AHTS assets in lively S&P activity*. 2024. URL: https://www.rivieramm.com/news-content-hub/news-content-hub/eager-buyers-scoop-up-valuable-ahts-assets-in-lively-sampp-activity-80052 (visited on 12/11/2025).

[48] Tethys. *Fixed Offshore Wind*. URL: https://tethys.pnnl.gov/technology/fixed-offshore-wind (visited on 12/11/2025).

[49] The North Sea Summit. *Offshore wind industry declaration*. Tech. rep. 2025.

[50] Jorick Tjaberings, Stefano Fazi, and Evrim Ursavas. “Evaluating operational strategies for the installation of offshore wind turbine substructures”. In: *Renewable and Sustainable Energy Reviews* 170 (Dec. 2022). ISSN: 18790690. DOI: 10.1016/j.rser.2022.112951.

[51] Wenbo Tu et al. “Time Domain Nonlinear Dynamic Response Analysis of Offshore Wind Turbines on Gravity Base Foundation under Wind and Wave Loads”. In: *Journal of Marine Science and Engineering* 10.11 (Nov. 2022). ISSN: 20771312. DOI: 10.3390/jmse10111628.

[52] Bygging Uddemann. URL: https://bygging-uddemann.com/our-services/serial-production-of-concrete-structures/hull-spar-semisuberisble-gbf/ (visited on 12/06/2025).

[53] Johanne Tomine Vartdal. *An Investigation of Offshore Wind Installation Strategies A Discrete-Event Simulation Model Used to Investigate Installation Vessel Operability*. Tech. rep. 2017.

[54] Martijn van Wijngaarden et al. *GRAVITY BASED FOUNDATIONS FOR OFFSHORE WIND TURBINES: CYCLIC LOADING AND LIQUEFACTION*. Tech. rep. 2018. URL: http://asmedigitalcollection.asme.org/OMAE/proceedings-pdf/OMAE2018/51302/V009T10A026/2536448/v009t10a026-omae2018-77082.pdf.

[55] Wind Europe. *Wind energy in Europe - 2024 Statistics and the outlook for 2025-2030*. Tech. rep. Wind Europe, Feb. 2025.

[56] Sarah McLean Yvan Gelbart. *Scaling up: spec changes in the new generation of heavy lift wind installation vessels*. 2025. URL: https://www.spinergie.com/blog/spec-changes-in-the-new-generation-of-heavy-lift-wind-installation-vessels.